MODELING OF LIFE HISTORY STRATEGIES IN ORGANISMS

WITH INDETERMINATE GROWTH, WITH A FOCUS ON THE

DISTRIBUTION AND LIFE HISTORY OF THE GUMBOOT

CHITON *CRYPTOCHITON STELLERI*

by

JOSHUA PRATT LORD

A THESIS

Presented to the Department of Biology
and the Graduate School of the University of Oregon
in partial fulfillment of the requirements
for the degree of
Master of Science

September 2010

"Modeling of Life History Strategies in Organisms with Indeterminate Growth, with a

Focus on the Distribution and Life History of the Gumboot Chiton *Cryptochiton stelleri*,"

a thesis prepared by Joshua Pratt Lord in partial fulfillment of the requirements for the

Master of Science degree in the Department of Biology. This thesis has been approved

and accepted by:

_____

Dr. Alan L. Shanks, Chair of Examining Committee

_____13 Aug 2010_____

Date

Committee in Charge: Dr. Alan L. Shanks, Chair
                                Dr. Cynthia D. Trowbridge
                                Dr. Richard B. Emlet

Accepted by:

_____

Dean of the Graduate School

An Abstract of the Thesis of

Joshua Pratt Lord   for the degree of   Master of Science

in the Department of Biology   to be taken   September 2010

Title: MODELING OF LIFE HISTORY STRATEGIES IN ORGANISMS WITH

INDETERMINATE GROWTH, WITH A FOCUS ON THE DISTRIBUTION

AND LIFE HISTORY OF THE GUMBOOT CHITON *CRYPTOCHITON*

STELLERI

Approved: _____

Dr. Alan L. Shanks

The gumboot chiton *Cryptochiton stelleri* is the largest intertidal invertebrate herbivore on rocky shores in the Pacific Northwest. This study documented the larval development, metamorphosis, distribution and life history of this species. Growth rings in valves of *Cryptochiton stelleri* and *Katharina tunicata* were used to determine age and showed life spans of at least 40 years for *C. stelleri* and 17 years for *K. tunicata*. Field surveys in southern Oregon showed that *C. stelleri* populations are densest in small coves as a result of mortality, food availability, or larval retention. Growth curves based on length, weight and volume were created for several intertidal invertebrates. When incorporated into energy allocation models,

length-based curves can underestimate growth and exaggerate an energetic shift from growth to reproduction. Estimates of food intake and reproductive output showed that continuous growth leads to higher food intake and increased fecundity in several organisms with indeterminate growth.

CURRICULUM VITAE

NAME OF AUTHOR: Joshua Pratt Lord

PLACE OF BIRTH: Grand Forks, North Dakota

DATE OF BIRTH: April 14, 1986

GRADUATE AND UNDERGRADUATE SCHOOLS ATTENDED:

University of Oregon, Eugene, Oregon
Colby College, Waterville, Maine

DEGREES AWARDED

Master of Science, Biology, 2010, University of Oregon
Bachelor of Arts, Biology, 2008, Colby College

AREAS OF SPECIAL INTEREST

Marine Biology
Ecology

PROFESSIONAL EXPERIENCE

Teaching Assistant, University of Oregon, Eugene, OR, Summer 2010
    Supervisor: Cynthia Trowbridge

GK-12 Fellow, National Science Foundation, Oregon Institute of Marine Biology,
    Coos Bay, OR, 2008-2010
        Supervisors: Janet Hodder, Alan Shanks, Patricia Mace

Student Teaching Assistant, America Reads and Counts, Colby College,
    Waterville, ME, 2004-2008
        Supervisor: Sherrill Saulter

Research Assistant, Biology Department, Colby College, Waterville, ME,
Summer 2007
Supervisor: W. Herbert Wilson

Biological Science Technician, Coweeta LTER Hydrologic Lab, Otto, NC,
Summer 2006
Supervisor: Barton D. Clinton

GRANTS, AWARDS AND HONORS

NSF GK-12 Fellowship, Oregon Institute of Marine Biology, 2008-2010
Presidential Scholarship, Colby College, 2004-2008

PUBLICATIONS

Lord, J.P. 2010. How symbiosis creates diversity. *Science and Children* **47(5):**
64-66.

ACKNOWLEDGEMENTS

TABLE OF CONTENTS

I. GENERAL INTRODUCTION 1

II. PATCHY SMALL SCALE DISTRIBUTION AND RECRUITMENT
    PATTERNS OF THE GUMBOOT CHITON *CRYPTOCHITON STELLERI* 4

    Introduction... 4
    Materials and Methods.. 9
        I. Distribution... 9
        II. Age-frequency 13
    Results.. 14
        I. Distribution... 14
        II. Age-frequency 17
    Discussion... 23
    Bridge... 30

III. LARVAL DEVELOPMENT, METAMORPHOSIS, AND EARLY GROWTH
     OF THE GUMBOOT CHITON *CRYPTOCHITON STELLERI* 31

    Introduction... 31
    Materials and Methods.. 32
    Results.. 36
    Discussion... 47
    Bridge... 50

IV. LONGEVITY AND GROWTH RATE OF THE GUMBOOT CHITON
    CRYPTOCHITON STELLERI AND THE BLACK LEATHER CHITON
    KATHARINA TUNICATA 51

    Introduction... 51
    Materials and Methods.. 56

LIST OF FIGURES

LIST OF TABLES

CHAPTER I

GENERAL INTRODUCTION

The gumboot chiton or giant Pacific chiton, *Cryptochiton stelleri*, is the largest

species of chiton in the world and is a common inhabitant of the rocky shores of

northwestern North America and northern Japan, yet much about its biology remains a

mystery. A relative dearth of studies exist on this mollusk, and those studies that have

been done often contradict one another on topics from spawning to development to

growth rate (Heath, 1897; Okuda, 1947; Tucker and Giese, 1962; MacGinitie and

MacGinitie, 1968; Palmer and Frank, 1974). Therefore, this study seeks to define or

clarify several of the debated aspects of the life history and behavior of *Cryptochiton

stelleri*.

I find *Cryptochiton stelleri* to be one of the oddest looking creatures in the

intertidal, and I have heard it described as anything from a blob to a meatloaf. It appears

this way because not only is it large (up to 36 cm long, pers. obs.) and brick red, but it is

the only species of chiton that does not have exposed dorsal plates. *C. stelleri* is found

from the mid-intertidal zone down to 60 meters subtidally and ranges from San Nicolas

Island in California to Alaska along the western coast of North America and over to

northern Japan (Tucker and Giese, 1962; MacGinitie and MacGinitie, 1968; Yates,

1989). It feeds on a variety of macroalgae, most notably the red algae *Mazzaella*, *Odonthalia,* and *Cryptopleura* and the green alga *Ulva* (MacGinitie and MacGinitie, 1968; Yates, 1989). While some studies have suggested that the gumboot chiton fasts during the winter months, other studies have not found this to be the case; seasonal feeding patterns could vary with site (Tucker and Giese, 1962; MacGinitie and MacGinitie, 1968; Palmer and Frank, 1974). This species is reportedly the longest-lived chiton in the world and has been estimated to live over twenty years (MacGinitie and MacGinitie, 1968).

I became interested in *C. stelleri* after spotting it commonly in the intertidal zone at Cape Arago and Sunset Bay, Oregon, and realizing how little was known about the habits of this large and common herbivore. Since it remains one of my favorite intertidal animals, I could not believe how little definitive information was known about the growth, habitat preference and larval development of this species. I found the fact that very few people had discovered small (< 15 cm long) *C. stelleri* of particular interest. Serendipitously, I was conducting a survey of the biodiversity in purple sea urchin burrows at Sunset Bay State Park during July 2008, and I found three young (about 5 cm) gumboots in the urchin burrows. After this discovery, I began closely searching the urchin beds for young *C. stelleri* and had significant success. In the next couple months, I discovered over fifty gumboots smaller than fifteen centimeters, all found in urchin burrows. Why would they do this? What induces them to settle and metamorphose? Could these urchin pits serve as *C. stelleri* nurseries? How quickly do they grow? All of

these questions led me to formulate this thesis. My goal was to generate an accurate description of the distribution, larval development, growth, and behavior of *C. stelleri*.

I first wanted to determine where *C. stelleri* individuals were found and what their population structure was. Chapter II of this thesis focuses on the distribution and recruitment patterns of *C. stelleri* at several sites on the southern Oregon coast. Chapter III describes the larval development and metamorphosis cues of this species of chiton. Chapter IV uses growth bands in the shell plates of *C. stelleri* and the leather chiton *Katharina tunicata* to estimate ages and growth rates of these species. The unusual growth patterns of these species of chitons led me to assess the way growth and size are measured in Chapter V, which examines the effect that different measures of size can have in models of life history and energy allocation in several intertidal invertebrates with indeterminate growth. This thesis fills in many of the gaps in what is known about the life history of *C. stelleri* and challenges some of the ways in which size and growth rate are used in energetic models.

CHAPTER II

PATCHY SMALL SCALE DISTRIBUTION AND RECRUITMENT PATTERNS OF

THE GUMBOOT CHITON *CRYPTOCHITON STELLERI*

Introduction

Intertidal herbivores can have significant ecological impacts on the algal

composition and overall species assemblages on rocky shores around the world

(Lubchenco, 1978; Moreno and Jaramillo, 1983; Dethier and Duggins, 1985; Jenkins and

Hartnoll, 2001). Chitons such as *Katharina tunicata* have widespread direct and indirect

effects on the population dynamics of the rocky shore by altering macroalgal density

(Dethier and Duggins, 1985). *K. tunicata* and urchins like *Strongylocentrotus purpuratus*

and *S. droebachiensis* can completely change the surrounding community by causing

shifts in habitat type (Leighton et al., 1966; Moreno and Jaramillo, 1983; Himmelman,

1984; Dethier and Duggins, 1985; Chapman and Johnson, 1990). Where dominant

herbivores such as these species exist in high densities they control the habitat, sculpting

the regions in which they reside. The mechanisms by which *S. purpuratus* and *K.*

tunicata shape the intertidal community are well studied and well understood. This is a

sharp contrast to the lack of information on the ecological importance of the gumboot

chiton, *Cryptochiton stelleri*, the largest herbivore in the intertidal zone of the Pacific

Northwest.

Cryptochiton stelleri is the only member of its genus and is a fairly common inhabitant of rocky intertidal shores from south of Monterey, CA, all the way north along the northeast Pacific coast and around to northern Japan. It is a generalist herbivore, feeding on the blades of algal genera *Mazzaella, Cryptopleura, Nereocystis, Saccharina* and *Ulva*, among others (Heath, 1905b; Yates, 1989). As such, *C. stelleri* is less likely to control the abundance of a specific species of algae and more likely to have an impact on the overall abundance of macroalgae in its intertidal and shallow subtidal habitat. Therefore, *C. stelleri* is more likely to affect competing generalist herbivores and organisms that benefit from open space. Because space is an important factor influencing intertidal community assemblages (Dayton, 1971), *C. stelleri* could potentially create space for limpets or other grazers by removing shading macroalgae, as the leather chiton *K. tunicata* does (Dethier and Duggins, 1985).

The feeding ecology of *C. stelleri* along the central Oregon coast was studied in depth by Yates (1989). His study confirmed the generalist nature of feeding in this species and found that adults feed preferentially on red algae such as *Mazzaella* and *Cryptopleura*, even though other algal species are consumed as well. A critical factor in determining the ecological impact of *C. stelleri* is population density because high densities of this large herbivore could alter the macroalgal abundance on the rocky intertidal shore. However, little is known about the distribution and population density of this species.

The distribution of *Cryptochiton stelleri* within its geographic range is not well known (Petersen and Johansen, 1973; Palmer and Frank, 1974; Yates, 1989). On a

smaller scale, Yates (1989) suggested that the absence of *C. stelleri* at some sites could be due to high amounts of wave action. However, it is unclear whether this is a result of physical limitation or is tied to diet, because several leafy algae that *C. stelleri* feeds on are only present in areas that are relatively protected from intense wave activity.

Small-scale (local) distribution and abundance can be vital to the success of a population, especially in terms of reproduction at both an individual and population level. Many species must sustain a minimum density in order to be reproductively successful, including barnacles (Kent et al., 2003; Munroe and Noda, 2009), mussels (Downing et al., 1993), urchins (Levitan et al., 1992), and some plants (Kunin, 1997). For example, the sea palm *Postelsia palmaeformis* is unlikely to persist at low population densities due to limited gamete dispersal (Dayton, 1973; Paine, 1988). Density can be especially important for free spawning species such as *Cryptochiton* because a critical concentration of sperm is needed for successful fertilization of eggs (Levitan et al., 1992, Young et al., 1992). Decreased fertilization success of non-aggregated populations has led to behavioral adaptations such as seasonal aggregations of spawning individuals (Young et al., 1992). This may be the case with *C. stelleri* populations, because there have been accounts of intertidal aggregations of spawning *C. stelleri* during the spring (Okuda, 1947). However, because these aggregations have not been widely reported it is possible that this behavior is not commonly displayed by *C. stelleri* or is due to differences in seasonal temperature regimes between northern Japan (where Okuda's study was based) and North America.

Despite the effect that density can have on the reproductive output and ecological importance of a population, there have been no studies on the within-site distribution of *Cryptochiton stelleri*. While the range of this species is relatively extensive, there is no available information regarding *C. stelleri* abundance within this range. The local distribution (areas of high and low population densities within a site) should indicate what types of habitats *C. stelleri* prefers. Distribution patterns could also offer clues about what drives the distribution of this species and why *C. stelleri* is more or less common in different parts of its range. Knowledge of the distribution of juvenile *C. stelleri* individuals could also provide information about cues for larval metamorphosis, since juveniles will be most commonly found in areas of high recruitment success.

Juveniles (< 3 cm) and small (< 15 cm) *C. stelleri* have been reported as very rare in the intertidal and subtidal in California and the Pacific Northwest (Tucker and Giese, 1962; MacGinitie and MacGinitie, 1968; Palmer and Frank, 1974; Yates, 1989). During a feeding study on *C. stelleri* between 1982 and 1986, Yates (1989) only found 12 individuals less than 15 centimeters in length, and only three juveniles, despite working in areas with very high densities of *C. stelleri*. Yates suggested that the lack of juveniles could be due to sporadic recruitment. Given the reports above that describe the rarity of individuals in these size classes, recruitment must either be very sporadic or consistently low enough that these younger life stages remain rare. It is also possible that small individuals are very cryptic or have different habitat preferences than the adults, making them more difficult to find. Knowledge of the distribution, size, and abundance of all life

stages of *Cryptochiton stelleri* could highlight differences in population structure and recruitment success between sites or tidal levels.

The distribution of all benthic life stages of *C. stelleri* could also be influenced by seasonal changes in food availability, wave action, temperature or other seasonal factors. Vertical migration in the intertidal and subtidal zones has been tied to seasonal differences in food availability for the green crab *Carcinus maenas* (Hunter and Naylor, 1993) and several species of limpets (Branch, 1975). Seasonal migration can also occur for other reasons, such as in the limpet *Lottia digitalis*, which migrates to lower in the intertidal during the summer in order to avoid desiccation stress caused by higher temperatures and decreased wave action (Frank, 1965a). This migration to different levels of the intertidal or subtidal can also occur over a lifetime in some species, such as intertidal snails *Chlorostoma funebralis* (Paine, 1969) and *Monodonta labio* (Takada, 1996). The prevalence of either seasonal or lifetime vertical migration patterns in other mollusks indicates the possibility that these changes in distribution occur with *C. stelleri*. However, no studies have focused on this topic or discussed the implications of this possibility, even though Snow (1951) suggested this for *C. stelleri*. If *Cryptochiton* does migrate vertically over its lifetime, then the resulting variation in size with tidal level could result in ecological importance that varies vertically in the intertidal and subtidal zones. Seasonal vertical migration could cause the ecological impact of *C. stelleri* to vary with changes in season.

Because of the lack of information concerning the distribution of *C. stelleri*, it is unclear what drives the distribution of this species. Even at sites with dense populations

of this species, there is no shortage of preferred macroalgae such as *Mazzaella,*

Cryptopleura, Ulva, and *Nereocystis* (pers. obs.), suggesting that *C. stelleri* may not be

food limited. While the sunflower star *Pycnopodia helianthoides* has been observed

feeding on *C. stelleri,* it has never been reported to prefer *C. stelleri* over more common

prey items such as purple urchins, *S. purpuratus* (Duggins, 1983). There have also been

reports of predation by the sea star *Pisaster ochraceus,* the fish *Scorpaenichthys*

marmoratus, and sea otters. However, none of these predators feed primarily on *C.*

stelleri, indicating that population numbers are not likely limited by predation (Yates,

1989). Therefore, the factors limiting the population size and distribution of *C. stelleri*

are unclear.

This study focused on the distribution of juvenile, small, and adult *C. stelleri*

along the southern Oregon coast in order to better understand the population structure of

this species. The size and abundance of *C. stelleri* individuals was measured in this study

in order to and compare how population size structure differs among sites. Exact

locations of individual *C. stelleri* were monitored to determine whether this species

displayed any sort of seasonal or ontogenetic vertical migration pattern.

Materials and Methods

I. Distribution

In order to determine the local distribution, size frequency, and population sizes

of *Cryptochiton stelleri* along the southern Oregon coast, surveys were conducted at six

sites (Fig. 2.1). The southernmost of the sites surveyed was Cape Blanco, OR
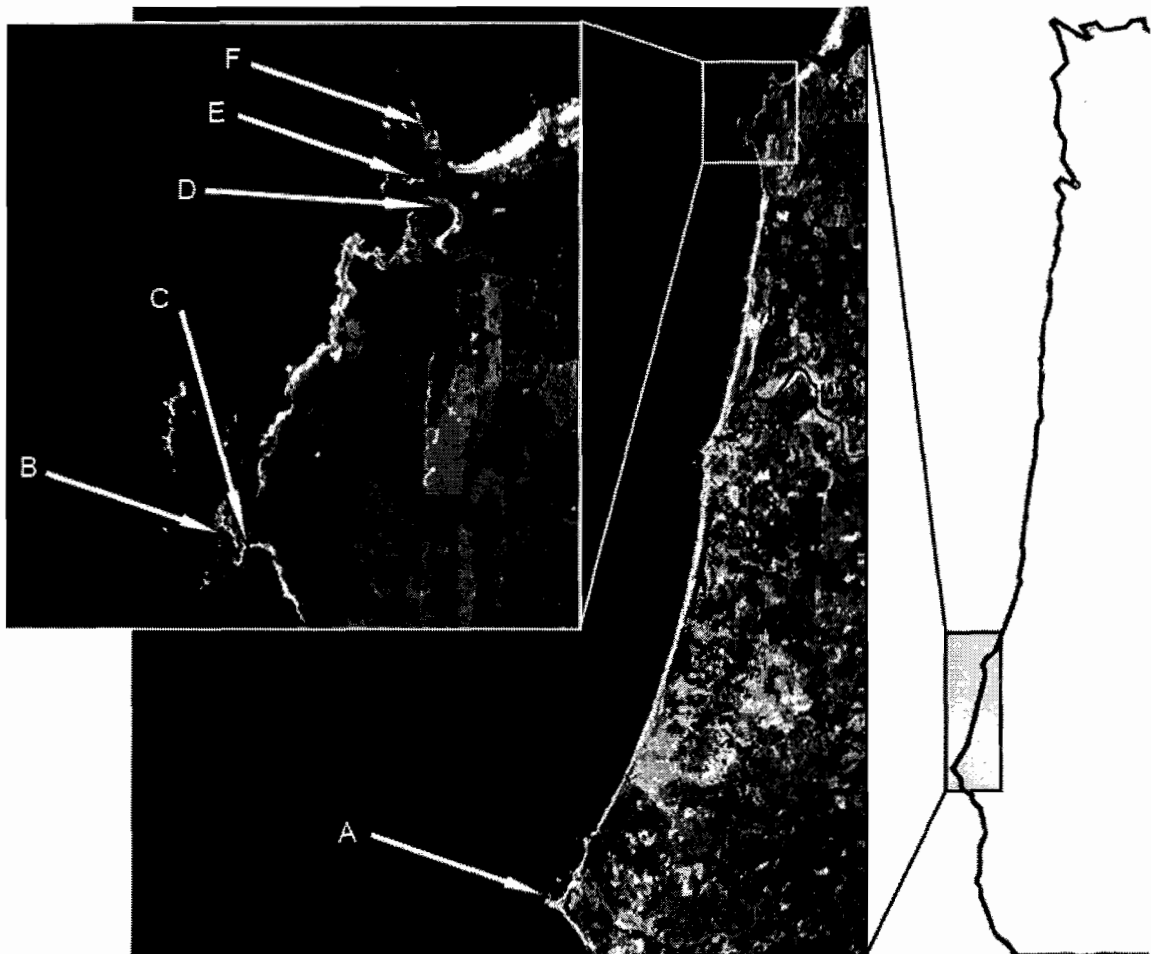
Figure 2.1. Locations of all six sites on the southern Oregon coast: (A) Cape Blanco; (B) Middle Cove; (C) South Cove; (D) Sunset Bay; (E) Qochyax Island; (F) Lighthouse Island.

(42°50.900N, 124°33.410W), a basaltic rocky shore with intertidal areas facing to the northeast, west, and south (Fig. 2.1A). All other sites were located just south of Charleston, Oregon (43°18.191'N, 124°23.198'W). Middle Cove of Cape Arago (Fig. 2.1B) is mostly composed of sandstone boulders and is a relatively protected intertidal area that faces west and has very little foot traffic. South Cove of Cape Arago (Fig. 2.1C) is a similar intertidal to Middle Cove, though it faces south and has more foot traffic. Sunset Bay (Fig. 2.1D) is another protected site with high foot traffic and is a small, west-facing bay with a long flat sandstone intertidal bench interspersed with deep tidal channels. Qochyax Island (Fig. 2.1E) is a small uninhabited island that is a couple hundred meters offshore and is accessible only on a negative low tide. It has an extensive rocky intertidal area with a variety of habitat types and aspects, including both exposed and protected areas and very little foot traffic. Lighthouse Island (Fig. 2.1F) is a long island with sandstone cliffs and is surrounded by rocky intertidal. It is fairly exposed on the south-facing side and moderately protected on the north-facing intertidal and also has low foot traffic.

The intertidal zone at these sites was sampled at low tides. Sampling was done year-round from July 2009 to August 2010, on every tide below -0.3 m, MLLW weather-permitting. *Cryptochiton stelleri* were found via haphazard search because they exist at densities too low to be accurately represented by transect sampling or other traditional sampling methods. Searches were extensive (2-3 days per site) and were conducted by zigzagging up and down through the intertidal within 2 meters of every intertidal location. One hundred meter transects were used initially but could not accurately

document the patchy distribution of *C. stelleri.* Because the goal of this study was to determine distribution over entire sites and not to determine total population size, haphazard search was the most effective method. The exact location of each individual was recorded by triangulating its position using a compass accurate to 0.1 degrees and two known landmarks at each site. This produced coordinates with a maximum error of 1.5 m for the location of each individual. Error was calculated by determining the difference in location resulting from a change of 0.1 degrees (compass accuracy) in angle from the furthest known landmark.

Individual *Cryptochiton stelleri* specimens were tagged at South Cove, Middle Cove, Cape Blanco, and Lighthouse Island in order to detect growth and seasonal movement patterns of individuals. Animals were tagged by inserting zip ties through the edge of the girdle and attaching numbered monel fish tags (National Band and Tag Co.). Zip ties were short (10 cm) and excess tie length cut off after attachment. This method of tagging is similar to that used by Palmer and Frank (1974), who used monofiliment line through the girdle and marked with beads. It is also similar to Yates (1989), who used spaghetti tags, also through the girdle. After marking, *C. stelleri* usually rolled up into a ball but resumed normal movement minutes after being placed back in their original location. Individuals were observed until they reattached to the substratum.

Distribution data obtained via triangulation methods were entered using Google Earth® with overlaid infrared aerial photos of the intertidal zone taken by the Oregon Department of Fish and Wildlife (1:7200 scale). These data were then transferred into ArcMap© software and converted into GIS layers. To determine the amount of clumping

at different sites, data were analyzed in ArcMap® using the spatial analysis tool 'nearest neighbor.' This tool calculated the expected mean distances between individuals if their distribution was random and compared this to the observed mean distances between individuals. Getis-Ord General G, another spatial analysis tool, was used to determine if individuals were clustered by size at each intertidal site. This GIS software was also used to analyze variation in distributions at all sites between each sampling date in order to compare tidal and seasonal differences in the distribution of individuals.

To determine whether or not several intertidal predators could consume *C. stelleri*, sea stars *Evasterias troschelii, Pisaster ochraceus,* and *Pycnopodia helianthoides* and crabs *Pugettia producta* and *Cancer productus* were kept together in a 1m x 2m flowing seawater tank for two months with just *C. stelleri* individuals ranging from 10 to 30 cm in length as potential prey items.

II. Age-frequency

The size of each individual surveyed was measured by using displacement volume in seawater. Volume was determined to be the most reliable of all size measurements, as it had the least variability (< 1%) when repeatedly measuring the same individual. In addition, volume was significantly correlated with more common measures such as weight and length, so it was a good indicator of *C. stelleri* size but with less variability and uncertainty than other methods. Length was used by Yates (1989), but individuals can vary their length significantly. Air weight has also been used to measure *C. stelleri* size (Palmer and Frank 1974), but water content can also vary greatly

depending on if the chiton was submerged in water or exposed to air when collected. Volume in the present study was measured to the nearest 5 mL using water displacement in a 4-liter graduated plastic container.

Volume was converted to age based on data derived from growth lines in the shell plates of *C. stelleri* (Lord, Chapter 4). A growth function relating age to volume was calculated using IDBS XLfit 5® and was used to estimate age for all surveyed gumboots. Age-frequency histograms were then created for each site and each season and peaks (possible cohorts) in these histograms were compared between sites and sampling dates. Each peak (cohort) in these data were identified using Peakfit® software and major peaks were defined as those at least two times the average number of individuals of each age for each site. Major peaks were then compared between sites in order to determine how uniform recruitment and survival were in *C. stelleri*.

Results

I. Distribution

Field surveys showed a patchy distribution of *C. stelleri* at all six surveyed sites (Fig. 2.2). Average nearest neighbor distance showed significant ($p < 0.05$) clumping at Cape Blanco, South Cove, Middle Cove, Sunset Bay, and Lighthouse Island. Slightly less clumping was found at Qochyax Island (Fig. 2.2D), but this was likely a result of the small area in which *C. stelleri* was found. Nearest neighbor statistics only included areas where *C. stelleri* was present, so did not take into account large areas where no individuals were found. Qochyax Island had a limited area in which *C. stelleri* was

present, but within this area there was not a significant amount of clumping (p = 0.1). There were no individuals of this species present in areas of very high wave action at any sites, as none were found in the outer areas of Lighthouse Island (Fig. 2.2A), Cape Blanco (Fig. 2.2B), Cape Arago (Fig. 2.2C), Qochyax Island (Fig. 2.2D) or Sunset Bay (Fig 2.2E). Gumboot chitons were found almost exclusively in small coves within sites (Fig 2.2C,E) or in northeast-facing habitats (Fig. 2.2A,B,D).

Populations were also clumped based on size at several of the sites (Fig. 2.2). Getis-Ord G High/Low clustering analysis showed significant (p < 0.05) clustering of large individuals (by volume) at Qochyax Island, Lighthouse Island, South Cove and Cape Blanco. Clustering based on size was not significant at Middle Cove and Sunset Bay. Few individuals of *C. stelleri* were found in areas of high sand scour, evidenced by the lack of individuals near beaches in the interior of Lighthouse Island, South Cove, Sunset Bay and Cape Blanco.

Eighty five of 92 specimens shorter than 15 cm in length were found in (mostly) abandoned pits of urchins (*Strongylocentrotus purpuratus*) at all six sites. The seven not found in pits were juveniles less than 2 cm in length. Three of these were in small holes made by boring clams and near the leafy red alga *Cryptopleura*. The remaining 4 juveniles were on flat surfaces within a bed of *Cryptopleura*, which is their preferred food source (Lord, Chapter 3). All juveniles were found below -0.3 m MLLW. Of the over 300 *Cryptochiton stelleri* specimens that were tagged, only 41 were found six months later due to the propensity of the tags to fall out of the girdle. Many specimens were found with marks where a tag had been previously, though they were soon
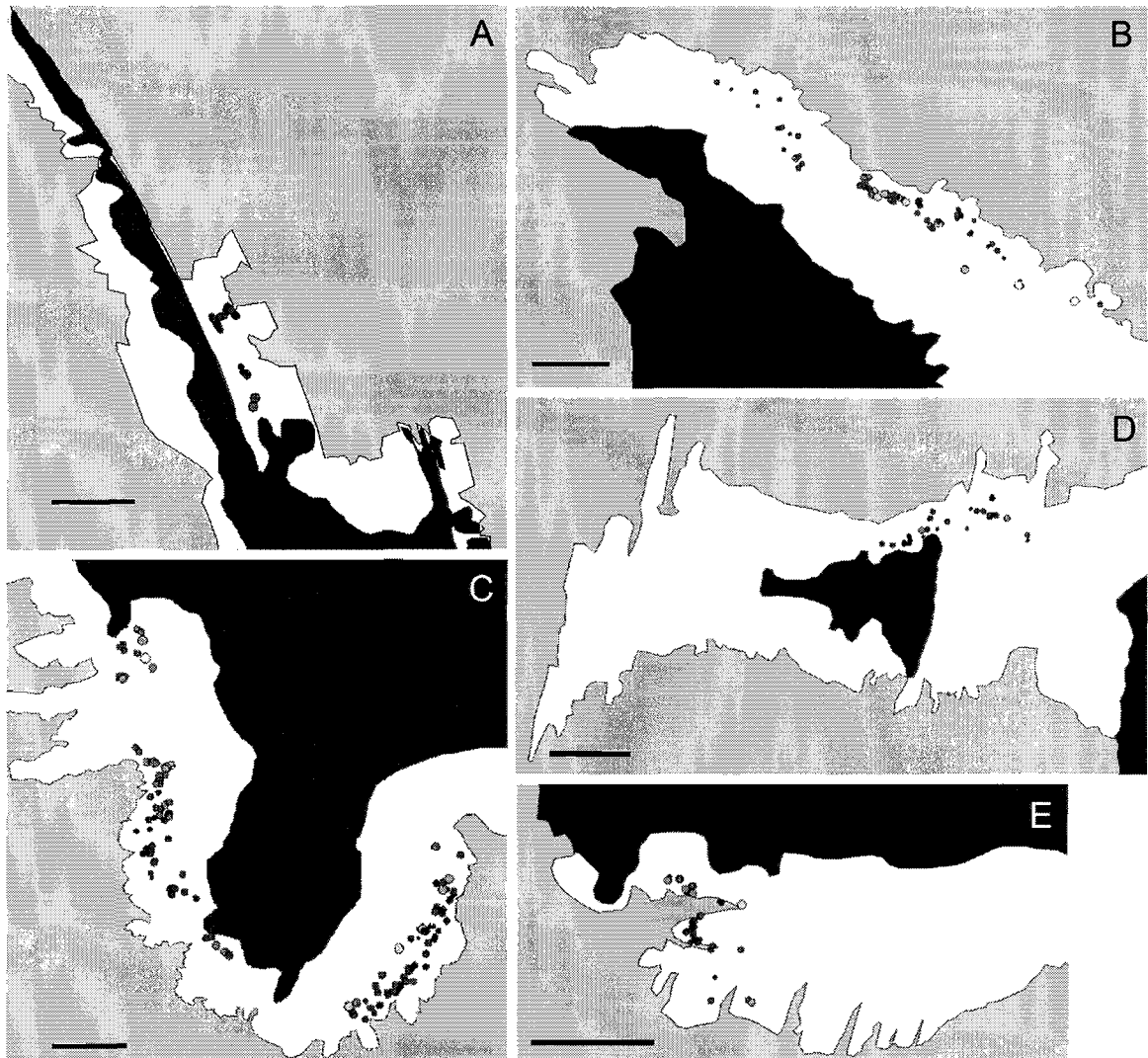
Figure 2.2. Size and distribution of *C. stelleri* at all sites surveyed in May 2010. Size and lightness of circles are relative to the size of the specimens; small dark circles represent small gumboot chitons and large white circles represent the largest gumboot chitons. Light gray fill represents the ocean, white is intertidal, and dark gray is terrestrial. Scale bar = 50 m. (A) Lighthouse Island; (B) Cape Blanco; (C) Middle Cove (on left) and South Cove (on right) of Cape Arago; (D) Qochyax Island; (E) Sunset Bay.

indiscernible because of the rapid healing process of *C. stelleri*. There was not a significant difference between sites in the distance moved between November 2009 tagging and May 2010 recovery, although the range was higher at South and Middle Cove than Sunset Bay. South Cove (n=19) and Middle Cove (n=12) chitons had ranges of approximately 3 to 22 meters traveled, while Sunset Bay (n=9) chitons were between 3 and 12 meters from their initial location.

Distributions did not change noticeably at Middle or South Cove of Cape Arago (Fig. 2.3) or at Sunset Bay (Fig. 2.4) between November 2009 and May 2010. These three sites are shown because they were the only three surveyed during November due to high wave activity. The 'directional distribution' tool in ArcMap® created standard deviation ellipses for each population during each season and these maps indicated that there was no consistent pattern of population movement with season at these site.

In the predation experiment, no *C. stelleri* were eaten by any of the predators over a two month period. All *C. stelleri* remained attached to the bottom and sides of the tank, never falling off or lying upside-down like they do occasionally in the intertidal zone at low tide. This is relevant because in the intertidal *C. stelleri* often uses aerial respiration at low tide, during which they expose their gills and often fall off rocks, thus exposing their muscular foot to potential predators.

II. Age-frequency

All surveyed *Cryptochiton stelleri* specimens were estimated to be between one and 40 years old. These estimates were based on growth curve data (Lord, Chapter 4) for
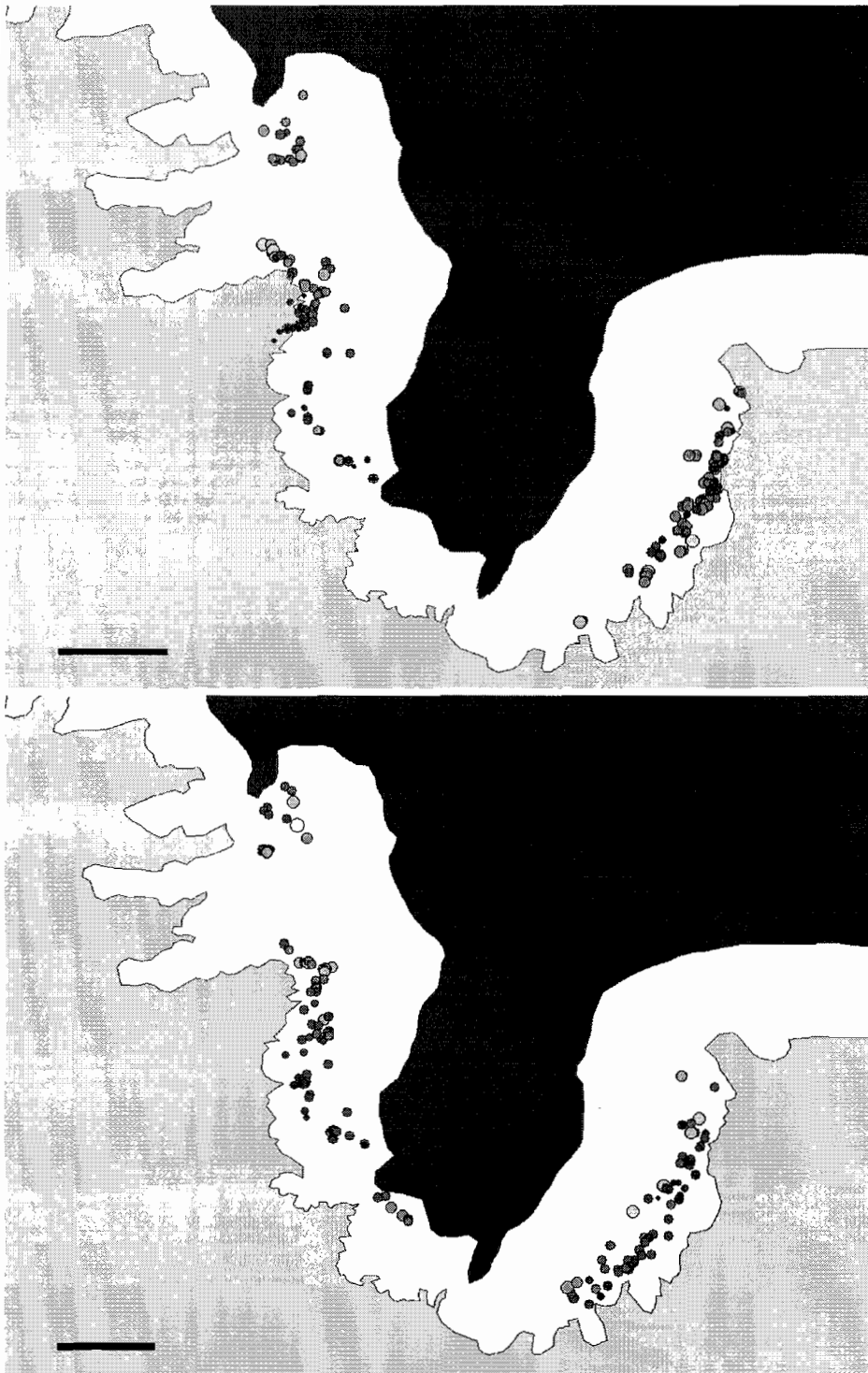
Figure 2.3. Distribution of *C. stelleri* at Middle and South Cove of Cape Arago in (A) November 2009 and (B) May 2010. Distribution did not change noticeably with season. Scale bar = 50 m. Light gray fill represents the ocean, white is intertidal, and dark gray is terrestrial.

Figure 2.4. Distribution of *C. stelleri* at Sunset Bay in (A) November 2009 and (B) May 2010. Like at Cape Arago, distribution did not change noticeably between seasons. Scale bar = 50 m. Light gray fill represents the ocean, white is intertidal, and dark gray is terrestrial.

C. stelleri that show a good regression between age and size. Age-frequency histograms at all sites showed the highest number of individuals at intermediate ages. While close to 100 young (< 15 cm) *C. stelleri* individuals were discovered in all seasons, the cryptic nature of these age classes and their urchin pit habitat makes it very likely that specimens less than 10 years of age are underestimated in these age-frequency histograms. This did not adversely affect peak fitting because relative peaks still appeared at young ages. Major peaks (< 2x average number) were compared between sites and there was no major peak that was present at a specific age at all sites, although a few peaks were shared by multiple sites (Fig. 2.5). Peaks at 22 and 24 years old were present to some extent at all sites except Cape Blanco. Sunset Bay, Qochyax Island and Lighthouse Island shared a major peak at 16 and 20 years (Fig. 2.5A,D,F). Cape Blanco, Middle Cove, and Sunset Bay shared peaks at 30 years (Fig. 2.5B,C,F) but few other peaks were shared between more than two sites. Distance was measured as a straight line between sites and similarity was calculated as the number of shared peaks over the number of total peaks for each pair of sites.

There was a significant correlation between the number of shared peaks and the $\log_{10}$ of distance between sites (Pearson's correlation coefficient, $r^2 = 0.46$, $t = -3.34$, df = 13, $p < 0.01$) (Fig. 2.6). The distances were $\log_{10}$ transformed because all of the sites were relatively close together with the exception of Cape Blanco, which would make a test of correlation impossible. The two sites with the highest percentage (66%) of peaks in common were Sunset Bay and Qochyax Island, which were the closest sites to each other, at 0.37 km (Table 2.1). The second most similar sites (60%) were South Cove and
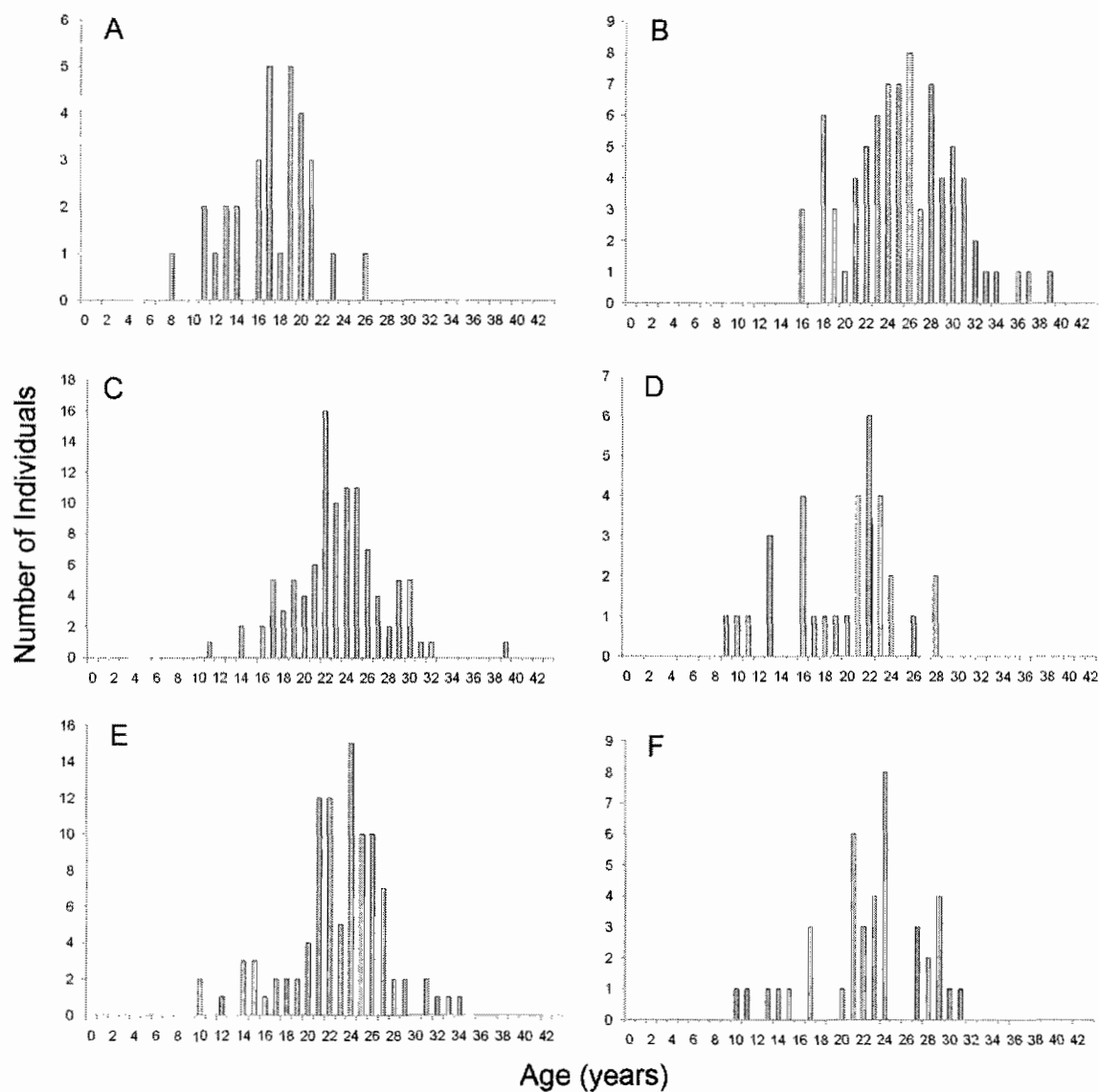
Figure 2.5. Age-frequency histograms for all six sites surveyed in May 2010. No peaks are shared between all sites, although most sites have a peak at around 20-22 years. The lack of young individuals is partially a result of their cryptic nature. (A) Lighthouse Island; (B) Cape Blanco; (C) Middle Cove; (D) Qochyax Island; (E) South Cove; (F) Sunset Bay.
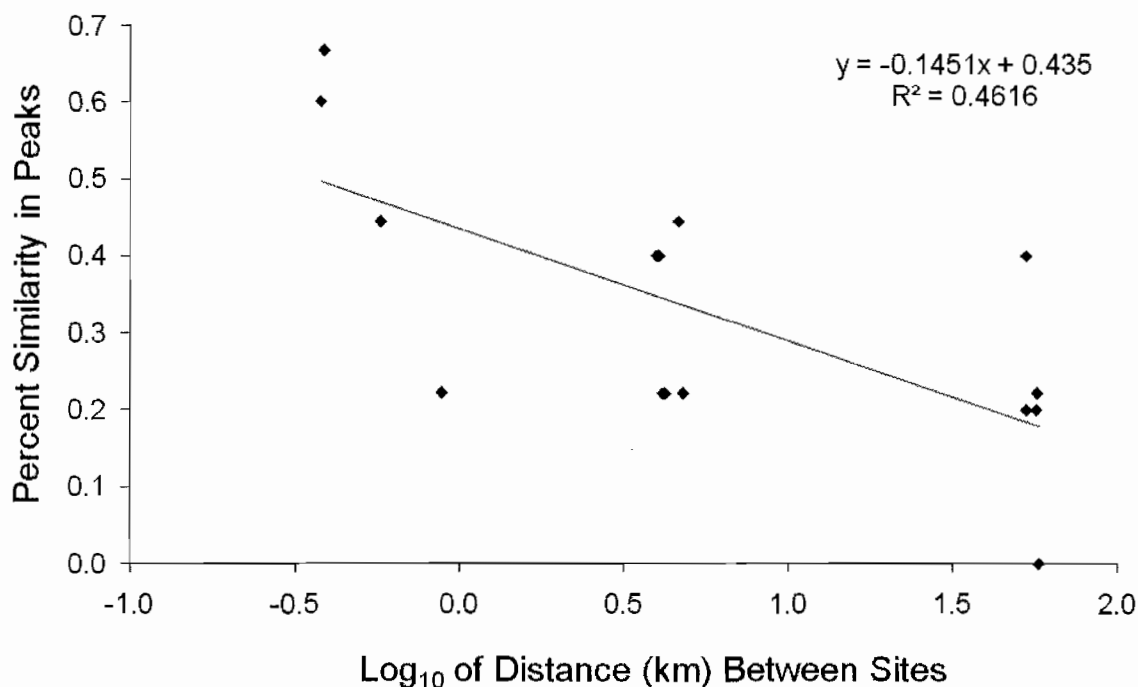
Figure 2.6. Distances ($\log_{10}$ km) and similarity in age-frequency peaks between six different sites (15 pairs of sites). Distances were $\log_{10}$ transformed in order to compare between sites since five sites were relatively clumped (within 10 km) and the sixth site was approximately 55 km south of the others. Correlation coefficient and equation of the best fit line are shown.

Table 2.1. Distances and similarities in age-frequency peaks between six different sites on the southern Oregon coast. There is a significant negative correlation between the distance and similarity between sites. Sites are arranged north to south in both columns and rows, with Lighthouse Island the northernmost site and Cape Blanco the southernmost.

Sites	Lighthouse Island	Qochyax Island	Sunset Bay	Middle Cove	South Cove	Cape Blanco	
Lighthouse		0.58	0.89	4.67	4.83	57.9	Distance (km)
Island	X	0.44	0.22	0.44	0.22	0.00	Similarity (%)
Qochyax			0.37	4.19	4.25	57.3	Distance (km)
Island		X	0.66	0.22	0.22	0.22	Similarity (%)
Sunset				4.00	4.07	57.06	Distance (km)
Bay			X	0.40	0.40	0.20	Similarity (%)
Middle					0.38	53.2	Distance (km)
Cove				X	0.60	0.20	Similarity (%)
South						53.1	Distance (km)
Cove					X	0.40	Similarity (%)

Middle Cove of Cape Arago, which were 0.38 km apart. The northern-most site, Lighthouse Island, did not share any peaks with the southern-most site, Cape Blanco. Cape Blanco only shared an average of 21% of its age-frequency peaks with other sites, all of which were at least 50 km north of Cape Blanco. The closest site to the north of Cape Blanco was South Cove, which was the most similar site to Cape Blanco in terms of age-frequency peaks, at 40% (Fig. 2.6, Table 2.1).

No correlation ($p > 0.4$) was found between upwelling start date or strength and age-frequency histogram peaks or gaps. There was also no correlation ($p > 0.4$) between El Nino years and the peaks or gaps in age-frequency histograms at any of the sites.

Discussion

The patchy distribution of *Cryptochiton stelleri* at each of six sites (Fig. 2.2) raises several questions about the life history and ecological impact of this species. It is not surprising that *C. stelleri* specimens were not found in areas of high wave action or high sand scour because these types of habitat generally do not have the types of thin bladed seaweeds upon which *C. stelleri* feeds. In addition, *C. stelleri* does not clamp to the substratum with the same force and tenacity that *Katharina tunicata* or other wave-tolerant chitons do, and is often found unattached to the substrate at low tide (pers. obs.). Therefore, it is likely that both physical and dietary limitations result in the absence of *C. stelleri* in areas of high wave action or sand scour.

However, the clumped distribution of *C. stelleri* found by this study was present at sites where this species is abundant (Fig. 2.2), so the clumped distribution is not likely

due to sand scour or extreme wave action. Sand scour generally occurred at the edges of the surveyed sites and wave action is similar within the protected sites, so these factors are not likely to influence distribution within these sites. A clumped distribution is not unusual for chitons (Grayson and Chapman 2004, Connelly and Turner 2009). During spring, summer and fall, leafy red algae such as *Cryptopleura* and *Mazzaella splendens* and greens such as *Ulva lactuca* are abundant throughout all sites surveyed. Therefore, the clumped distribution of *C. stelleri* is not due to food distribution. Distribution patterns are also unlikely to be driven directly by predation, since *C. stelleri* was not eaten by any predator. Sea stars *Evasterias troschelii, Pisaster ochraceus,* and *Pycnopodia helianthoides* and crabs *Pugettia producta* and *Cancer productus* did not feed on *C. stelleri* in this study, though field observations have been made of sea stars consuming *C. stelleri*. It is likely that sea stars and crabs can consume *C. stelleri* if it becomes detached from the rocks, exposing the muscular foot.

It seems more likely that *C. stelleri* is limited to protected areas even within sites in order to avoid being dislodged from the rocks. Dislodgement could result in mortality from wave action or increased predation risk. At all sites, *C. stelleri* was most common in small coves within each site. This was especially evident at Lighthouse Island (Fig. 2.2A), Middle Cove (Fig. 2.2E), and Sunset Bay (Fig. 2.2C). These areas could be acting as larval traps where slower, swirling water may allow larvae to settle out of the water column. Settlement and recruitment in small coves may also lower mortality rates of new recruits and juveniles which are undoubtedly susceptible to wave bashing.

Because *C. stelleri* under 15 cm in length were found almost exclusively in abandoned sea urchin pits, it is also possible that the distribution of small *C. stelleri* is driven by the presence of these pits. With smaller individuals limited to these cryptic habitats and large individuals able to move at least 20 meters, this could explain the clumping of large individuals in areas where small specimens are not present. Encrusting coralline algae is also common in urchin beds because of macroalgal consumption by the urchins. The cue for settlement and metamorphosis by *C. stelleri* is encrusting coralline algae (Lord, Chapter 3), which is ubiquitous throughout all of the sites. Therefore, this is not a limiting factor in the settlement or recruitment of *C. stelleri*, but urchin pits covered in encrusting coralline algae could serve as a good spot for *C. stelleri* to settle and survive. If urchin pits act as a nursery for young individuals, this would explain the pattern of large *C. stelleri* being clumped, since areas without urchin pits are only going to be occupied by large individuals that have moved there later in life. Given that smaller herbivores such as *Katharina tunicata* (Dethier and Duggins, 1985) and *Strongylocentrotus purpuratus* (Leighton, 1966; Estes and Duggins, 1995) can have great ecological impact, high densities of *C. stelleri* could have a large effect on seaweed abundance. Because *C. stelleri* food intake scales linearly with body weight and volume (Lord, Chapter 5), grazing impacts in areas with high densities of large individuals could be especially significant.

While *C. stelleri* will move out of the urchin pits over the course of their lives, they do not display seasonal variation in distribution (Figs. 2.3, 2.4) and do not move up or down in the intertidal with age. Snow (1951) mentioned that *C. stelleri* move down in

the intertidal during the winter and then up during the spring. This has been described in a variety of other species, including crabs (Hunter and Naylor, 1993) and several species of limpets (Branch, 1975). However, year-round surveys in the present study did not reflect this pattern at any of these southern Oregon sites. There were also no vertical patterns in size or age of *C. stelleri* like those shown in *Chlorostoma funebralis* (Paine, 1969) and *Monodonta labio* (Takada, 1996). The lack of vertical migration with season by *C. stelleri* may be due to its ability to go months without eating (Yates, 1989) or to the fact that it already inhabits fairly protected habitats. By living in protected areas, there may be no need for *C. stelleri* to move up or down in the intertidal zone to avoid the intense wave action from winter storms in Oregon.

More about larval settlement patterns can be ascertained from age-frequency data (Fig. 2.5) for each site and similarity in cohort peaks within age-frequency distributions between sites (Table 2.1). Peaks in the age-frequency histograms represent large cohorts. The success of these large cohorts could be due to high recruitment or to low mortality at some life stage. It is unlikely that predation on adults would vary greatly between cohorts, so the most likely causes of the variation between cohort sizes are differences in settlement or juvenile survival. While predation experiments have not been done with juvenile *C. stelleri*, it is likely that crabs and sea stars or even fish could easily detach and consume these small individuals with tiny plates. Therefore, a good recruitment year for any of these predators could cause high juvenile mortality for *C. stelleri*. However, population levels of *C. stelleri* are not very high at any site compared to other species of chitons, limpets, and other mollusks. It is unlikely that any life stage of *C. stelleri* would

be a primary food source for a predator, especially given the small protective holes or pits that small individuals often inhabit.

Therefore, the most likely cause of variations in cohort size is larval supply and settlement success. This species of chiton spawns annually (Tucker and Giese, 1962; Lord, Chapter 3) and has lecithotrophic larvae. Differences in number of planktonic predators could have an impact, since larvae can remain competent for up to two months even though they can settle and metamorphose in as few as five days after spawning (Lord, Chapter 3). Oceanographic conditions such as the directions of currents could affect settlement as well, as could wave action or other small-scale near-shore oceanography conditions. For example, populations may have successful self-recruitment when local barriers form and limit the movement of planktonic larvae out of a cove or bay. At several sites along the southern Oregon coast, upwelling can cause these barriers to form at the mouths of coves such as Sunset Bay, potentially trapping larvae inside and enhancing local recruitment (Shanks and McCullogh, 2003).

Shared peaks in cohort size between sites could be a result of either large-scale dispersal of larvae to multiple sites in the same period or local oceanographic conditions that enable successful settlement at multiple sites. No peaks were shared between all sites and very few peaks were shared by more than three of the six sites, suggesting that successful cohorts were not driven by large-scale oceanography because if that were the case then all sites would likely share peaks in the age-frequency histograms. There was also no correlation between upwelling strength or start date and the age-frequency histogram peaks or gaps. This suggests that local conditions are more likely to affect the

success of a recruitment class or cohort. The significant negative correlation between the number of shared cohort peaks and distance between sites further supports this conclusion (Fig. 2.6.). The high similarity in peaks between the closest sites (Middle Cove + South Cove, Sunset Bay + Qochyax Island) indicates that these sites either share larvae or have similar near-shore local oceanographic patterns (Table 2.1). There appears to be low population connectivity between sites, given the potentially short larval period of this species and the lack of shared peaks in age-frequency histograms, although genetic work is necessary to confirm this.

Limited larval supply, settlement, or high post-settlement mortality could also partially explain the relative scarcity of small *C. stelleri* reported by multiple studies (Tucker and Giese, 1962; MacGinitie and MacGinitie, 1968; Palmer and Frank, 1974; Yates, 1989). However, these studies report a lack of individuals < 15 cm in length, or < 13 years old (Lord, Chapter 4). A peak in the age-frequency distribution indicating a successful cohort occurs on average every 5 or 6 years at all my sites studied. It is highly unlikely that none of the sites in these studies had a successful cohort in the previous 13 years, so sporadic recruitment may only play a small role in the lack of these size or age classes. The present study found over 90 individuals in this 'rare' size range, with several at every site, and almost all of them were in sea urchin pits or other holes in the rocks. In areas without sea urchin pits, young *C. stelleri* presumably occupy crevices or live under rocks in the low intertidal zone. It is very likely that the use of these cryptic habitats by young individuals is the reason why they are not found often. Juvenile *C. stelleri* are yellow unlike the dark red adults, which may also cause confusion.

The surveys in this study show that the different life stages of *C. stelleri* prefer different microhabitats, with young (< 13 years) individuals occurring in cryptic habitats. They may choose these habitats to avoid predation or to avoid wave action, but their preference for these habitats coupled with the relatively low mobility of adults may enhance the clumped distribution of this species. Spatial and temporal differences in abundance and distribution are most likely a result of differential settlement and juvenile survival that are controlled by near-shore oceanography or other local factors. The resulting patchy distribution of *C. stelleri* may result in locally high algal consumption in areas of high density of this species within sites.

Bridge

Chapter II determined the distribution and population structure of *Cryptochiton stelleri* at six sites along the southern Oregon coast. In this chapter I attempted to explain the causes for some of the observed recruitment patterns seen at the different sites, however, to fully understand the settlement and recruitment patterns reflected in the distribution of *C. stelleri* the larval development process and metamorphosis cues had to be determined. The only previous study on *C. stelleri* larval development (Okuda, 1947) described unusual development for a chiton, so chapter III focused on accurately describing the larval development of this species. In addition, in this study I tried to determine the settlement and metamorphosis cues and juvenile growth rate of *C. stelleri*.

CHAPTER III

LARVAL DEVELOPMENT, METAMORPHOSIS, AND EARLY GROWTH OF THE

GUMBOOT CHITON *CRYPTOCHITON STELLERI*

Introduction

Cryptochiton stelleri is the largest invertebrate herbivore along the western coast

of North America, and, at up to 36 cm long, it is the largest chiton species in the world.

Its range stretches from central California to Alaska and westward to northern Japan.

Their habitat is from the mid-intertidal zone down to a depth of 60 m. Despite the

abundance of this species, small individuals (smaller than 15 cm long) are rarely found

(Palmer and Frank, 1974; Yates, 1989) and juveniles (Heath, 1897) and larvae (Okuda,

1947) have been described in only one publication. Even though larval development and

metamorphosis have been described for several species of chitons (Cowden, 1961;

Thorpe, 1962; Barnes and Gonor, 1973; Watanabe and Cox, 1975; Kniprath, 1980;

Rumrill and Cameron, 1983; Voronozhskaya, 2002), the life cycle of *C. stelleri* is largely

unknown.

The timing of spawning in *Cryptochiton stelleri* has been described in several

papers, but spawning times differ between publications, even at the same location (Heath,

1905a; Okuda, 1947; Tucker and Giese, 1962; Lawrence and Lawrence, 1965; Palmer

and Frank, 1974; Yates, 1989). During spawning, release of eggs by females triggers the

release of sperm by males (Tucker and Giese, 1962). Eggs are green and are released in a loosely connected gelatinous mass (Yates, 1989). Sperm are released freely and are activated (become mobile) when they contact seawater.

While the development of chiton species such as *Tonicella lineata* and *Mopalia muscosa* and others have been well documented (Barnes and Gonor, 1973; Watanabe and Cox, 1975), the only description of *Cryptochiton stelleri* development is by Okuda (1947). However, based on major differences between his paper and other literature with regard to egg color and spawning behavior in *C. stelleri*, Okuda may have been working with a different species. No photographs have been published documenting the development of *C. stelleri*, and the only illustrations are by Okuda and contain several inconsistencies. The present study seeks to accurately describe the spawning, larval development and metamorphosis of *C. stelleri*.

Materials and Methods

Adult specimens of *Cryptochiton stelleri* were collected from the rocky intertidal zone at South Cove, Cape Arago, Oregon (43°18.191'N, 124°23.198'W) on April 11, 2009. The low tide on that day was -0.21 m (actual) relative to MLLW, the sky was overcast, air temperature was 8°C and sea surface temperature was 10.1°C. While conducting intertidal surveys, four chitons were observed with released eggs near the paired gonopores in the pallial groove. These individuals were collected because they were the only females that appeared to have just-released eggs. Adults were brought to

the laboratory and eggs were isolated in culture dishes filled with 45 μm filtered seawater (not autoclaved). After the eggs were photographed under a compound light microscope, they were fertilized with sperm from a male that had released sperm in a running-seawater table that morning. Cultures were changed via reverse filtration with 45 μm Nytex mesh and then refilled with 0.45 μm filtered seawater every day for the first week and then every other day thereafter.

Cultures of *C. stelleri* were maintained at 11°C (± 1°C), roughly the ambient Oregon seawater temperature and kept in natural light, so were exposed to the same light timing as they would have been in the field. Photographs of development were taken regularly with a Sony 3CCD ExwaveHAD© microscope camera on a DIC compound microscope and observations were made throughout development.

Many species of chitons have lecithotrophic larvae that metamorphose and develop plates approximately one week after fertilization (Watanabe and Cox, 1975). The *C. stelleri* larvae in the present study did not change in size, shape, or behavior significantly after week one post-fertilization. It was highly likely that the larvae were competent, based on both morphology and timing. Chiton species including *Mopalia lignosa, Mopalia muscosa, Mopalia ciliata, Katharina tunicata,* and *Tonicella lineata* all are competent by eight days after fertilization, and the *C. stelleri* larvae from the present study were at 13 days post-fertilization (Thorpe, 1962; Barnes and Gonor, 1973; Watanabe and Cox, 1975; Rumrill and Cameron, 1983). In addition, *M. lignosa, M. muscosa* and *T. lineata* were competent after eyes and the dorsal plate field had formed, both which had already occurred in the *C. stelleri* larvae (Barnes and Gonor, 1973;

Watanabe and Cox, 1975). These observations suggest that a metamorphosis cue might be needed before they would complete development.

In an attempt to induce settlement and metamorphosis, beginning two weeks after fertilization several potential metamorphic cues were introduced into the culture dishes. One centimeter square pieces of the green alga *Ulva* and red alga *Mazzaella*, the food of adult *C. stelleri*, were placed in culture dishes with the larvae. Since the chemical gamma-amino butyric acid (GABA) from coralline algae has been shown to induce settlement in the chitons *Katharina tunicata* (Rumrill and Cameron, 1983) and *Tonicella lineata* (Barnes and Gonor, 1973), both shavings of and rocks covered with the encrusting coralline algae (likely multiple genera) were added. The phytoplankton species that are commonly used to feed larvae, *Rhodomonas lens* (Division Cryptophyta), *Dunaliella tertiolecta* (Division Chlorophyta), and *Isochrysis galbana* (Division Haptophyta), were also added from lab cultures to larval culture dishes as potential metamorphosis cues. This was done in case different kinds of phytoplankton were a settlement cue.

Presence of adults is another cue that has been shown to induce settlement and metamorphosis in some species (Bayne, 1969; Burke, 1984; Coon et al., 1985). Adult specimens of *C. stelleri* were kept in 3 L filtered seawater for an hour, after which five mL of this water was added to larval culture dishes as another potential cue. Elevated temperature has been shown to induce metamorphosis in some species of mollusks (Boettcher, 2005); the temperature of the cultures was raised to 25° C. These cues were added sequentially to five 11.4 cm wide glass culture dishes, with each dish containing

approximately 15 larvae. After two days, the water was changed and another potential

cue was tested in the order listed in Table 3.1. This wide variety of cues, including some

that have not been shown to induce metamorphosis or settlement, were tested because

settlement cues are known for very few species of chiton and are not known for *C.*

stelleri (Barnes and Gonor, 1973).

Table 3.1. List of potential metamorphosis cues tested. Treatments were done
consecutively on the same 5 culture dishes (approx. 15 larvae in each dish) and are listed
in the order in which they were tested.

Treatment (potential cue)	Duration (hours)	Replication (# dishes)	Sources
1 cm^2 pieces of alga *Mazzaella splendens*	48	5	Adult food (Yates, 1989)
1 cm^2 pieces of alga *Ulva lactuca*	48	5	Adult food (Yates, 1989)
Rocks covered in encrusting corallines *Lithothamnion* and *Clathromorphum*	48	5	Barnes and Gonor, 1973
Shavings of encrusting corallines *Lithothamnion* and *Clathromorphum*	48	5	Barnes and Gonor, 1973
Increased phytoplankton concentrations (*Rhodomonas, Dunaliella, Isochrysis* sp.)	48	5	
Water from tank with adult *C. stelleri*	48	5	Burke, 1984
Temperature increased to 25 °C	48	5	Boettcher, 2005

Cryptochiton stelleri collected at the South Cove of Cape Arago were kept in

flowing seawater tanks at the Oregon Institute of Marine Biology and spawned again the

following year on May 6, 2010. The eggs were fertilized with sperm from males that also

spawned in the lab. Larvae were again raised in 11.4 cm culture dishes in flowing

seawater at approximately 12 °C and were kept in 45 μm filtered seawater. After the

larvae hatched out of the hulls, four treatments were set up, with 4 culture dishes of 50

larvae each for each treatment. One was a control, with nothing added to the filtered

seawater. Treatment two had a small rock covered with encrusting coralline algae in

each dish. Treatment three had encrusting coralline algae extract added; this was extracted by scraping the coralline algae off rocks, grinding it down with a mortar and pestle, adding filtered seawater, and then centrifuging the mixture in 15 mL vials to extract the supernatant. Treatment four had *Cryptopleura* extract, a delicate leafy red alga that juvenile *C. stelleri* eat, prepared with the same procedure as coralline algae extract.

On April 12, 2009, a horizontal plankton tow was made near the mouth of Coos Bay, Oregon, in order to search for *C. stelleri* eggs and larvae. The tow was approximately 100 m in length and the net mesh was 200 μm. Searches in the intertidal zone for juveniles were performed along the Oregon coast at Sunset Bay, Cape Arago, and Cape Blanco throughout the spring and summer. Juveniles collected at Cape Blanco on July 22, 2009, were raised in a 20 cm x 20 cm container (15 cm high, mesh sides) in a flowing seawater table at the Oregon Institute of Marine Biology. The length and weight of the juveniles were measured once a week through March 2010 and time-lapse photos were taken every 5 minutes of the juveniles during August 2009 in order to determine movement patterns in presence of other juveniles.

Results

The four female *C. stelleri* from which eggs were collected in April 2009 were not spawning at the time of capture, so egg release was not observed. The green eggs were stuck in the mucous covering the gills, towards the posterior end of the pallial

groove. A male was observed releasing sperm in a flowing seawater table on the same morning that the eggs were discovered. Both the eggs and sperm sank in seawater. The male released sperm from the raised posterior end of his body all day, stopped during the night, and then released again the following day; this individual released sperm for about 30 hours. Seven males in May 2010 released sperm in the same manner. Some females raised their posterior ends while spawning in May 2010, while others lay entirely upside down to release or showed no visible difference in behavior while spawning.

The April 12, 2009, near-surface plankton tow near the mouth of Coos Bay, Oregon, yielded four unfertilized chiton eggs that were the same color and diameter as those of *C. stelleri*. They could be identified because no other chiton with an egg near 300 μm has a hull with a diameter of 600 μm. Due to high wind and waves, no plankton tows were conducted in the ocean to search for more eggs and larvae. There are no known intertidal populations of *C. stelleri* within two miles of the site of the plankton tow, though subtidal populations may exist.

Unfertilized ova of *Cryptochiton stelleri* averaged 301 μm in diameter (SD=3.16, n=15) with a hull diameter of approximately 600 μm (SD=18.1, n=15). The eggs were extremely yolky, and the hull further obstructed a clear view of the embryos. Fertilization was observed shortly after gametes were mixed together in culture (Fig. 3.1A). The first holoblastic (total division) cleavage occurred 4 h, 40 min post-fertilization, and subsequent divisions occurred approximately every 40 min (Table 3.2).
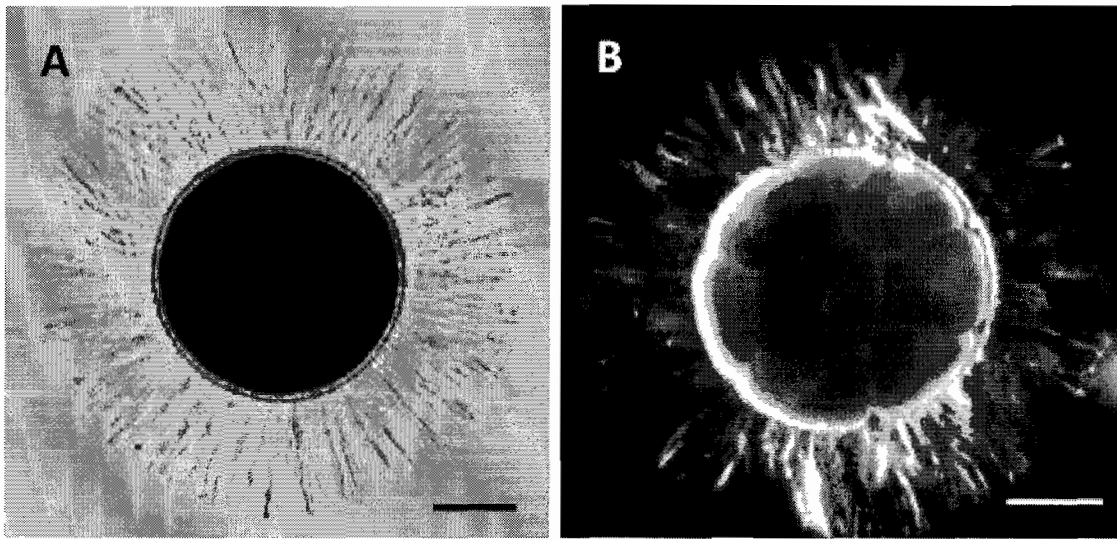
Figure 3.1. *Cryptochiton stelleri* early development: (A) fertilized egg with surrounding hull. (B) 16 cell stage with spiral cleavage evident. Scale bar = 100 μm.

Table 3.2. Developmental timetable for *Cryptochiton stelleri*, with times given for all notable stages of early development. Eggs were collected from the South Cove of Cape Arago and gametes were mixed on April 11, 2009.

TIME POST FERTILIZATION	STAGE
0	Gametes mixed
< 1 minute	Fertilization envelope forms
4 hours, 40 minutes	First cleavage: 2 cell stage
5 hours, 20 minutes	Second cleavage: 4 cell stage
5 hours, 55 minutes	Third cleavage: 8 cell stage
6 hours, 40 minutes	Fourth cleavage: 16 cell stage
11 hours, 10 minutes	Fifth cleavage: 32 cell stage
17 hours, 10 minutes	Blastula
26 hours, 55 minutes	Cilial cells form, 4 patches of cilia
46 hours (≈2 days)	Hatching from hull, become pelagic
70 hours (≈3 days)	Prototroch formed from ciliary patches
90 hours (≈4 days)	Elongation of post-trochal region, eyes form
118 hours (≈5 days)	Settle to bottom, bumps on dorsal side appear (plate precursors)
5 days	Metamorphosis; loss of prototroch and apical tuft, beginning of plate calcification

By 27 h post-fertilization, four distinct patches of cells developed cilia. The eggs remained on the bottom of the dishes until hatching. At 46 h, the early trochophore hatched and was characterized by an apical tuft and prototroch, which propelled the bright green larvae rapidly around the culture dish (Fig. 3.2). A large amount of yolk remained and there was no indication of plate formation or any bumps that could be precursors of plate formation (Fig. 3.2).

Over the next two days the post-trochal region elongated, a pair of red larval eyes appeared behind the prototroch, and dorso-ventral flattening occurred as the foot developed (Fig. 3.3A). At about five days after fertilization, the larvae developed seven dorsal bumps and settled to the bottom of the culture dishes where the larvae began creeping (Fig. 3.3B). Over the next five weeks, these bumps became more defined and dark dorsal spicules formed around the edge of the girdle; however, loss of the prototroch and plate formation did not occur, suggesting that the larvae were awaiting some cue to undergo metamorphosis. The addition of different kinds of seaweeds, high phytoplankton concentrations, water containing the scent of conspecific adults, and warm water temperatures all failed to induce metamorphosis. The larvae died in culture approximately 8 weeks after hatching, having failed to metamorphose.

The embryos in May 2010 developed on a similar timeline, beginning to hatch around two days after fertilization. The trochophores that were in the coralline algae extract and coralline algae-covered rock treatments began metamorphosing three days after hatching (~5 days post-fertilization). Larvae were competent to metamorphose after the post-trochal region had elongated, seven dorsal bumps had formed, and the larvae
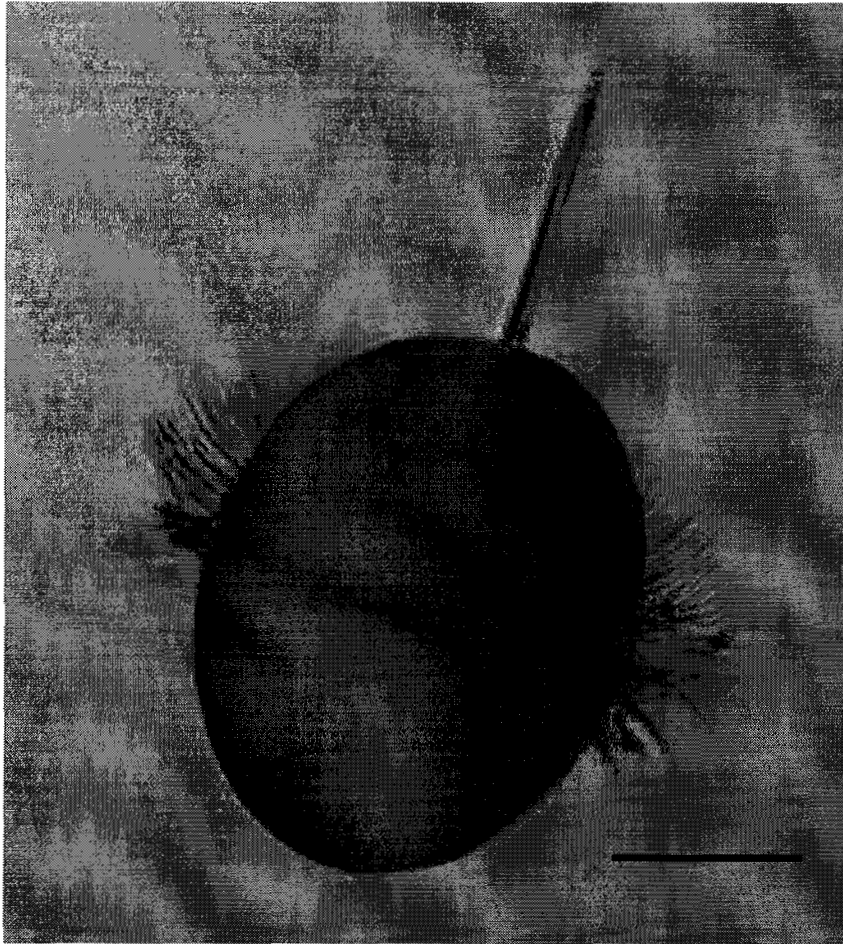
Figure 3.2. Two-day old trochophore larvae, just after hatching. Note the lack of dorsal plates or bumps that are the precursors to plate formation. There is no elongation of the post-trochal region, and the eyes and foot have yet to develop. Scale bar = 100 μm.
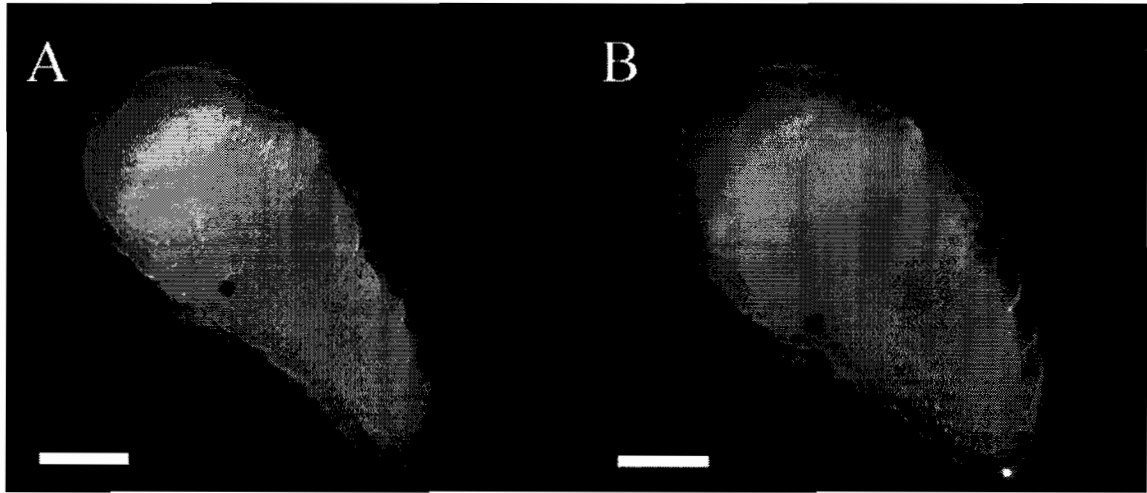
Figure 3.3. Photographs of late trochophores of *Cryptochiton stelleri*. Dorsal side is facing the upper right corner of the photo. (A) Elongation of post-trochal region is visible as well as some dorso-ventral flattening. Foot and seven plate precursors are evident underneath the body surface, and yolk is still visible. (B) The seven bumps that are plate precursors are visible on the outer surface of the larval body as well. As in (A), the eyes and prototroch are present. Scale bar = 100 μm.

spent most of their time on the bottom of the dishes (Fig. 3.4). In the control and

Cryptopleura-extract treatments, larvae stayed in this stage for over two months, until

they were induced to metamorphose with encrusting coralline algae extract.

Metamorphosis consisted of a loss of the prototroch and apical tuft and the beginning of

the formation of seven shell plates. The shell plates begin as thin lines (Fig. 3.5A) and

slowly expanded until they covered the body of the juvenile. Post-metamorphosis, the

larvae were observed feeding on diatoms and cyanobacteria that were present on the

bottom of the culture dishes. Fecal pellets were discovered, some composed entirely of

cyanobacteria and others containing largely diatoms with silica skeletons that were not

broken down by the addition of bleach. Grazing trails were formed on the bottoms of the dishes but did not show any pattern and crossed repeatedly over other trails.

Four juvenile *C. stelleri* were discovered on the red alga *Cryptopleura* at Cape Blanco, Oregon, on July 22, 2009. They measured between 7.6 and 12.6 mm long and, unlike the adults, their dorsal plates were still exposed (Fig. 3.6). Juveniles were yellow with tufts of red spicules partially covering the girdle, giving them an orange appearance. The mouth, foot, and all other anatomical features appeared to be fully developed and the juveniles fed on *Cryptopleura*. Feeding was captured on time-lapse video and the red alga was visible in the gut through the juvenile foot.

Via time-lapse photography, movement patterns were observed. Juvenile *C. stelleri* tend to move more at night (3.60 mm/h) than during the day (1.9 mm/h) but this difference was not significant (ANOVA, df = 4, F = 2.42, p = 0.13) due to the small sample size and high variance. In January 2010, six months after the juveniles were captured and presumably nine months after they metamorphosed, the juvenile *C. stelleri* began to feed on *Ulva lactuca* as well as the *Cryptopleura* sp., which they had been feeding on since capture. By one year, juveniles could feed on *Mazzaella splendens,* a common adult food source. After July 2009, juveniles grew an average of 1.96 mm or 0.14 g per month in captivity and were approximately 30 mm long by March 2010 (Fig. 3.7). This growth rate appears to be similar to that in the field; three additional juveniles collected in the field were in the same size range as those kept in the lab: one was found on Nov. 11, 2009, at Middle Cove of Cape Arago (13 mm), another on Dec. 5, 2009, at Cape Blanco (15 mm), and the third on Feb. 3, 2010, at Cape Blanco (19 mm).
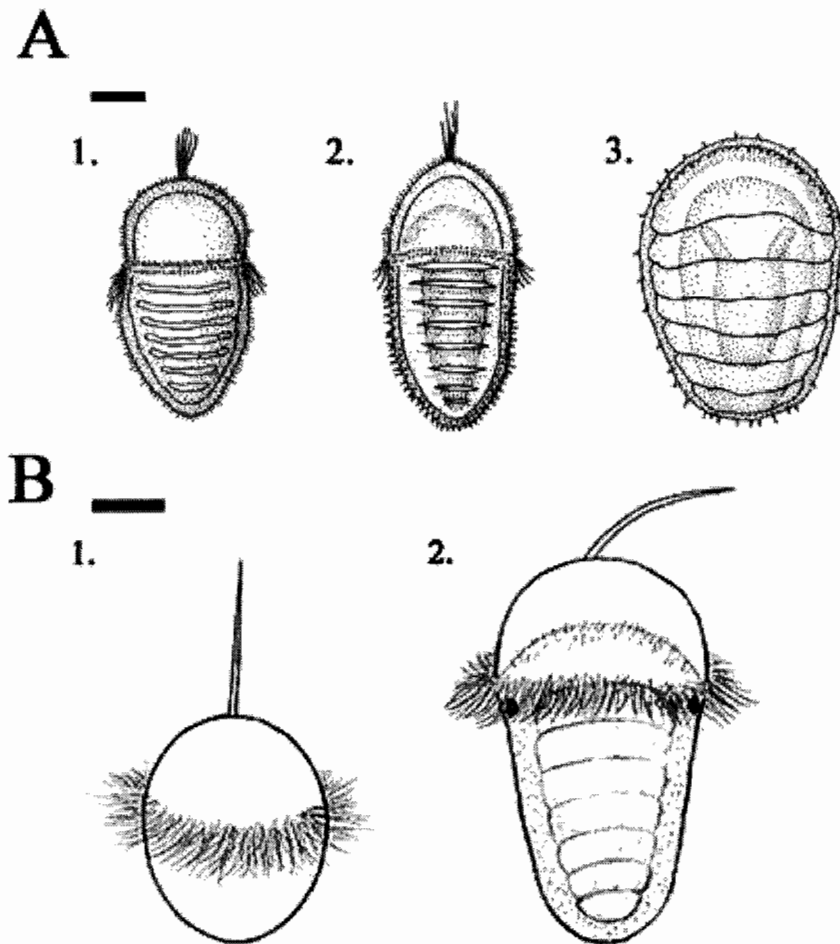
Figure 3.4. Contrasting descriptions of *C. stelleri* development: (A) Different stages of *C. stelleri* development (modified from Okuda, 1947). Scale bar = 100 µm. (1) Just after hatching; (2) Larvae ready to settle; (3) Recently settled. (B) Observed stages of *C. stelleri* development in this study. Scale bar = 100 µm. (1) Just after hatching—no plate formation or post-trochal elongation; (2) Settled. Dorsal bumps are plate precursors as no calcification has occurred.
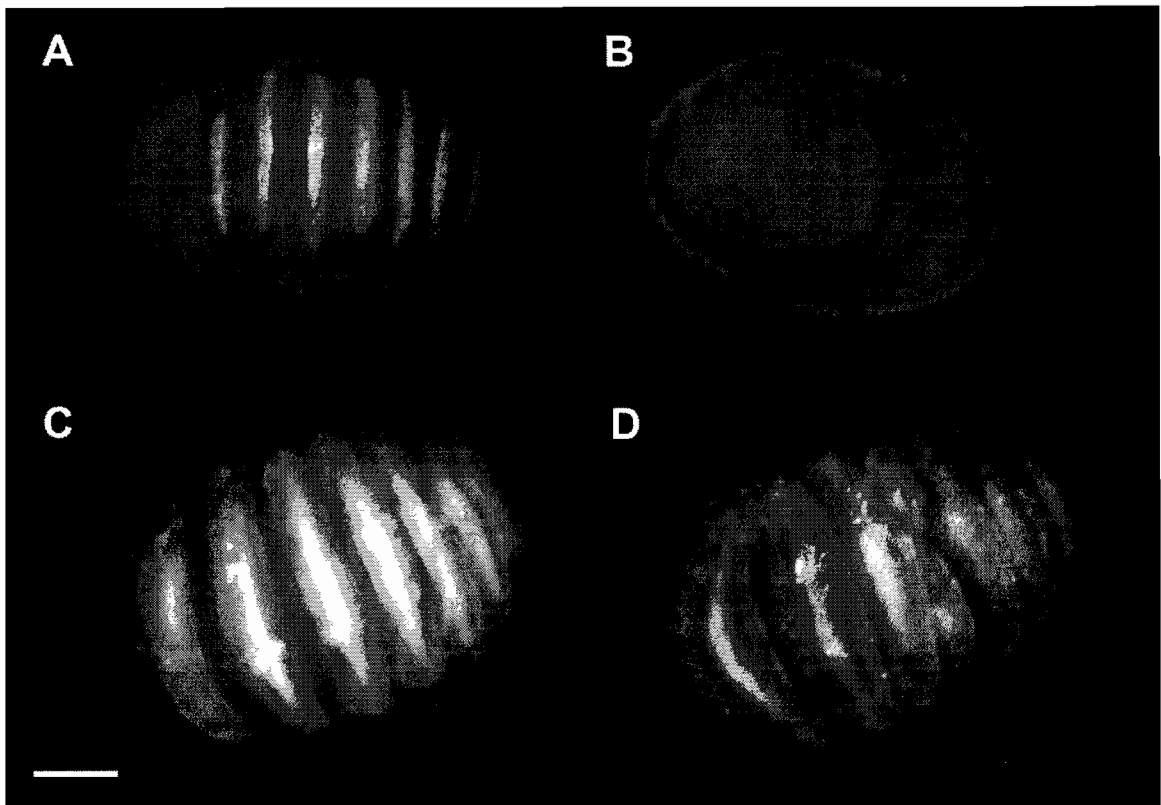
Figure 3.5. Photographs of newly metamorphosed juveniles of *Cryptochiton stelleri*. (A) Dorsal view of one day post-metamorphosis juvenile with valves beginning to form. (B) Ventral view of one day post-metamorphosis juvenile with two red eyes and the foot visible. (C) Dorsal view of juvenile five days after metamorphosis; valves have developed further. (D) Dorsal view of juvenile 14 days after metamorphosis with valves completely covering the mantle and foot. Scale bar = 100 μm.
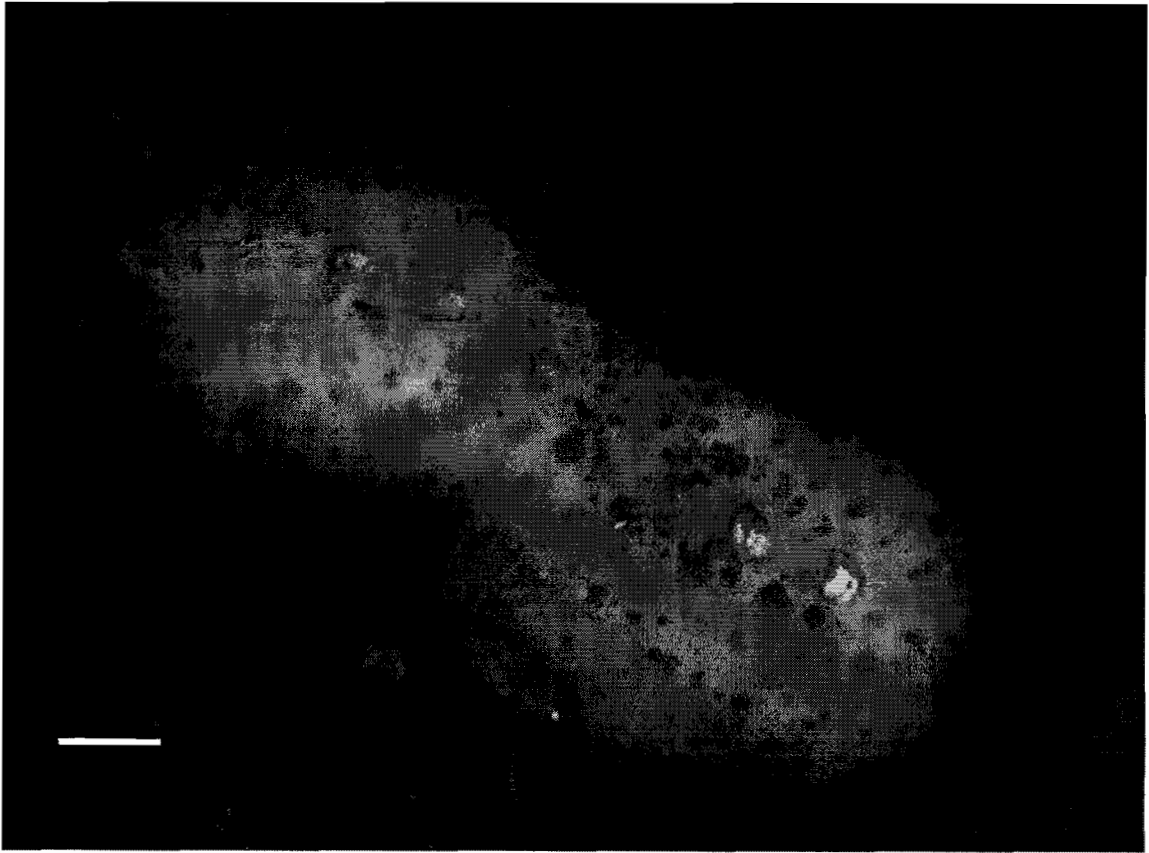
Figure 3.6. Juvenile *Cryptochiton stelleri* discovered at Cape Blanco, Oregon. Eight exposed plates are visible as they have not yet been overgrown by the mantle. Red spicules can be seen starting to cover the surface of the mantle. Scale bar = 1 mm.
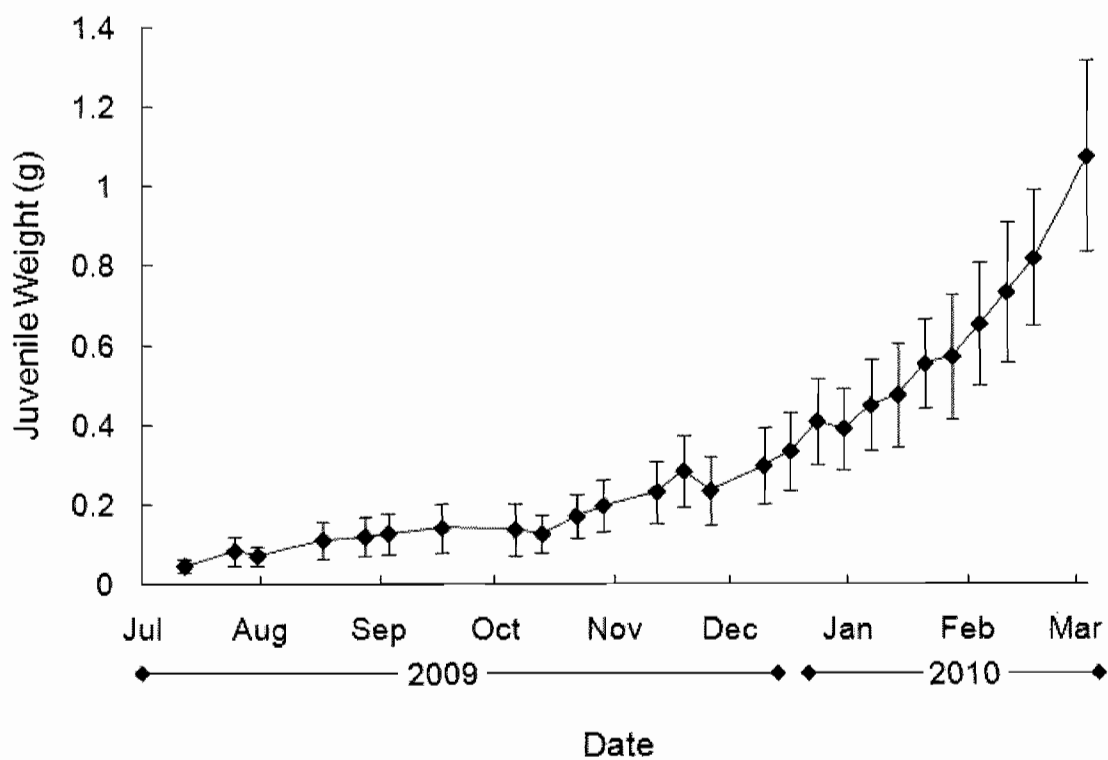
Figure 3.7. Growth rate of juvenile *C. stelleri* raised in flowing seawater tables (N = 4). SE bars indicate the small variation in the growth and sizes of the juvenile specimens. Growth rate is in terms of wet weight, measured to 0.01 g.

Discussion

The major developmental stages of *Cryptochiton stelleri* were compared with those described by Okuda (1947), the only other study on the development of this species. Okuda's study has several differences relative to the current study: he described *C. stelleri* eggs as red or cinnamon-colored instead of green and he described hatching occurring after four days instead of two (Strathmann, 1985). Okuda's study has been used as the primary source for the description of the development of *C. stelleri* and one figure in particular (Fig. 3.4A) has been disseminated in at least two texts (Giese and Pearse, 1979; Shanks, 2001). Okuda stated that plate formation and post-trochal elongation occurred before or soon after hatching (Fig. 3.4A); in contrast, these characteristics did not appear soon after hatching in the present study (Fig. 3.2); post-trochal elongation commenced two days after hatching and plate precursors appeared three days post-hatching (Fig. 3.3). Plates did not begin to calcify until metamorphosis, which could occur as soon as three days post-hatching. Like the anomalous egg color, this difference could result from Okuda having studied a different undescribed species.

This speciation could be a possibility given the distance between Japan and the Pacific Northwest of the United States. The short larval period of *C. stelleri,* physical differences in body and egg color, and the fact that multiple species of chitons have been split into different species on the two coasts the Pacific are reasons that Japanese *Cryptochiton* could be a different species. (D. Eernisse, UC Fullerton, pers. comm.). However, no non-brooding chitons have been shown to begin plate formation as early in the developmental process as the pre-hatching shell formation described by Okuda

(1947). Therefore, the current study provides a new description of embryonic and larval development of *C. stelleri*.

The short larval period, the developmental timetable, and non-feeding larvae described in this study are similar to most other described species of chitons (Giese and Pearse, 1979; Rumrill and Cameron, 1983; Shanks, 2001). Eggs of *C. stelleri* at 300 μm diameter (600 μm with the hull) are the largest of any NE Pacific chiton, slightly larger than the brooder *Lepidochitona fernaldi*, which has an egg diameter of 270 μm but a hull diameter of only 280 μm. The trochophore larva of *C. stelleri* looks similar to that of other chitons, but is slightly larger, 300 μm at hatching (Fig. 3.2). The appearance of only seven plates is consistent with other chiton species as well, since many chitons do not develop the eighth plate until well after metamorphosis (Voronozhskaya et al., 2002). While calcareous plates did not form from the plate precursor bumps before metamorphosis, the head, foot, girdle, and spicules all developed, indicating that these aspects of development may be more closely tied to development time than a metamorphic cue.

The potential metamorphic cues tested (warmer temperatures, high phytoplankton concentrations, presence of *Cryptopleura* (juvenile food source) and water in which adults had been maintained) failed to induce metamorphosis. Metamorphosis was triggered solely by the addition of coralline algae extract, which has been shown to induce species such as *Tonicella lineata* (Barnes and Gonor, 1973), *Katharina tunicata* (Rumrill and Cameron, 1983), *Haliotis diversicolor* (Bryan and Qian, 1998) and other species of mollusks to metamorphose (Morse et al., 1979). This consistency between a

diverse group of mollusks could be a result of a highly conserved ancestral trait, or could have evolved convergently in several different mollusk species. The reason for *C. stelleri* to use this specific cue is unclear, because encrusting coralline algae is present in many locations with high wave action in which *C. stelleri* would be unable to survive and because no stages of the *C. stelleri* life cycle feed on coralline algae. This may indicate a high amount of localized recruitment for this species, because *C. stelleri* is more abundant in small coves (Lord, Chapter 2) and a ubiquitous cue for metamorphosis may be most useful if larvae generally remain in these protected habitats. It is also possible that coralline algae is used as a mechanism for ensuring that metamorphosis occurs at a relatively low tidal level, where encrusting coralline algae is found.

The documentation of larval development, metamorphosis and observed growth rate of juveniles helps define the early life history of *Cryptochiton stelleri* (Fig. 3.6). The only published description of these juveniles in the literature are by Heath (1897) and brief mentions by Eernisse (2004) and Vendrasco et al. (2008). Juveniles are seldom found and little is known about their growth, feeding or behavior, though ongoing study will hopefully fill this void. The description of *C. stelleri* larval development, metamorphosis cue, plate formation and juvenile growth fills in major gaps in the knowledge of the life history of this species.

Bridge

Chapter III described the development, metamorphosis, and early growth rate of *C. stelleri*. The metamorphosis cue is encrusting coralline algae, a common cue to induce settlement and metamorphosis in mollusks. Encrusting coralline algae are abundant in many types of intertidal environments in southern Oregon, so this is not likely the factor driving the distribution of *C. stelleri* documented in chapter II. Since *C. stelleri* has been reported to be very long-lived (MacGinitie and MacGinitie, 1968), juveniles could not be raised to adults in order to figure out the growth curve for this species. In addition, the flexibility and lack of hard external structures in this species eliminated the possibility of mark-recapture techniques that are often used to determine growth rate. Chapter IV uses annual growth bands in the valves of *C. stelleri* to estimate age and growth rate for this species. Another large chiton, *Katharina tunicata*, is also used in this chapter in order to compare growth rates and growth ring formation in these two species.

CHAPTER IV

LONGEVITY AND GROWTH RATE OF THE GUMBOOT CHITON

CRYPTOCHITON STELLERI AND THE BLACK LEATHER CHITON *KATHARINA*

TUNICATA

Introduction

Growth rate is one of the most fundamental life history parameters and is critical

in developing models of the overall health, structure, and reproductive output of a

population. Comprehensive knowledge of population structure is vital to the

understanding of population dynamics for any species, especially those that are long-

lived, because size and longevity have an immense impact on the lifetime reproductive

output of an individual or population (O'Farrell and Botsford, 2005). Growth rate

information is available for many marine organisms, especially those with commercial

value such as fish and bivalves (Gang et al., 2008; Abele et al., 2009). Despite the

relative abundance of growth rate data in general, the establishment of growth curves for

some marine animals has been fraught with difficulty. This is particularly true for the

chitons, Class Polyplacophora.

The gumboot chiton, *Cryptochiton stelleri* Middendorff, 1847 is the largest

invertebrate herbivore in the intertidal zone throughout much of its range (central

California to Alaska, Japan), but the population dynamics of this species remains

unknown. It is the largest species of chiton in the world, at up to 36 cm long and up to 2000 g (pers. obs.) and is relatively abundant on rocky intertidal shores. This species feeds on a variety of seaweeds, including *Cryptopleura, Mazzaella, Ulva, Nereocystis,* etc. (Yates, 1989). Growth rates and factors influencing growth or distribution are not well known, leaving the life history of *C. stelleri* largely undescribed. Unlike most chiton species, *C. stelleri* has valves fully covered by the girdle (making marking difficult) and small valves relative to their body size. This species is also very flexible, which makes measurements of length highly variable. Previous studies have attempted to use growth lines on the outside of the valves to age this species, but the researchers decided that the lines were too obscure to use (MacGinitie and MacGinitie, 1968; Palmer and Frank, 1974). The covered valves, flexible morphology, and unclear growth lines of this species have confounded previous attempts to elucidate the growth rate of *C. stelleri.*

Several sources have suggested that *C. stelleri* is quite long-lived, but actual age measurements are not available (MacGinitie and MacGinitie, 1968; Palmer and Frank, 1974; Yates, 1989). Heath (1905b) estimated *C. stelleri* longevity at approximately four years, but this was based on limited data. The MacGinities (1968) estimated that the largest *C. stelleri* individuals were at least 20 years old, but this estimate was based on limited observations of growth rings on the shell plates. Palmer and Frank (1974) expressed doubts about the growth ring method of the MacGinities (1968), but were unable to obtain any useful growth rate information from weight measurements of *C. stelleri.* We know little about the growth rate, longevity, or age structure of *Cryptochiton stelleri* populations anywhere in its range.

The fact that *C. stelleri* is believed to be a long-lived species is not only a reason why understanding its growth rate is important, but also complicates establishing a growth curve. In addition, the early life history stages of this species remain a mystery, with only a few studies even mentioning the discovery of juvenile or young individuals (Heath, 1897; MacGinitie and MacGinitie, 1968; Yates, 1989). This scarcity of individuals from the early part of the life history of this fairly common organism poses problems for establishing a growth curve, especially via methods such as following the growth of age classes. Heath estimated the age of a 27 mm juvenile at a few months, but this was not supported by any data, and not enough of these juveniles have been found to make a proper estimate (Yates, 1989). Even individuals less than 15cm in length are fairly uncommon in parts of Oregon, as a four-year study by Yates (1989) found fewer than a dozen individuals this size along the central Oregon coast.

The black leather chiton *Katharina tunicata* is the second largest chiton in the northeastern Pacific, at up to 12 cm in length (Himmelman, 1978). It is common intertidally from Kamchatka (Russia), through the Aleutian Islands, and down the Pacific coast to Catalina Island in southern California (Himmelman, 1978). Like *C. stelleri*, *K. tunicata* feeds largely on macroalgae, in this case the kelp *Saccharina sessilis* and occasionally erect coralline algae (Dethier and Duggins, 1984). The only published study on the age or growth of *K. tunicata* was done by Heath (1905a), who estimated that this species can live for three years in central California. However, this estimate was not supported by data. Like *C. stelleri*, little about the life history of *K. tunicata* is known.

The debatable and often imprecise nature of aging chitons was illustrated clearly in a review of molluskan lifespans by Comfort (1957). Using a variety of sources, he listed the best-known estimates of lifespan for many mollusks, including several chitons. The difference between these estimates and present growth information is indicated by a multitude of examples. The maximum age of *Chiton tuberculatus* was listed as twelve years by Crozier (1918), but was later estimated at approximately two years (Glynn, 1970). Heath (1905a) gives a lifespan of three years for *Katharina tunicata* in central California, but the present study estimates a considerably longer lifespan. The molluskan lifespan paper by Comfort also cites Heath (1905b) in estimating maximum *Cryptochiton stelleri* age at approximately four years. Since then, multiple studies have estimated *C. stelleri* to live at least twenty years, although this has never been confirmed by any growth data (MacGinitie and MacGinitie, 1968; Palmer and Frank, 1974). These inconsistencies in chiton age estimates underscore the difficulties in ascertaining age of chitons.

Some of the problems with determining growth rate stem from variability in what body measurement is used as an indicator of size. A study on the chiton *Plaxiphorella aurata* used the width of the 4th shell plate to estimate growth (Gappa and Tablado, 1997). They found that *P. aurata* live 6-7 years and display an asymptotic growth pattern best estimated by the von Bertalanffy Growth Function (von Bertalanffy, 1938). A growth curve for *Acanthopleura gemmata* has also been established using the 4th shell plate as a proxy for individual size (Soliman et al., 1996). In contrast, Glynn (1970) used body length to measure growth in *Acanthopleura granulata* and *Chiton tuberculatus*.

Still other research on chiton growth has focused on growth rings or annuli in the shell plates in order to determine lifespan and growth rate (Crozier, 1918; Baxter and Jones, 1978; Jones and Crisp, 1985). The use of growth lines has become commonplace in research on molluskan aging, especially in the case of commercially important bivalves (Ropes, 1987; Black et al., 2008, 2009; Black, 2009).

Growth in the chiton *Acanthopleura granulata* slows when out of the water at low tide and this produces daily growth rings (Jones and Crisp, 1985). This ring formation pattern results in an extremely high number of rings present on the valves of these chitons, with rings clumped in groups of 28, associated with the days of the tidal cycle. However, not all rings are created equal, as much heavier and more well-defined growth rings are laid down annually in many species of chiton (Crozier, 1918; Baxter and Jones, 1978). Each ring represents a time of very slow growth, while the larger gaps in between indicate faster growth. Growth rings are produced annually in many organisms because of seasonal fluctuations in food availability, climate, and seasonal spawning (Merrill et al., 1961; Feder and Paul, 1974; Baxter and Jones, 1978; Bennett et al., 1982; Black, 2009).

The present study closely examined the ontogeny of *C. stelleri* and used the growth rates of juveniles and young individuals to support age estimates based on growth rings. Growth rings visible in the shell plates or valves of these chitons were used to establish growth and longevity estimates for *C. stelleri* and *K. tunicata*. Difficulties in measuring *C. stelleri* and *K. tunicata* size and age were minimized by using an array of different measurements of size, including weight, volume, length, circumference, valve

weights, valve lengths, and valve widths. This wide range of morphological measurements allowed for extensive allometric comparisons, which both exposed limitations of growth curves based on linear measures of size and revealed a considerable amount of information about the growth rates of *Cryptochiton stelleri* and *Katharina tunicata.*

Materials and Methods

This study was conducted primarily along the central Oregon coast. *Cryptochiton stelleri* individuals that were sacrificed in order to measure the growth rings in their valves were taken from Cape Blanco near Port Orford, Oregon (42°50.900'N, 124°33.410'W), and Lighthouse Island, Sunset Bay, and Cape Arago, all near Charleston, Oregon (43°18.191'N, 124°23.198'W). Only five individuals were taken from each site in January 2010, in order to minimize the impact on this species that is not superabundant along the Oregon coast. The majority of the valves that were used to analyze growth lines were from individuals that washed up dead on the beach, so were not killed for the purpose of this study. Forty dead chitons were collected from a beach near Fort Ebey State Park, Washington in February 2009, and 14 individuals were collected from the south end of Ansilomar Beach near Monterey, California in December 2009. *Katharina tunicata* specimens that were measured and sacrificed were taken from South Cove, Cape Arago, Oregon, ten kilometers south of Charleston, Oregon.

Cryptochiton stelleri that were washed up on the beach in Washington and California were too deteriorated to obtain any body size information, so all external body

measurements were done solely on live individuals from the sites in Oregon. External measurements included body length and circumference when curled up in a ball. Circumference was determined by first picking up and holding specimens until they were tightly curled and then measuring the circumference longitudinally. The reliability of this method was tested by making repeated measurements of 15 specimens, which were given time to uncurl between each measurement (each measured five times). The maximum and minimum measurement for each specimen differed by an average of 1.8%, indicating that circumference was a consistent measure. Other external measurements for *C. stelleri* and *K. tunicata* included volume (water displacement) and weight in air. All measurements were made after specimens had been kept in a flowing seawater table for a week so that weight and volume measures would not be biased by differential water or air content.

Specimens were relaxed, then killed with a 7.5% magnesium chloride solution the same day external measurements were taken and one week after field collection. Once the valves were removed, valves were weighed on a digital scale and then photographed and measured digitally using ImageJ (available at http://rsb.info.nih.gov/ij). The valve measurements, length (at the shortest point) and width (at the widest point), were done on all intact valves from all California, Oregon, and Washington *Cryptochiton stelleri*, for a total of over 300 valves measured and weighed from 70 individuals. The same measurement process was done for *Katharina tunicata*, using the third, fourth, and fifth valves, which were the largest in this species.

I. Growth ring counts

In order to observe growth rings on the valves, the valves were cross-sectioned using a Dremel® rotary tool with a diamond-coated cutting blade. For each specimen of *C. stelleri*, as many as all eight valves were used, with cross sections taken along the long and short axis of each valve. Consequently, each *C. stelleri* individual had up to 16 cross sections used to estimate age, with an average of six for each specimen. Several of the dead, washed up specimens had broken valves which were unusable. *Katharina tunicata* valves (valves 3,4,5) were also cross-sectioned along the long and short axis, producing approximately six valve cross sections per specimen. Valves of both species were then polished with increasingly fine silicone carbide grinding paper, with a final grit of 1200.

Clear dark growth rings were visible on *K. tunicata* valves with the naked eye after cross-sectioning and polishing. Only major growth rings were visible and were counted under a dissecting microscope. The acetate peel technique was necessary to view *C. stelleri* growth rings; the etching process and acetate peels were done according to the method described by Black et al. (2009). Acetate peels were taped to microscope slides and examined for growth rings on a compound light microscope. The distances between valve rings were measured using an eyepiece micrometer and photos were taken of acetate peels using an Optixcam Summit 5.0 series® digital microscope camera. Photographs of valves were analyzed for the density of valve lines using the plot profile function in ImageJ in order to compare the growth of *C. stelleri* individuals from California, Oregon, and Washington. This was done by making transects down the middle of each valve and analyzing the gray values along this transect. The plot profile

function plots gray values on a scale from zero (black) to 255 (white), with peaks in gray value indicative of a major growth ring.

Growth lines faded out towards the center of the valves on older *C. stelleri* specimens, so an additive process was used to estimate the number of rings for these individuals. Since smaller specimens had all of their growth rings intact and visible to the center, the distance between each ring and the next was measured and a dataset was compiled that included the number of rings present at each distance from the center of the valve. In those older individuals with growth rings that faded out towards the center of the valve, the rings/distance dataset was used to estimate the number of faded missing rings. For example, if smaller specimens averaged 4 growth rings in the first 8 millimeters from the center of the valve and an older specimen had 10 visible growth rings but then the rings faded out around 8 mm from the center, it could be estimated that the older specimen likely had $10 + 4 = 14$ rings. Because growth rate could differ with location, this additive process was done separately for Washington, Oregon, and California specimens.

In order to complete the early stages of the growth curve for *C. stelleri*, additional growth rate information was obtained by raising juvenile and young *C. stelleri* in flowing seawater tanks at the Oregon Institute of Marine Biology, Charleston, Oregon. Four juveniles were collected on the north side of Cape Blanco, Oregon on Jul 22, 2009, on a - 0.67 meter low tide (MLLW). Laboratory growth rates were verified by the finding of three more juveniles in the field four months later that were in the same size range as those kept in the lab for those four months. One was found on Nov. 11, 2009, at Middle

Cove of Cape Arago, another on Dec. 5, 2009, at Cape Blanco, and the third on Feb. 3, 2010, at Cape Blanco. Juveniles were fed red algae of the genus *Cryptopleura* and older individuals (>5 cm) were fed a constant supply of the algae *Mazzaella splendens, Ulva lactuca,* and *Nereocystis luetkeana.* The length, width, and weight of the juveniles were measured once a week from August 2009 to February 2010.

II. Size-at-age curves

Juvenile measurements of size at age were combined with ring count information to create size-at-age curves showing the changes in several different morphological characteristics with age. This created multiple size-age datasets for the juveniles that could be added to the adult *C. stelleri* datasets that plotted circumference, weight, and volume against age estimated from major growth lines on the valves.

Without using acetate peels, growth rings in *K. tunicata* were quite clear, making growth ring counting much simpler. After sectioning and polishing the valves, rings appeared as darker colored bands. These growth rings were apparent to the center of the valves, so the additive method used to estimate the number of rings for *C. stelleri* was unnecessary. Juvenile *K. tunicata* were not found at the time of collection, so were not included in the size-at-age curves for this species.

Growth data were fitted using XLFit® software (by IDBS) and the best fitting curves (highest r^2 value) were chosen. This software fits the data to over 700 different curves and presents the best fits. In order to create a complete size-at-age curve, *C. stelleri* specimens from Oregon sites (5 specimens from 3 sites) were combined using

individuals from more than one site gives the models more generality to geographically disparate populations. In contrast to the rarer *C. stelleri*, *Katharina tunicata* is very abundant at many sites (Himmelman, 1978), so abundance was not a concern and all specimens were taken from the South and Middle Coves of Cape Arago, Oregon. The size-at-age data for *K. tunicata* were fit with growth functions in the same manner as the data for *C. stelleri*.

Results

I. Growth ring counts

Upon inspection under a compound light microscope, the *C. stelleri* acetate peels showed clear major growth lines as bright rings separated by dark increments of faster growth (Fig. 4.1). This allowed rings to be easily counted and the space between the major rings to be measured. Black and white photographs were taken of the acetate peels and, along a transect of the photograph of the peel, the brightness of the growth lines showed up well in a plot profile of gray values in ImageJ (Fig. 4.1). Spikes or peaks in the gray value coincided with major growth lines (Fig. 4.1). In order to set a protocol for counting growth lines, a major growth ring was established as one that was at least twice the standard error above the average gray value along the transect. For *K. tunicata,* only major rings were visible under the dissecting microscope, so discerning between major and minor rings was not an issue. The additive method for counting rings (previously
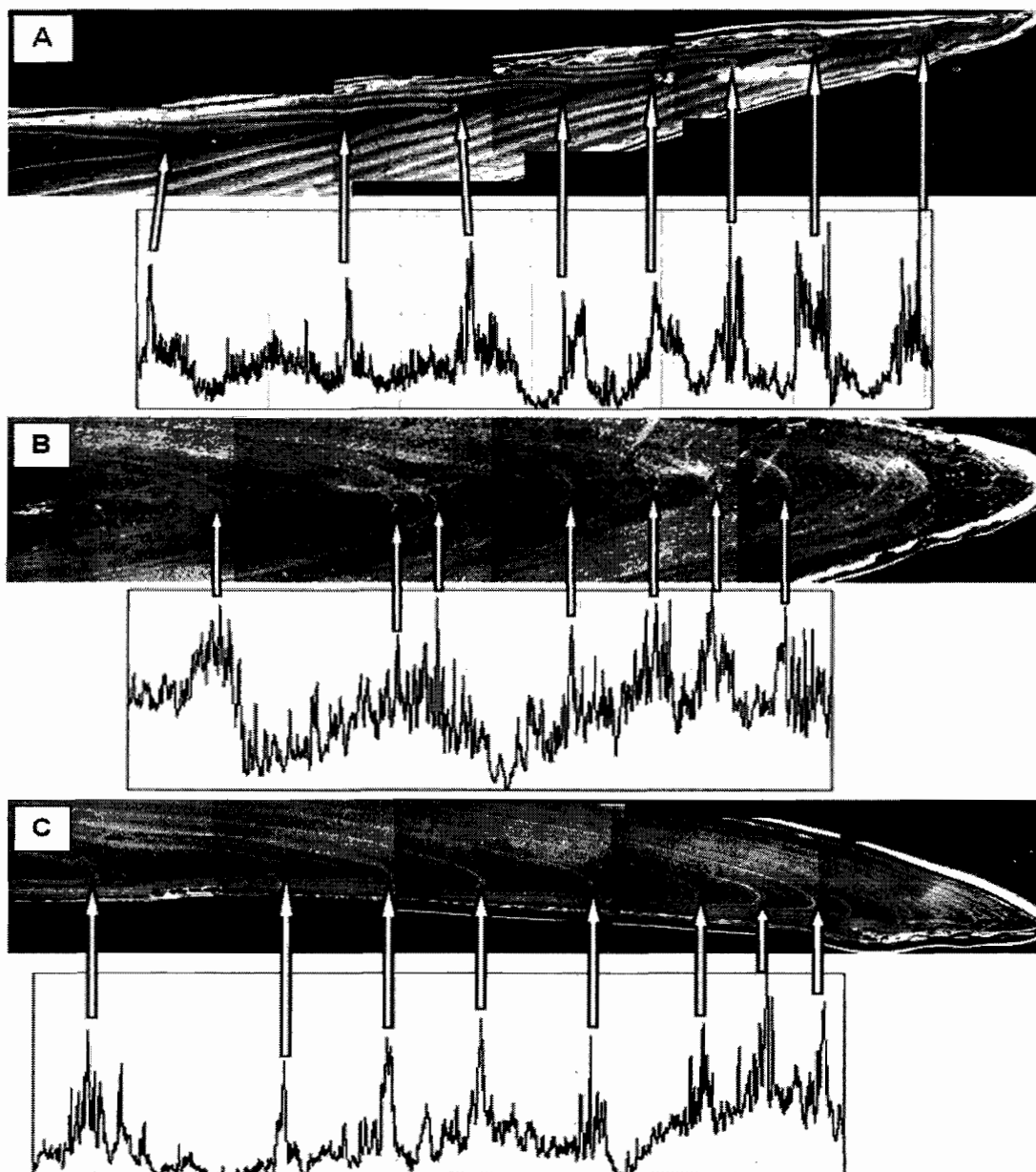
Figure 4.1. Photographs of acetate peels of sectioned *C. stelleri* valves from Washington, California, and Oregon. Graph shows associated plots of gray values from ImageJ, with peaks in gray value associated with each growth line because of the brightness of the line compared to the dark region of growth in between lines. (A) Acetate peel of valve cross-section from Washington. Growth lines are clearly defined, with very few smaller growth rings between major rings. (B) Acetate peel of valve cross-section from California. Growth lines are more obscure, with many pronounced smaller lines in between each growth band. (C) Acetate peel of valve cross section from Oregon. Growth lines are more clearly defined than California, but less clear than in individuals from Washington.

described) was fairly precise, as the curves estimating the numbers of growth rings to the center had a 95% confidence interval of approximately +/- 2 rings (Fig. 4.2).

Cryptochiton stelleri valves from Fort Ebey, Washington (Fig. 4.1A) showed very distinct growth rings, with very few smaller growth lines between the major potentially annual bands. The major growth rings on the valves from Ansilomar, California (Fig. 4.1B) were much less pronounced and were obscured by a large number smaller growth rings clumped around each major ring. This distinction between Washington and California is clear on both the acetate peels and the gray value graphs. Valves from Oregon showed distinct growth lines similar to those from Washington, but slightly less defined. Valves and graphs in Fig. 4.1 were chosen as representative examples of the differences in banding in the valves of Washington, Oregon (Fig. 4.1C) and California specimens.

There were no significant differences in spacing between major growth rings in valves from the three different states. The spacing between the bands is indicative of the time between ring deposition, or the growth rate of the valves, which did not vary significantly between states. However, there were differences (one way ANOVA, df = 110, F = 15.39, p < 0.0001) in the dispersion of smaller growth rings around each major growth band. Both Washington (Tukey's HSD, p < 0.01) and Oregon (Tukey's HSD, p < 0.01) had growth lines that were significantly more tightly clustered (width of peak in gray value) than in the California valves (Fig. 4.3). These tightly clustered minor growth lines made major growth bands in Washington and Oregon valves very distinct. Valves from Oregon *C. stelleri* specimens were not significantly different from Washington

valves with regard to the clustering (of small growth marks around major growth rings (t-test, $p > 0.1$).

Juvenile *C. stelleri* appeared to grow at approximately the same rate in the lab as in the field; individuals growth in the laboratory from August through the fall were similar in size to individuals from the field found in the fall. The average weight of the lab-reared juveniles (raised since August 2009) in December 2009 was 0.190 grams, and the average weight of the juveniles discovered in the field November 2009-January 2010 was 0.195 grams (Fig. 4.4). This similarity in size suggests that the lab-reared individuals grew at approximately the same rate that they would have in the field.

II. Size-at-age curves

Counts of the major presumably annual growth rings were used to create size-at-age curves for *C. stelleri* and *K. tunicata*. The most common measurement of size used in growth curves is body length. However, length is an extremely inaccurate measure of adult *C. stelleri* size due to their ability to contract and extend themselves. In order to avoid this problem, circumference when curled up was used as a measure of size. Using ages determined from the growth rings, body circumference was plotted against age and fitted with a growth equation using XLfit® software. Juvenile growth rates observed in the lab were included to make the early ages of this model more accurate by including the circumference-age data from the juveniles with the circumference-age data estimated from adult growth rings (Fig. 4.5). The best fit ($r^2 = 0.96$) model used to fit these data was a growth function used to model the indeterminate growth of *Strongylocentrotus*
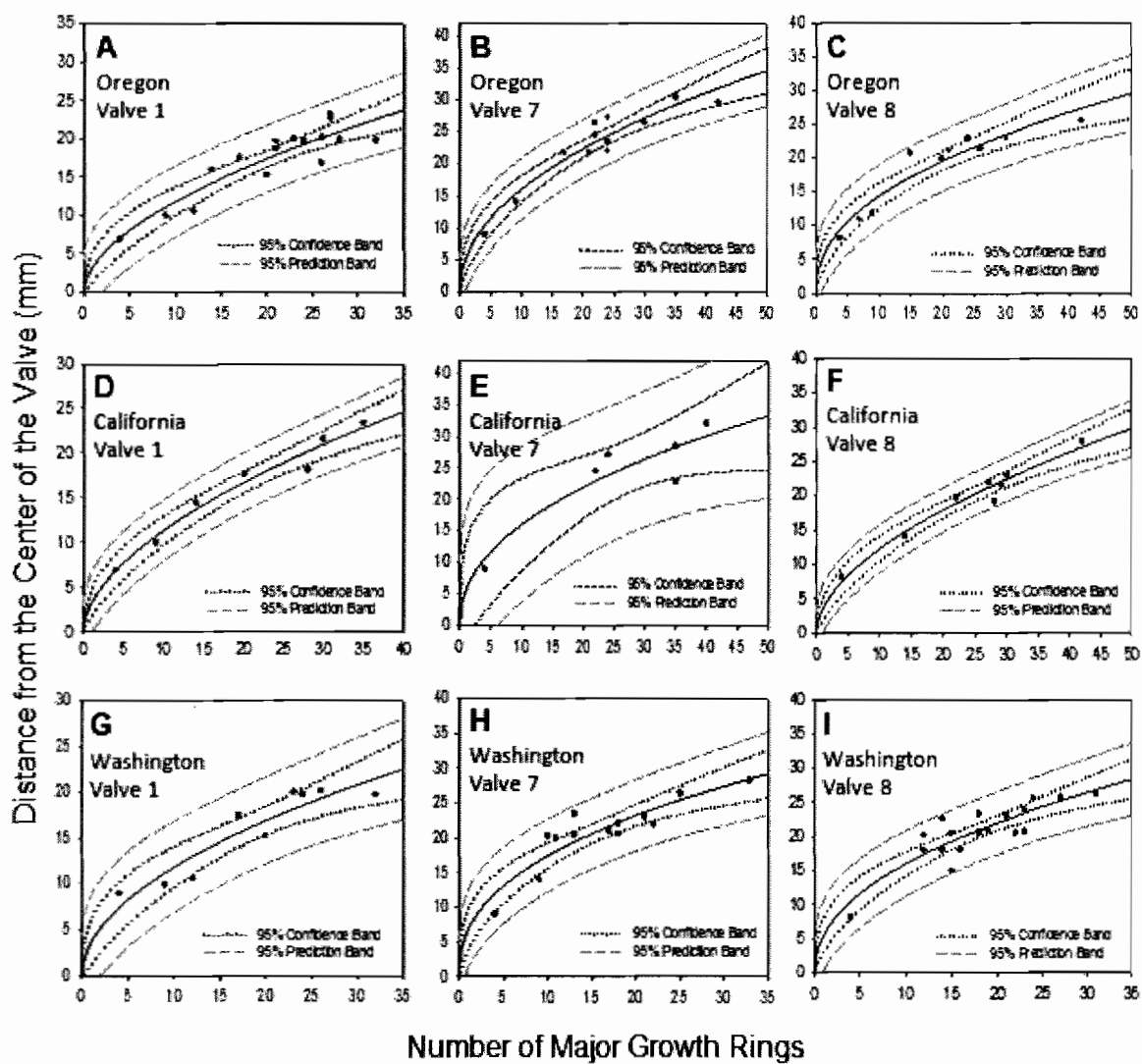
Figure 4.2. Curves used to help estimate the number of *C. stelleri* growth rings when valves had growth rings that faded towards the center. These curves were used to predict the number of rings that would be in that distance to the center of the valve. Curves are shown for Oregon (A,B,C), California (D,E,F), and Washington (G,H,I) valves. Since different valves are different size, curves had to be used separately for valve 1 (A,D,G), valve 7 (B,E,H), and valve 8 (C,F,I). 95% prediction and 95% confidence intervals are shown on each graph.
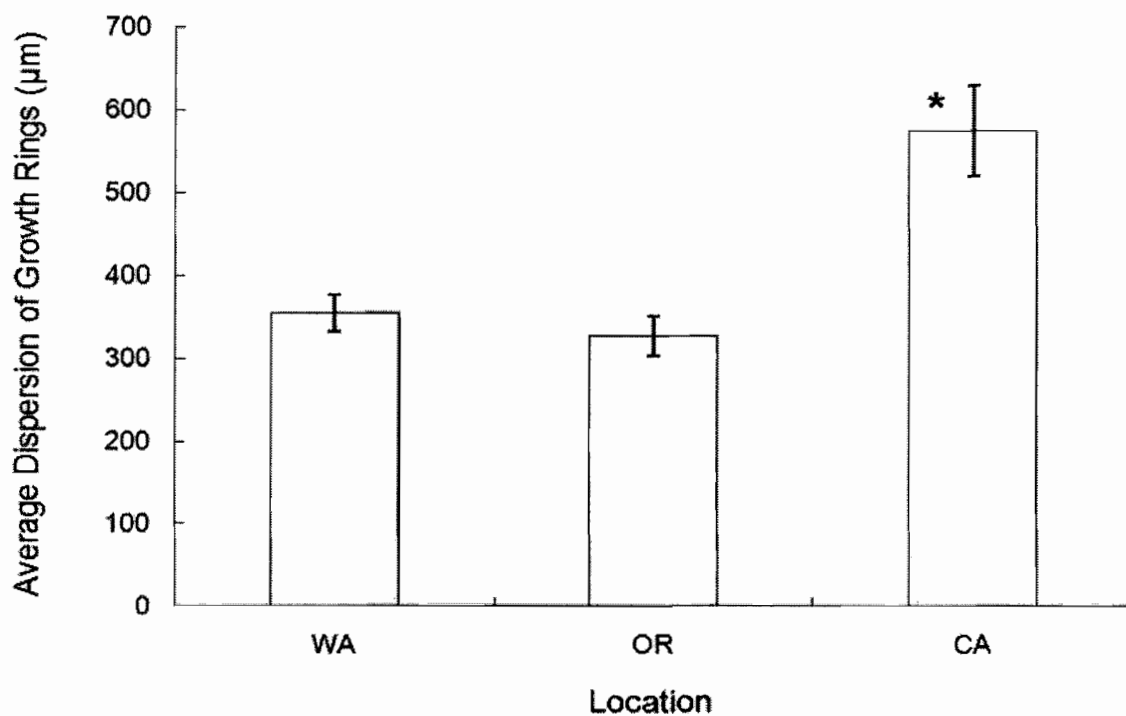
Figure 4.3. Average width or clumping (width of each peak in gray value) of small growth lines around each major growth line on acetate peels of valves from Washington, Oregon and California. Oregon (n=25) and Washington (n=32) valves had significantly narrower, clearer growth rings than valves from California (n=12). (±SE)
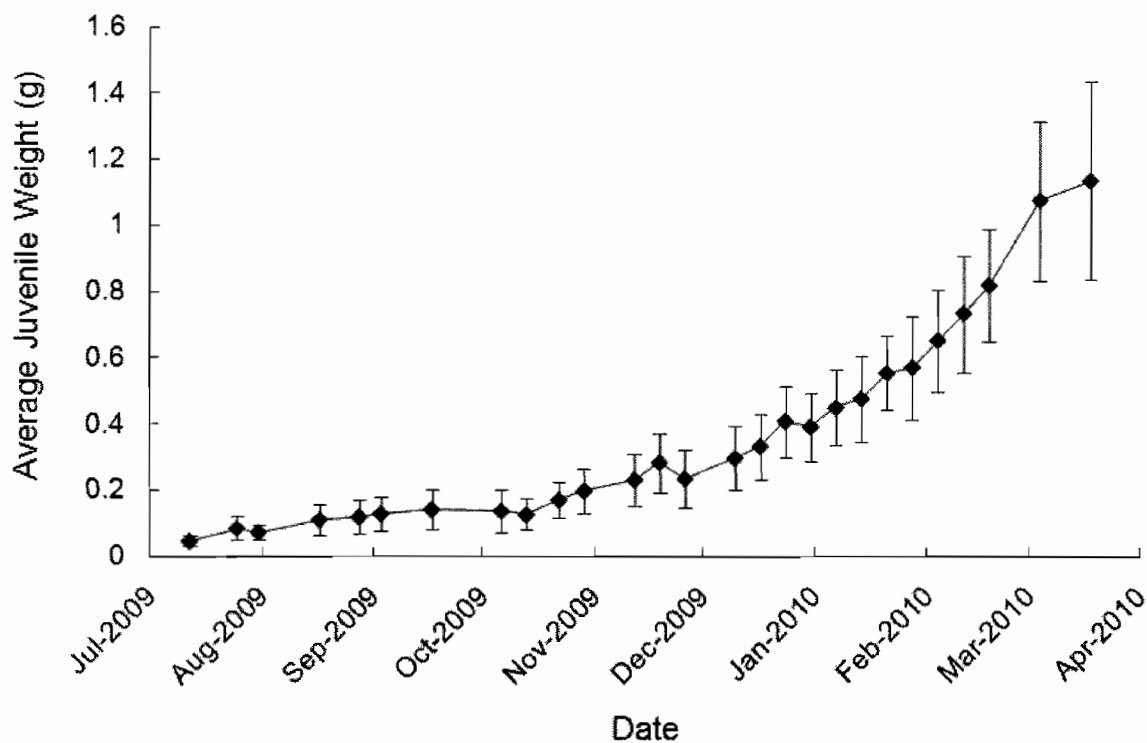
Figure 4.4. Average growth rate (±SE) of juvenile *C. stelleri* (n=7) in flowing seawater tanks at the Oregon Institute of Marine Biology. Body weight is plotted against the date of measurement. Juveniles were approximately three months old upon collection in August 2009. This is the first documentation of growth rates for these early stages of the life history of this organism.

franciscanus (Rogers-Bennett et al., 2003) (Table 4.1):

$$C(t) = A(1 - e^{-(Kt)}) + Bt$$

In this model, C(t) is the change in the circumference with time, A and B are parameters, K is a growth rate constant and t is time or age. A Chapman function (Table 4.2) was used to fit *K. tunicata* ($r^2 = 0.85$) size and age data, with body length used instead of circumference because the stiffer morphology of *K. tunicata* made length a reliable measurement.

Body volume was also plotted against estimated age, producing a different shaped curve for both species than the curves based on length and circumference (Fig. 4.5). In both species, growth as measured by volume increases with age and does not level off or slow down. Using volume measurements of size, *C. stelleri* growth rate that increases with age was best fit ($r^2 = 0.87$) by a growth function from Rogers-Bennett et al. (2003) (Fig. 4.5A) (Table 4.1). Volume-age and weight-age data for *K. tunicata* were best fit by the same function and show the same pattern of increasing growth rate with age (Fig. 4.5) (Table 4.2).

Body measurements were not available for Washington and California *C. stelleri* specimens because of their badly deteriorated condition. However, since the weight of the eighth valve was strongly correlated with body weight and volume (Fig. 4.6A), a size-at-age curve could be established by using the valve eight weight as a proxy for size and plotting it against age (number of presumptive annual rings). This was done for Washington and Oregon (from 15 sacrificed specimens) but there were not enough specimens of different sizes from California to compile an accurate size-at-age

Table 4.1. All equations shown are the curves that best fit the measure of *Cryptochiton stelleri* growth that is given in the first column. Best fit curves were chosen based on the functions with the highest r^2 value in XLFit®. The change (increase or decrease) in growth rate with age is in the last column and is based on the upward or downward slope of each of the curves.

Y	X	Best Fit Curve	Equation	R^2	Change in Growth Rate
Valve 8 Weight	Body Volume	Line	$W(v) = 0.0153v$	0.82	N/A
OR body circumference		Rogers-Bennett et al. (2003)	$C(t) = (31.97*(1.01 - (e^{-0.085t}))) + 0.17t$	0.96	(-) Decrease with age
OR body volume		Rogers-Bennett et al. (2003)	$V(t) = (-274.0*(0.49 - (e^{-0.060t}))) + 34.25t$	0.87	(+) Increase with age
OR body weight	Number of major growth rings (age)	Chapman Function	$W(t) = (2873.3*((1-e^{\wedge}(((-1)*0.0277)*x))^{\wedge}1.7855))$	0.91	(+) Increase with age
WA valve 8 weight		Modified power function	$W(t) = 0.1121t^{1.4016}$	0.69	(+) Increase with age
OR valve 8 weight		Modified power function	$W(t) = 0.0206t^{1.95}$	0.96	(+) Increase with age
OR valve 8 width		Modified power function	$W(t) = 7.688t^{0.5465}$	0.96	(-) Decrease with age
WA+OR+CA valve 8 weight		Modified power function	$W(t) = 0.0753t^{1.538}$	0.80	(+) Increase with age
WA+OR+CA valve 8 length		Morgan-Mercer-Flodin	$L(t) = [(-19.95*5.77) + (110.9(t^{0.35}))] / (5.77+(t^{0.35}))$	0.71	(-) Decrease with age

Table 4.2. All equations shown are the curves that best fit the measure of *Katharina tunicata* growth that is given in the first colum. Best fit curves were chosen based on the functions with the highest correlation coefficient in XLFit®. The change (increase or decrease) in growth rate with age is in the last column and is based on the upward or downward slope of each of the curves.

Y	X	Best Fit Curve	Equation	R^2	Change in Growth Rate
Valve 4 Weight	Body Volume	Line	$W(v) = 0.0388v$	0.88	N/A
Body length		Chapman function	$L(t) = 109.35*(1-exp((-.298)x))^{1.436}$	0.85	(-) Decrease with age
Body volume	Number of major growth rings (age)	Two power fits	$V(t) = (1.61*(t^{1.24})) + (2.4*(t^{1.23}))$	0.85	(+) Increase with age
Body weight		Rogers-Bennett et al. (2003)	$W(t) = (-8.4(1.02 - (e^{-1.04t}))) - 9.33t$	0.84	(+) Increase with age
Valve 4 weight		Rogers-Bennett et al. (2003)	$W(t) = (-0.59(.956 - (e^{-2.06t}))) + 0.324t$	0.84	(+) Increase with age
Valve 4 width		Rogers-Bennett et al. (2003)	$W(t) = (88.65(1.03 - (e^{-0.071t}))) - 1.99t$	0.93	(-) Decrease with age
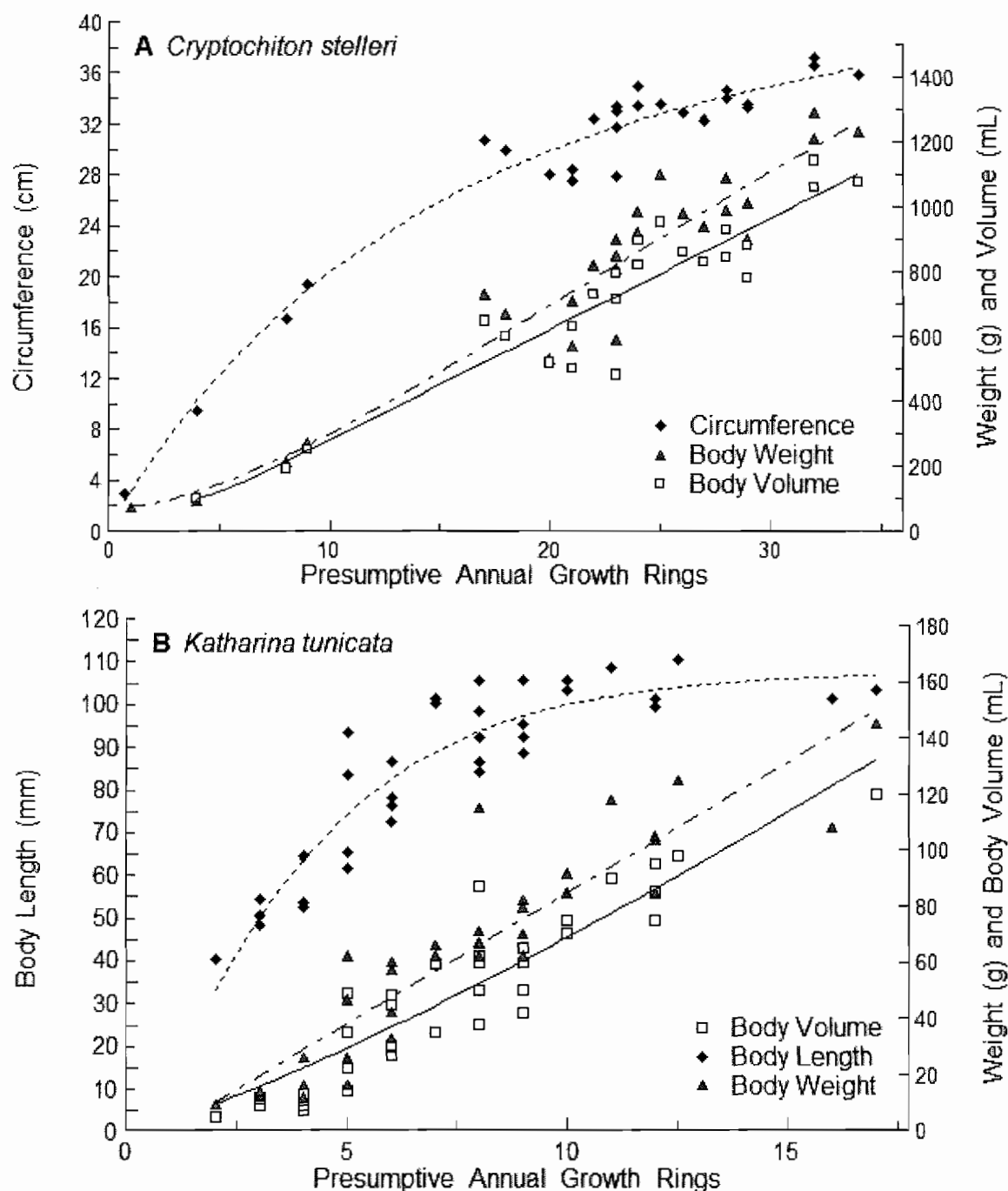
Figure 4.5. Size-at-age curves based on weight, volume, and a linear measure of size for *C. stelleri* and *K. tunicata.* Body length and body volume are both plotted against presumptive annual growth rings. Growth functions from Rogers Bennett et al. (2003), which modeled indeterminate growth, were fit to the data. (A) Size-at-age curves for *C. stelleri* (n=25). Circumference is used as a linear measure of size instead of length because of the flexibility of the organism. (B) Size-at-age curves for *K. tunicata* (n=35).

curve (Table 4.1). These data were best fit with a modified power model of the form:

$$W(t) = A*B^t$$

W(t) is the change in valve eight weight with time or age and A and B are growth

parameters (Table 4.1). For *K. tunicata*, valve four weights were the most strongly

correlated with volume (Fig. 4.6B). Valve four weight and width were both plotted

against age (presumptive annual growth rings) (Fig. 4.7B) and the equations used to fit

these curves are shown in Table 4.2.

In order to get a general estimate of the relationship between valve 8 weight (as a size

proxy) and age for *C. stelleri*, data from all three locations (Washington, Oregon,

California) were combined and a modified power function was fit to these data (Fig. 4.8).

This combined growth curve had the equation:

$$W(t) = 0.0753t^{1.538}$$

The data fit well into one curve ($r^2 = 0.80$), indicating the lack of drastic

differences in size-at-age between the three locations. The width of valve 8 was also

plotted against age for the combined dataset from all three states, and these data were best

fit ($r^2 = 0.709$) by the Morgan-Mercer-Flodin (MMF) equation shown in Table 1.

Discussion

I. Growth ring counts

Age estimates have not been previously published for *Katharina tunicata*.

Previous attempts to estimate age for *Cryptochiton stelleri* have been unsuccessful.

MacGinitie and MacGinitie (1968) attempted to use growth lines as an estimate of
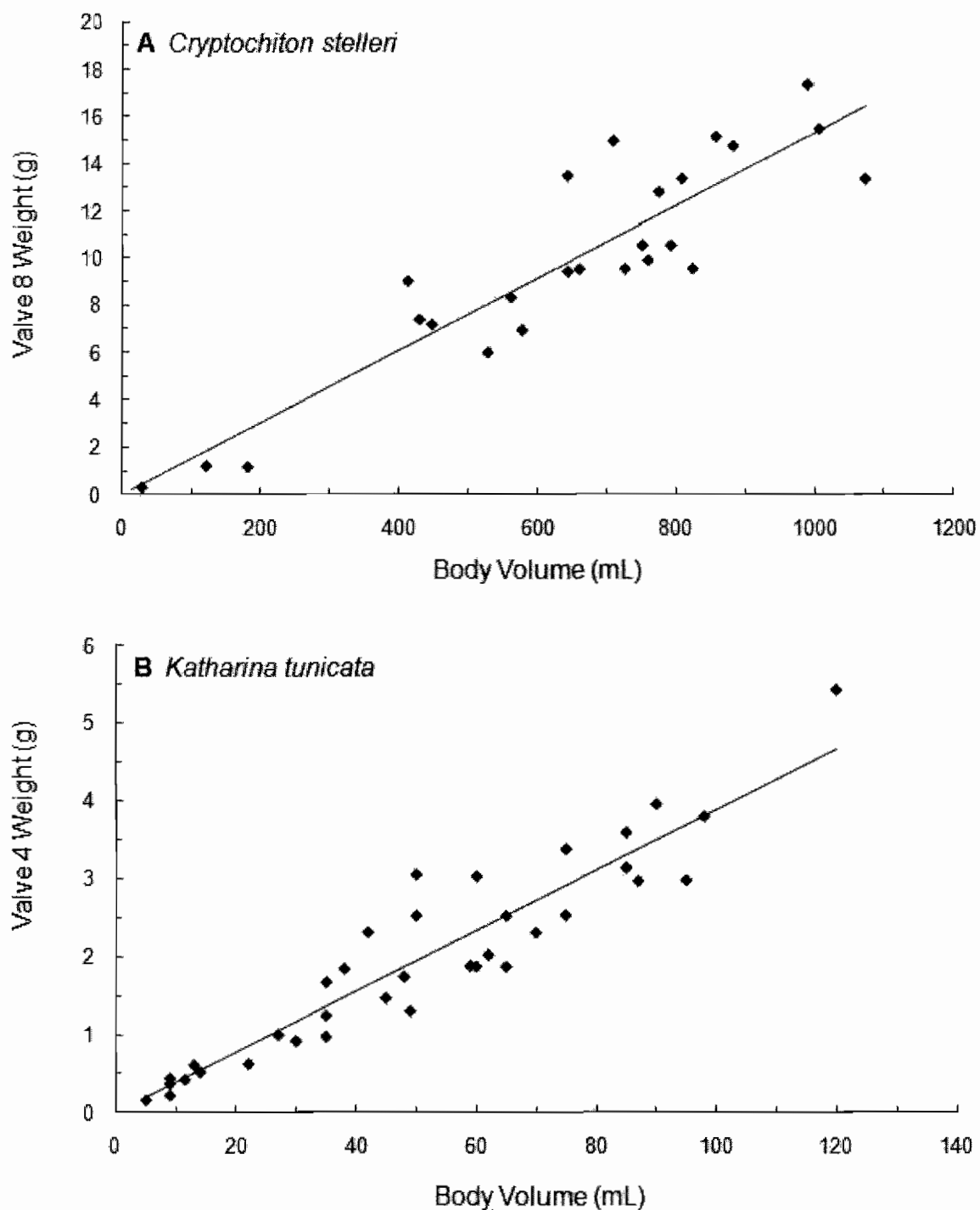
Figure 4.6. Correlation between valve eight weight and body volume in *C. stelleri* and *K. tunicata* collected near Charleston, OR. A significant and positive linear correlation exists between these two variables for both (A) *C. stelleri* (n=25) and (B) *K. tunicata* (n=35).
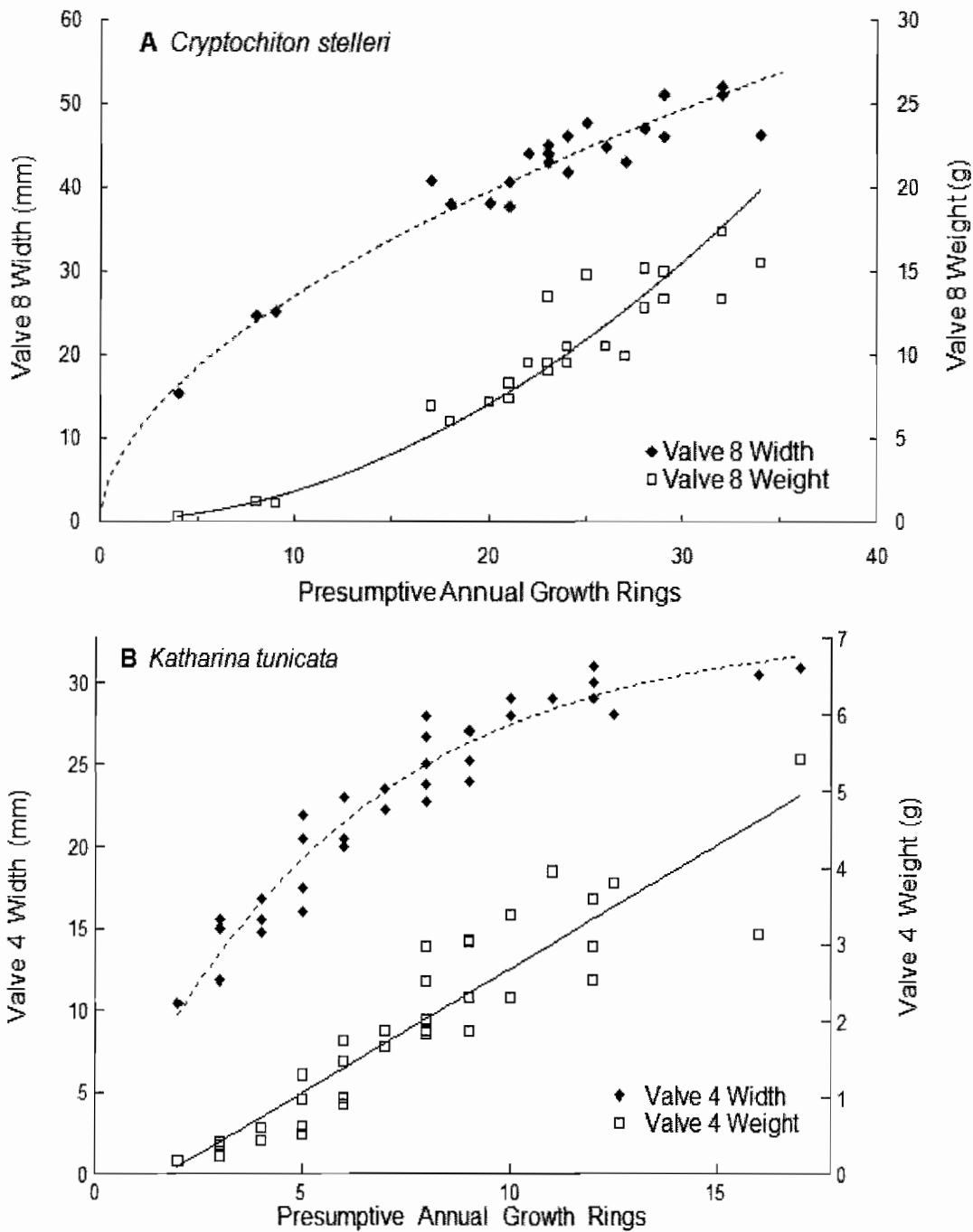
Figure 4.7. Size-at-age curve for age and valve width and valve weight data for Oregon specimens of *C. stelleri* and *K. tunicata*. For both species, the valve width growth rate slows with age, while the valve weight growth rate increases with age. (A) Size-at-age curve for *C. stelleri* valve 8 width and valve 8 weight plotted against presumptive annual growth rings. (B) Size-at-age curve for *K. tunicata* valve 4 width and valve 4 weight plotted against presumptive annual growth rings.
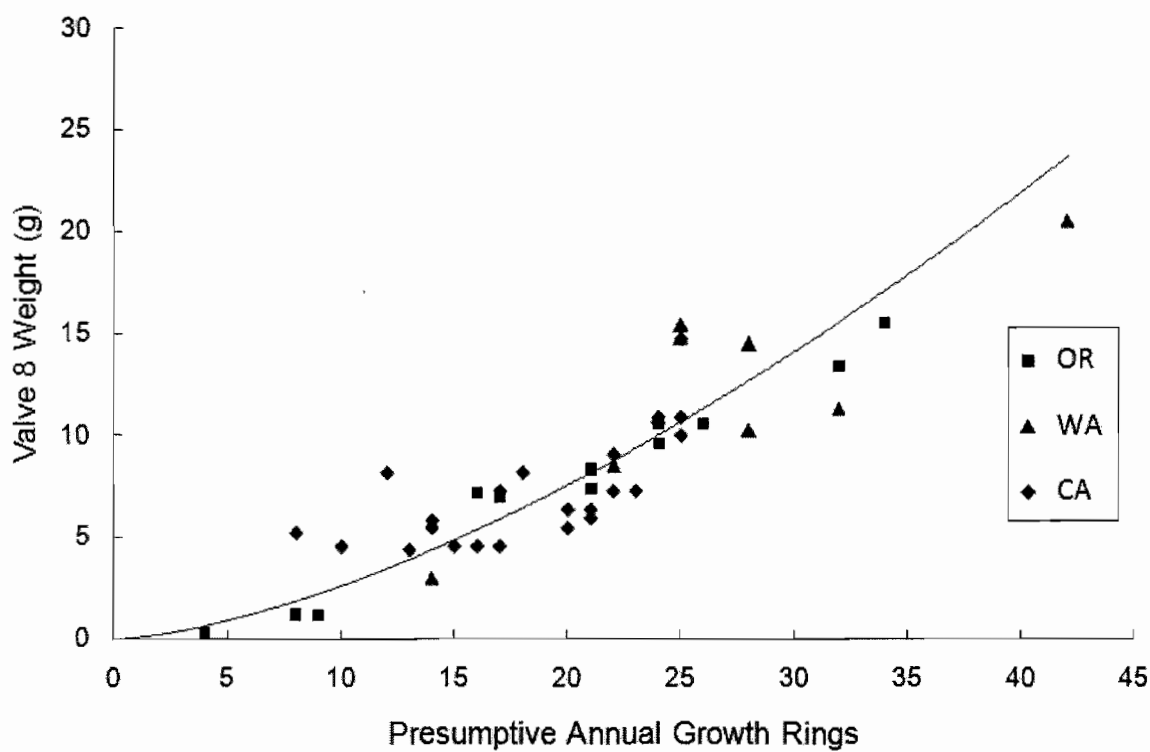
Figure 4.8. Combined size-at-age curve for *C. stelleri* valve eight weight from Washington (n=32), Oregon (n=25), and California (n=12) specimens. The growth rate increases with age when shell weight is used as a measure of size and is plotted against age (presumptive annual growth rings).

C. stelleri age, but were unable to make the necessary counts because the bands faded towards the center of the shell plate. This ring counting method was further called into question by Palmer and Frank (1974), who were doubtful of their ability to clearly elucidate growth lines from the shells. There are vague lines apparent on the external surface of the valves, so it is possible that these superficial lines were the ones referenced by previous studies. The lines used in the present study were only visible on the polished cross sections of the valves.

In the current study, the cross sectioning of valves and use of the acetate peel technique allowed for the successful detection of unambiguous growth lines (Fig. 4.1). By both examining acetate peels under a compound light microscope and analyzing the gray value plot profile of these peels, growth rings were clearly elucidated. The additive method was used to estimate the total number of rings on each *C. stelleri* valve successfully solved the problem of estimating age when growth lines faded towards the center of the valve. Accuracy was further enhanced by using estimated ring counts from at least three valves for every individual, with the average counts used to provide the overall age estimate for that individual. Since growth differs by valve and by location, the curves used to estimate the numbers of rings to the center were made separately for all eight valves from Washington, Oregon, and California specimens (Fig. 4.2). *Katharina tunicata* growth lines were clear and did not fade towards the center of the valves, so the additive method was not necessary to attain accurate estimates of the number of growth rings.

One of the difficulties with growth ring counts, or marginal increment analysis (MIA), is discerning between multiple growth rings. This process can be subjective because of the small distances separating often indiscrete growth lines (Campana, 2001). In the current study, the subjective nature of MIA was minimized by the use of image analysis software to create gray value profiles of each valve coupled with an objective protocol for determining what was a major growth line based on the gray value. Further, randomizing the order of valves processed and taking multiple counts of the same specimen using more than one shell plate further safeguarded against experimenter bias. Despite all of these measures, the biggest safeguard against counting errors may have been the clarity of the growth lines (Fig 4.1); the growth increments in the large valves of this organism could even be distinguished under a low power dissecting scope. While image analysis was not used for *K. tunicata*, the large valves and clarity of the growth lines ensured accuracy.

In order to create size-at-age curves from ring count data, I needed to establish that the major growth rings were annual. Annual growth rings are commonly formed during winter, when a slowdown in growth can result from gonad production, colder temperatures, increased storms, and lower food availability (Crozier, 1918; Baxter and Jones, 1978; Brousseau, 1979; MacDonald and Thomas, 1980; Picken, 1980; Thompson et al., 1980). The production of annual growth rings is especially common among organisms with annual food supplies such as phytoplankton or macroalgae. Annual rings have been shown to form in chitons, limpets, bivalves, fish, and corals, among other organisms (Merrill et al., 1961; Parry, 1978; Brousseau, 1979; Bayne and Worrall, 1980;

MacDonald and Thomas, 1980; Picken, 1980; Thompson et al., 1980; Jones, 1981; Schone, 2003). *Cryptochiton stelleri* and *Katharina tunicata* spawn once per year in the spring (Tucker and Giese, 1962; Himmelman, 1978; Yates, 1989) and feed predominantly on seasonally abundant macroalgae (Dethier and Duggins, 1984; Yates, 1989), so it is likely that the major growth rings are annual.

II. Size-at-age curves

Since the weight of the eighth valve was strongly and positively correlated with *C. stelleri* volume (Fig. 4.6), valve eight weight was used to construct size-at-age curves using all of the available data including the samples from Oregon (OR), as well as the Washington (WA) and California (CA) specimens that were too decomposed to measure any soft tissue morphology. By using the weight of the eighth valve, size-at-age curves could be created for all sites (WA, OR, CA) combined (Fig. 4.8), establishing a general estimate of *C. stelleri* growth. This combined size-at-age curve (Fig. 4.8) displayed roughly the same trend as did curves for the individual states (Table 4.1). Many organisms display differing growth rates with latitude (Dehnel, 1955; Conover and Present, 1990; Conover et al., 1997; Linse et al., 2006; Royo et al., 2006; Howes and Lougheed, 2007), but since the specimens from Washington and California each came from just one site, no definite conclusions can be made about latitudinal variation in growth rate for this species. However, the specimens examined did not appear to differ in growth rate with latitude.

Valves of *C. stelleri* from Washington, Oregon, and California displayed very different distribution of smaller lines around the major presumptive annual growth lines (Fig. 4.1). The narrow, intense growth rings present in the Oregon (Fig. 4.1C) and Washington (Fig. 4.1A) valves are much clearer and more well-defined than in the valves from California specimens, which had a large number of smaller growth rings clustered around the annual rings (Fig. 4.1B). There were no significant differences in major growth line spacing (growth rate) between Washington, Oregon, and California, but the major growth lines on California valves were significantly less distinct than at the other sample sites (Fig. 4.3). This difference could be a result of less seasonality in the warmer and calmer climate of Monterey, California, which could allow *C. stelleri* to be more active during winter. Differences in climate also result in a more constant supply of macroalgae in California (including *Mazzaella splendens*) which could reduce the impact of season on *C. stelleri* growth (Dyck and DeWreede, 2006). Any of these factors could allow individuals of this species to have a growth rate less dependent on season, resulting in less defined growth lines.

Circumference (*C. stelleri*) and length (*K. tunicata*) are the first external morphological measures for which size-at-age curves were constructed. Linear measurements of growth such as these are by far the most prevalent measures incorporated into modeling of growth rates and creation of growth curves for chitons, gastropods, bivalves, fish, and many other organisms (Rao, 1976; Fournier and Breen, 1983; Basson et al., 1988; Bosman and Hockey, 1988; Fouda and Miller, 1981; Ebert and Russell, 1992; Katsanevakis, 2006; Johnson and Black, 2008; Navarte et al., 2008; Kilada

et al., 2009). These circumference-age (*C. stelleri*) and length-age (*K. tunicata*) curves appear similar to typical growth curves, with growth rate slowing with age: these data are fit well with a slowing but indeterminate growth function developed by Rogers-Bennett et al. (2003). Shell width also showed a decrease in growth rate with age (Fig 4.7), indicating that linear shell growth slows with age as well. These curves showing asymptotic or decreasing growth rate with age are typical for linear measurements such as length, width, or diameter.

Volume and weight are measures of absolute size and show a much different growth pattern than the curves based on linear measurements (Fig. 4.5). When size was measured with body volume or body weight, growth rate increased slightly at all ages (Fig. 4.5). This same relationship also existed between valve weight and age for both *C. stelleri* and *K. tunicata* (Fig. 4.7), as valve growth rate based on weight increased with age. This demonstrates that the amount of material added to the shell plates each year increases with age.

The similarity in size-at-age curves for body volume and valve eight weight indicates that a growth function with growth rate slowly increasing over time is the best descriptor of the growth of *C. stelleri* and *K. tunicata*. These growth functions are not asymptotic, unlike the growth curves based on length or circumference, so they can be better used to estimate age. Based on multiple size-at-age curves, the oldest *C. stelleri* specimen in this study was estimated at around 40 years, making *C. stelleri* the oldest species of chiton in the world. The oldest *K. tunicata* specimen in this study was

approximately 17 years old, making it the second-oldest chiton species in the northeast Pacific.

This study provides detailed empirical data on growth and longevity of *Cryptochiton stelleri* and *Katharina tunicata*. It also highlights the differences between growth curves based on linear measures of size and absolute measures of size such as volume. Growth curves based on length, circumference, and valve width all showed decreases in growth rate with age, typical of a growth curve for an indeterminately growing species (Sebens, 1987). In contrast, absolute measures such as body volume, body weight, and shell weight showed an increasing growth rate when plotted against age. The creation of growth curves based on various measures of size for *C. stelleri* and *K. tunicata* allowed a comparison of different aspects of growth and highlighted the intriguing life histories of these chitons.

Bridge

Chapter IV described the growth rates, developed techniques to measure the age of *Cryptochiton stelleri* and *Katharina tunicata* and highlighted the different patterns of growth when one looks at length vs. volume as a measure of the size of the chiton. Both of these species add more shell material later in life than they do when they are young, which is unexpected since the general paradigm is that growth rate slows down with age. Models of life history and energy allocation for most invertebrates and intertidal organisms show a tradeoff from growth to reproduction as the organism gets older, eventually reaching a point where growth is minimal and virtually all energy is allocated to reproduction. The unusual growth patterns of the chiton species examined in Chapter IV led me to investigate growth and energy allocation in a variety of intertidal species in Chapter V. Chapter V focuses on the impact that using different measures of size can have on models of life history and energy allocation.

.

CHAPTER V

IMPACT OF DIFFERENT MEASURES OF SIZE ON ENERGY

ALLOCATION MODELS

Introduction

The size of an organism is of great importance to its ecology and reproductive

output. Regardless of how size is defined, it has an undeniable effect on feeding, growth

rate, and other ecological factors in a wide variety of species (Peters, 1983; Sebens, 1987;

Chase, 1999a; Woodward et al., 2005). In a multitude of organisms from plants to

terrestrial vertebrates to intertidal invertebrates, body size strongly influences

reproductive output and the amount of energy allocated to reproduction (Thompson,

1979; Gibbons and McCarthy, 1986; Lively, 1986; Shields, 1991; Clauss and Aarssen,

1994; Cattaneo-Vietti et al., 1997; Crespi and Teo, 2002). Ecological interactions such as

predation and competition are strongly affected by size as well, even resulting in shifts in

growth rates and life history strategies to cope with the ecological importance of size

(Dayton, 1971; Paine, 1976; Tegner and Dayton, 1981; Osenberg and Mittelbach, 1989;

Chase, 1999a; Arendt and Reznick, 2005). Body size can be important on the individual

and population level as well as on both the immediate and evolutionary time scale,

because organisms may evolve life history patterns to optimize size. However, the way

that size is measured can impact the outcomes of life history and growth or energy allocation models.

Body size is an integral part of life history theory, which concerns lifetime energy allocation with the maximization of lifetime reproductive output (R_o) as the adaptive 'goal' of an organism (Rinke et al., 2008). In order to establish an energetic balance that will allow the optimization of R_o, organisms must account for energetic costs for somatic growth, maintenance, and reproduction (Jokela, 1997). A multitude of studies have presented models that attempt to account for a wide array of factors that influence the energetic budget of organisms. These models focus largely on the well-reported energetic shift between growth and reproduction that occurs in most organisms as they grow older and larger (Heino and Kaitala, 1996, 1999; Kozlowski, 1996a,b; Jokela, 1997; Chase, 1999b; Kozlowski and Gawelczyk, 2002; Kozlowski et al., 2004). This shift occurs at different ages and life history stages for different organisms, and there are a variety of potential reasons for alterations in the timing and rate of this shift in energy allocation from growth to reproduction.

According to several of these life history models, the shift in energy allocation is a balancing act aimed at maximizing lifetime reproductive output by optimizing the size of the organism (Reiss, 1989; Kozlowski, 1996a; Heino and Kaitala, 1999; Kozlowski and Gawelczyk, 2002; Sebens, 2002). In many organisms, individuals with larger body sizes produce more gametes, so ideally, in these species, size would be maximized (Thompson, 1979; Gibbons and McCarthy, 1986; Lively, 1986; Shields, 1991; Clauss and Aarssen, 1994; Cattaneo-Vietti et al., 1997; Crespi and Teo, 2002). However,

growth and energy allocation vary greatly based on the life history strategy of the organism involved.

There are two main life history strategies with regard to when and how much energy to put into growth and reproduction: determinate and indeterminate growth. Organisms with determinate growth reach a size plateau, at which point they cease to grow larger and put all excess energy into reproduction (Sebens, 1987). This group includes most terrestrial vertebrates (Forseth et al., 1994), as well as pinnipeds (Winship et al., 2001), dolphins (Miyazaki, 1977), and some crustaceans and fish (Sebens, 1987). Organisms with indeterminate growth may slow down their growth rate with age, but even the largest show some growth (Sebens, 1987; Kozlowski et al., 2004). This was recognized in one of the first publications on size relationships and allometry, in which Julian Huxley wrote, "rate of growth may, and doubtless does, slow down with increasing size and age" (1932). A wide array of organisms display indeterminate growth; this includes plants, many fish, amphibians, and most soft-bodied invertebrates (Sebens, 1987; Kozlowski, 1996b; Rinke et al., 2008).

Indeterminate growth has been described using multiple growth functions, and Kozlowski (1996b, 2004) explains that indeterminate growth could be estimated best with the von Bertalanffy growth function (von Bertalanffy, 1938), which is a common model of asymptotic growth. The von Bertalanffy has been used to express growth curves for a variety of fish (Ricker, 1975; Chen et al., 1992; Hood and Schlieder, 1992; Essington et al., 2001; Lester et al., 2004), mussels (Steffani and Branch, 2003), whelks (Ebert and Lees, 1996), and sea urchins (Ebert and Russell, 1992; Rogers-Bennett et al.,

2003), as well as a variety of other organisms. In all of these instances, this curve was used for organisms with indeterminate growth in order to model the way that the length or diameter of the organism changed with age. Both Kozlowski (1996b) and Rogers-Bennett et al. (2003) describe several other growth functions as well, and all of these equations show size in indeterminately growing organisms approaching an asymptote with age. The one exception is the Tanaka function (Tanaka, 1982). Only the Tanaka function expresses truly infinite increase with no built-in asymptote, even though indeterminate growth is being described.

A reason why asymptotic functions are most commonly used in models of life history and energy allocation is that size is often expressed in linear terms. Length, width, and diameter are commonly used measures of size, especially in mollusks, and several growth and size-at-age curves have been developed using these linear measures of size (Frank, 1965b,c; Kenny, 1969; Suchanek, 1981; Brown and Quinn, 1988; Ebert and Russell, 1992; Ebert and Lees, 1996; Steffani and Branch, 2003; Grupe, 2006). Essentially, when size is measured as length, width, or diameter, only one dimension of size and growth is being accounted for. This is not a problem in itself, as growth curves based on both length and weight can provide insights into the growth of an organism. However, the asymptotic growth patterns shown by length-based growth curves are clearly incorporated into energy allocation models, which may be problematic.

The aforementioned shift from growth to reproduction is well reported (Heino and Kaitala, 1996; Kozlowski, 1996a,b; Jokela, 1997; Chase, 1999b; Heino and Kaitala, 1999; Kozlowski and Gawelczyk, 2002), but appears to be based partially on the apparent

decrease in growth that appears in length-based growth curves of many organisms. Because volume and weight presumably go up as the approximate cube of length, growth and size-at-age curves based on weight and volume may not approach an asymptote. As such, growth could not be described by asymptotic models such as the von Bertalanffy growth function, impacting models of life history and energy allocation. Measures of reproduction such as gonad mass, gonad index, or gonadosomatic index are most often based on mass, and if they are compared to one-dimensional measures of growth, then the resulting patterns could be partially an artifact of the allometric relationship between length (or diameter) and weight (or volume), complicating the idea of 'optimal size.'

The present study investigates the potential impact of using weight and volume (absolute measures) instead of length or diameter (linear measures) in growth curves, with the purpose of determining how these relationships could impact models of energy allocation and life history patterns. The present study compiled linear and absolute size data with previously published size-at-age curves in order to compare the two different curves for the black turban snail *Chlorostoma funebralis*, mussels *Mytilus californianus* and *Mytilus galloprovincialis*, chitons *Katharina tunicata* and *Cryptochiton stelleri*, and limpets *Lottia pelta, Lottia persona*, and *Lottia digitalis* (Frank, 1965b,c; Suchanek, 1981; Ebert and Lees, 1992; Steffani and Branch, 2003). The present study also compares how shell measurements and fecundity change with size and age in several gastropods and chitons. By determining the relationships between growth, reproduction, and various measures of size, the accuracy of life history and energy allocation models can be assessed for organisms with indeterminate growth.

Materials and Methods

I. Growth curves

Organisms used for this study were from rocky intertidal areas along the south central Oregon coast, just south of Charleston, Oregon (43°18.191'N, 124°23.198'W). All species used were measured during February or March 2010, and all conspecific specimens were always measured on the same day to avoid between individual variability. In order to create growth curves from absolute measures of size such as weight and volume, ten Oregon intertidal species with published growth curves were measured during March 2010. All growth curves created in this study were fitted with growth functions using XLFit® 5 (IDBS software) in order to determine the best-fitting curves.

Sea urchins *Strongylocentrotus purpuratus* and *Strongylocentrotus franciscanus,* black turban snail *Chlorostoma funebralis,* mussels *Mytilus californianus* and *Mytilus galloprovincialis,* chitons *Cryptochiton stelleri* and *Mopalia muscosa,* and limpets *Lottia pelta, Lottia persona*, and *Lottia digitalis* were collected at the sites listed in Table 5.1. Sample sizes and measurements made on each species are listed as well (Table 5.1). These data were combined with published growth curves for each species; all published curves had a linear measurement of size plotted against age (Table 5.1). Both linear (length, diameter) and absolute measures (weight or volume) were measured for each species and were used to create linear and absolute growth curves. All measurements of size were made in the laboratory immediately after specimens were collected. Weight was measured with a digital balance, except for *S. franciscanus*, which was weighed with

a spring scale. Volume was measured using water displacement in 10 to 2000 mL

graduated plastic containers, depending on the size of the organism. The precision of the

weight and volume measurements for each organism are listed in Table 5.1. Linear

measurements of test diameter, body length, and shell width were measured to the nearest

0.1 mm using vernier calipers.

Table 5.1. Collection sites and measures of size used for all species for which absolute
growth curves were created. The previous studies from which linear growth curves were
taken are also listed.

Species	Field Collection Location	Present + Previous Study Linear Measure	Previous Study	Present Study Absolute Measure of Size	Present Study Accuracy	N
Strongylocentrotus purpuratus	Gregory Point	Test diameter	Grupe, 2006	Body Volume	< 5 mL	19
Strongylocentrotus franciscanus	Gregory Point	Test diameter	Ebert and Russell, 1992	Body Weight	< 10 g	13
Chlorostoma funebralis	Gregory Point	Shell width	Frank, 1965c	Body Volume	<1 mL	22
Mytilus californianus	Gregory Point	Shell length	Suchanek, 1981	Body Volume	< 5 mL	22
Mytilus galloprovincialis	Charleston, OR, Docks	Shell length	Steffani and Branch, 2003	Body Weight	< 0.01 g	18
Cryptochiton stelleri	South Cove of Cape Arago	Circumference	Lord, unpubl. data	Body Volume	< 10 mL	25
Katharina tunicata	South Cove of Cape Arago	Body Length	Lord, unpubl. data	Body Volume	< 1 mL	19
Lottia pelta	South Cove of Cape Arago	Body Length	Frank, 1965b	Body Weight	< 0.01 g	11
Lottia persona	South Cove of Cape Arago	Body Length	Kenny, 1969	Body Weight	< 0.01 g	16
Lottia digitalis	South Cove of Cape Arago	Body Length	Frank, 1965b	Body Weight	< 0.01 g	14

For *Tonicella lineata, Mopalia muscosa, Katharina tunicata, Cryptochiton stelleri,* and *Lottia scutum*, valves or shells were removed, cleaned, and dried before measurements were taken. Valve or shell weight was measured on a digital balance to the nearest 0.01 gram. Valve width was measured to the nearest 0.1 mm at the widest point of the valve with vernier calipers. Shell length was measured at the longest point of the shell for the limpets *L. scutum* and *Acmaea mitra* (collected at Gregory Point). Shells of the predatory snails *Nucella lamellosa* and *Callianax biplicata* were collected at Yoakim Point, three kilometers south of Charleston, Oregon, and were weighed and measured in the same way as the limpets.

The length (mm) and volume (mL) for all chiton and limpet species used were plotted against each other to observe how length varied with volume. These plots were fit with curves using XLFit® 5 (IDBS software) and were compared with 3-D models of a chiton and a limpet. This was done in order to determine if the body shape of these organisms was changing as they grew, affecting growth patterns. The 3-D models were created in Google Sketchup® (Fig. 5.1) and were enlarged proportionally in one millimeter length increments. Using length and volume tools in that program, these models were used to estimate volumes at given sizes with no change in shape. A length-volume plot for the model was produced, showing how volume would vary with length with no change in body proportions as the animal grew. These length-volume plots were fit with curves and compared to the length-volume graphs created from the different species of chitons and limpets.
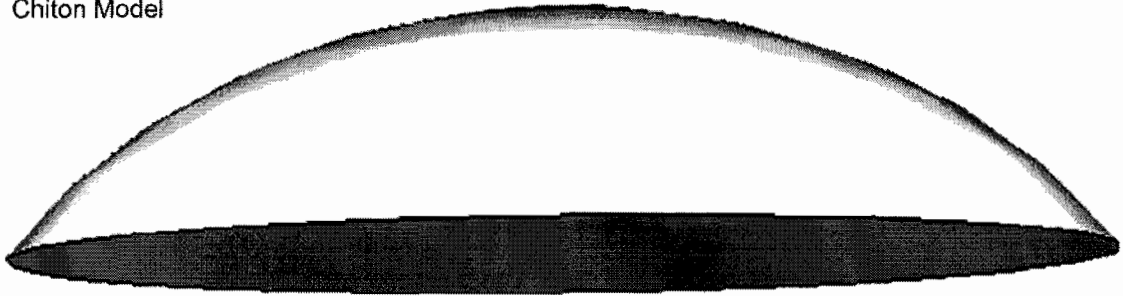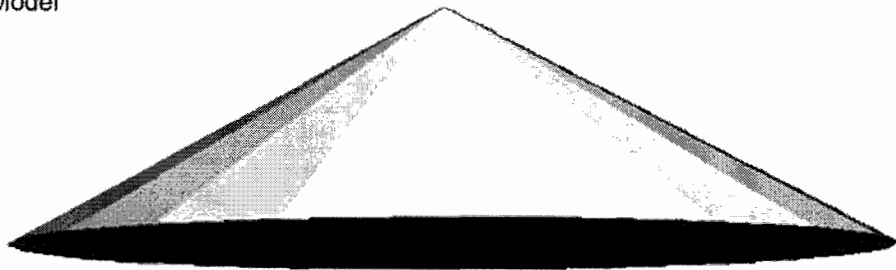
Figure 5.1. 3-D models of limpet and chiton body shape created in Google Sketchup®
and used to measure how volume changed with length if body shape remained the same.
(A) Chiton model drawn in the general shape of a chiton; (B) Limpet model drawn in
general shape of a limpet

II. Size and reproductive output

To determine the relationship between size and reproductive output, the following chiton and limpet species were collected from Gregory Point, five kilometers south of Charleston, Oregon during February 2010: *Tonicella lineata, Mopalia muscosa, Katharina tunicata, Cryptochiton stelleri,* and *Lottia scutum.* The following measurements were made on all 30 specimens of each of the five species: length (mm) or circumference (mm, *C. stelleri*), volume (mL), weight (g), valve 4 or shell weight (mm), and valve 4 or shell width (mm). Length was measured with vernier calipers to the nearest tenth of a millimeter, volume was measured to the nearest mL with water displacement in graduated containers, and wet weight was measured on a digital scale to the nearest tenth of a gram.

For each of these species, all gonad material was dissected out and diluted in 20, 120, or 500 mL plastic bottles (depending on the size of the species) filled with 45 μm filtered seawater so that subsamples could be accurately counted. The containers were stirred and shaken until all eggs were free from the gonad material. Ten 200 μL subsamples were taken from the suspended egg dilution with a micropipetter and placed in small rows on a dish under a dissecting microscope. Eggs in each 200 μL subsample were counted, the ten subsample values were averaged, and then these averages were multiplied by the diluted volume in order to estimate the total fecundity for that individual.

For all of the egg counts, the bottles used were randomly numbered so that there was no bias in the counting process. Numbers and counts were later matched up to plot

the counts against different measures of size for all specimens of each species. The rate at which egg counts varied with body length were compared to curves created with volume, weight, and shell sizes.

III. Feeding experiments

Feeding experiments were performed with the gumboot chiton *Cryptochiton stelleri*, and the black turban snail *Chlorostoma funebralis* in order to determine how feeding scales with size. These experiments were conducted in flowing seawater tables at the Oregon Institute of Marine Biology, with individual *C. stelleri* kept in 10 gallon aquaria and *C. funebralis* in 50 mL plastic containers covered with 1.0 mm mesh. The *C. stelleri* aquaria were supplied with flowing seawater via a single plastic tube going to each tank, all from the same flowing seawater source. The *C. funebralis* containers all floated freely in a single flowing seawater table. The red alga *Mazzaella splendens* is a common food item for *C. stelleri,* so this alga was collected from Gregory Point, 5 km south of Charleston, Oregon. Bull kelp *Nereocystis luetkeana* is a preferred food of *C. funebralis* (Steinberg, 1985) and was used for this experiment. Both *C. stelleri* and *C. funebralis* were provided with a constant supply of algae during April and May 2010.

For *C. stelleri*, specimen length, circumference, volume, and wet weight were measured before the experiment began. Shell diameter (at the widest point) and total wet weight were used to measure *C. funebralis* size. Feeding was determined by measuring seaweed weight consumed by each organism. For both species, seaweed was patted dry with paper towels and then weighed on a digital scale to the nearest 0.01 gram. It was

placed in each tank or container, then two days later was patted dry again, weighed, and new seaweed was added. Amount consumed was determined by subtracting the experimental seaweed weight (after two days) from the original weight. Seaweed controls were done to account for unrelated changes in seaweed weight and consisted of empty tanks or containers containing seaweed patted dry and weighed by the same process as the treatments.

Results

I. Growth curves

The formulas for all growth functions for linear and absolute measures of size plotted against age are described in detail in Table 2. This includes the growth function used to fit the curve using XLFit® (IDBS software), the correlation coefficient for each of the curves, and all parameters for each function. Data used to create length-age curves were taken from previous studies on each organism. Therefore, the age used in the growth functions was an estimate based on published growth curves and the length of the organism. In all instances, the linear measurements (length, test diameter, shell width) result in curves that go up steeply at first and then quickly slow, nearing an asymptote as linear growth slows down dramatically with size.

Using volume and weight resulted in differently shaped curves. Instead of size approaching an asymptote, these models of size continued a steady increase regardless of age. In *C. funebralis* (Fig. 5.2C) and *M. galloprovincialis* (Fig. 5.2E), volume and weight accretion slow with age, but never approach an asymptote. For the urchins *S. purpuratus*

Table 5.2. Functions describing relationships between age both linear (length, diameter) and absolute (weight, volume) measures of size. For each species, the x and y variables are listed, as well as the function that was fit to the data. Best fits were selected and correlation coefficients were calculated using XLFit® 5 software. The function named 'Rogers-Bennett' is an indeterminate growth function published in Rogers-Bennett et al. (2003).

Species	y	x	Function	Equation	R^2
Strongylocentrotus purpuratus	Test Diameter (mm)		Shifted Power	$y=(38.5*((x - 0.965)^{0.213}))$	1.00
	Volume (mL)		Rogers-Bennett	$y=(75.9*(0.87-(e^{-0.162x})))+3.18x$	1.00
Strongylocentrotus franciscanus	Test Diameter (mm)		Rogers-Bennett	$y=(82.3*(1.01-(e^{-0.310x})))+1.36x$	1.00
	Weight (g)		Rogers-Bennett	$y=(198.6*(0.75-(e^{-0.31x})))+19.6x$	1.00
Chlorostoma funebralis	Shell Width (mm)		Rogers-Bennett	$y=(21.1*(0.943-(e^{-0.403x})))+0.34x$	1.00
	Volume (mL)		Rogers-Bennett	$y=(14.2*(0.96-(e^{-0.040x})))-0.030x$	1.00
Mytilus californianus	Shell Length (mm)		Rogers-Bennett	$y=(65.7*(0.993-(e^{-1.02\,x})))+13.2x$	1.00
	Volume (mL)		Power Fit	$y=(-2.16 + (18.15*(x^{1.48})))$	1.00
Mytilus galloprovincialis	Shell Length (mm)		Rogers-Bennett	$y=(78.7*(0.98-(e^{-0.20x})))+0.246x$	1.00
	Weight (g)	Age	Chapman	$y=(36.9*((1-exp((-0.24)*x))^{3.27}))$	1.00
Katharina tunicata	Body Length (mm)		Chapman	$y=(109.4*((1-exp((-0.30)*x))^{1.44}))$	0.85
	Volume (mL)		Two Power Fits	$y=(1.61*(x^{1.24})) + (2.4*(x^{1.23}))$	0.85
Cryptochiton stelleri	Circumference (cm)		Rogers-Bennett	$y=(31.97*(1.01-(e^{-0.085x})))+0.17x$	0.96
	Volume (mL)		Rogers-Bennett	$y=(-156.1*(1.1-(e^{-0.396x})))+40.2x$	0.88
Lottia pelta	Shell Length (mm)		Rogers-Bennett	$y=(16.4*(1.29-(e^{-0.88x})))+3.23x$	1.00
	Weight (g)		Rogers-Bennett	$y=(-14.4*(0.15-(e^{-3.18x})))+2.22x$	1.00
Lottia persona	Shell Length (mm)		Rogers-Bennett	$y=(28.4*(0.99-(e^{-0.446x})))+1.13x$	0.98
	Weight (g)		Rogers-Bennett	$y=(-0.95*(0.966-(e^{-8.3*10E23})))+x$	1.00
Lottia digitalis	Shell Length (mm)		Rogers-Bennett	$y=(12.8*(1.01-(e^{-1.46x})))+1.78x$	0.93
	Weight (g)		Rogers-Bennett	$y=(-0.236*(1.37-(e^{-0.007x})))+0.34x$	0.99

Figure 5.2. Linear and multidimensional measurements of size plotted against age. Curves showing linear measurements plotted against age were extrapolated from the studies listed for each organism. These data were combined with multidimensional measures of size to create volume-age and weight-age curves (A) *Strongylocentrotus purpuratus*, Grupe, 2006 (B) *Strongylocentrotus franciscanus,* Ebert and Russell, 1992 (C) *Chlorostoma funebralis*, Frank, 1965c (D) *Mytilus californianus*, Suchanek 1981 (E) *Mytilus galloprovincialis*, Steffani and Branch, 2003 (F) *Katharina tunicata*, Lord (unpubl. data) (G) *Cryptochiton stelleri*, Lord (unpubl. data) (H) *Lottia pelta*, Frank, 1965b (I) *Lottia persona*, Kenny, 1969 (J) *Lottia digitalis*, Frank, 1965b.

(Fig. 5.2A) and *S. franciscanus* (Fig. 5.2B), the rate at which volume or weight is added goes up steeply at first and then slows to an apparently linear rate of increase at about 15 years of age. After the 15-year mark, *S. purpuratus* added approximately 16 mL of volume per year (Fig. 5.2A), while *S. franciscanus* adds approximately 20g of weight per year (Fig. 5.2B). *Mytilus californianus* (Fig. 5.2D), the chitons *C. stelleri* (Fig. 5.2G) and *K. tunicata* (Fig. 5.2F), and the limpets *Lottia pelta* (Fig. 2H), *L. persona* (Fig. 5.2I), and *L. digitalis* (Fig. 5.2J) increased their rate of absolute growth (volume) as they got older, evidenced by upward trending volume-age curves.

Linear (width) and absolute (weight) measures of shell size varied in the same manner as did the linear and absolute measurements of body size (Fig. 5.3). Shell width and shell weight for *K. tunicata* (Fig. 5.3A) and *C. stelleri* (Fig. 5.3B) were plotted against age, with best fitting equations shown on the graphs. Rate of increasing shell width slows with age in both species while the rate of accumulating shell weight is linear for *K. tunicata* (Fig. 5.3A) and gradually increasing for *C. stelleri* (Fig. 5.3B).

The length-volume plots created for all chiton and limpet species were best fit by an indeterminate growth function presented by Rogers-Bennett et al. (2003) (Table 5.3). All chiton (Fig. 5.4) and limpet (Fig. 5.5) species showed a very similar curve to the length-volume relationship created in the 3-D models of chiton and limpet growth, in which the shape of the 'organism' did not change as the model organism "grew" (Figs. 5.4, 5.5).
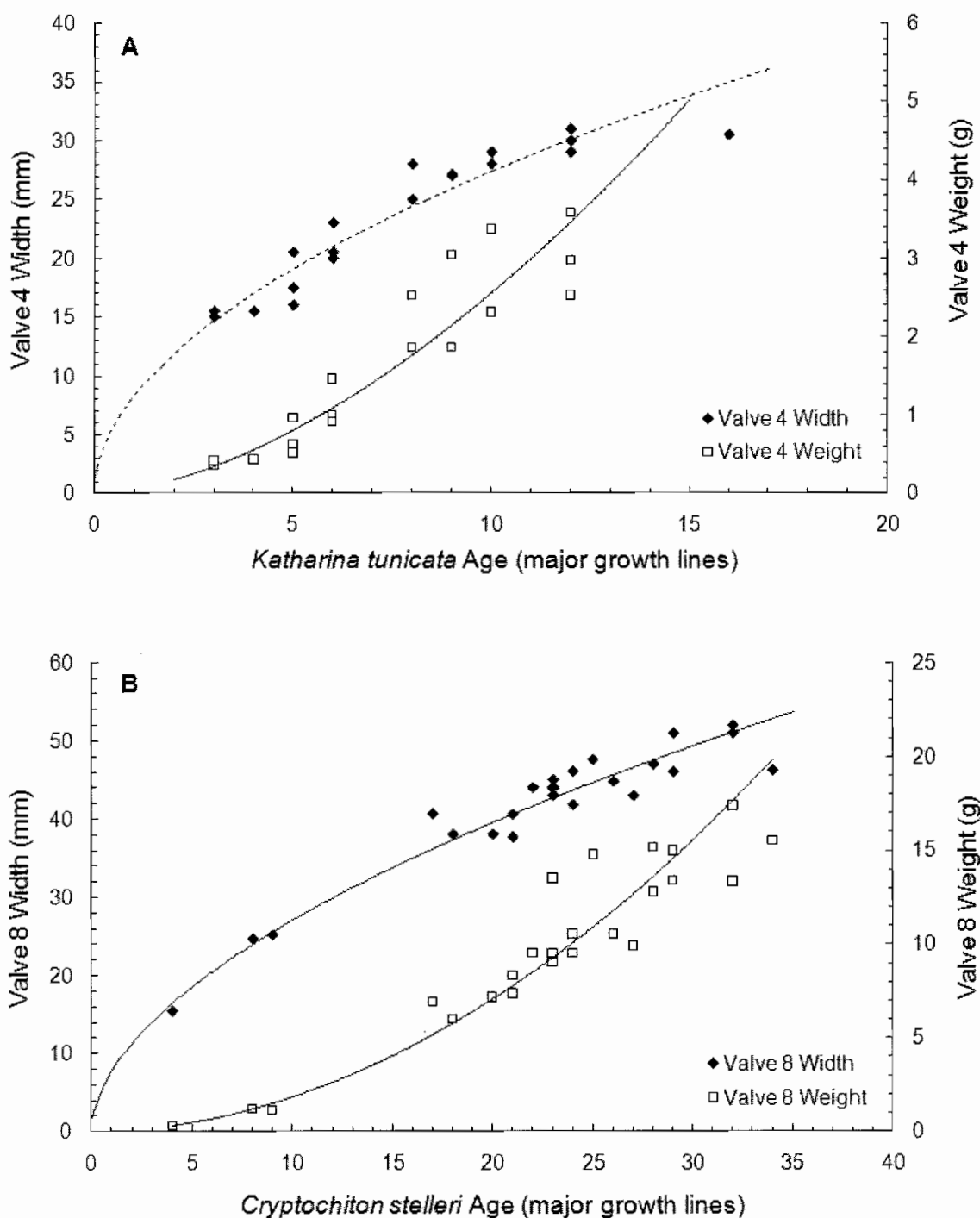
Figure 5.3. Valve weight and valve width plotted against age for *Katharina tunicata and Cryptochiton stelleri.* (A) *K. tunicata* valve four weight and valve four width plotted against age; (B) *C. stelleri* valve four weight and valve four width plotted against age.

Table 5.3. Functions describing the body volume-body length relationship for four species of chiton and the limpet *Lottia scutum*. Also included are volume-length data from multidimensional models of a limpet and a chiton, created in Google Sketchup®. Best fits were selected and correlation coefficients were calculated using XLFit® software. The function named 'Rogers-Bennett' is an indeterminate growth function published in Rogers-Bennett et al. (2003).

Species	Y	X	Function	Equation	R^2
Chiton model			Power Fit	$y=(-2.17+(26.36*(x^{0.329})))$	1.0
C. stelleri			Rogers-Bennett	$y=(210.8*(1.17-(e^{-0.006x}))) + 0.120x$	0.99
T. lineata		Body	Rogers-Bennett	$y=(13.3*(1.62-(e^{-1.57x}))) + 5.21x$	0.89
K. tunicata	Body	Volume	Rogers-Bennett	$y=(205.4*(1.19-(e^{-0.011x}))) - 0.77x$	0.97
M. muscosa	Length	(mL)	Rogers-Bennett	$y=(94.09*(1.176-(e^{-0.067x}))) - 0.99x$	0.95
Limpet Model	(mm)		Power Fit	$y=(0.118+(24.01*(x^{0.335})))$	1.0
L. scutum			Rogers-Bennett	$y=(64.8*(1.04-(e^{-0.46x}))) - 1.75x$	0.88
L. pelta		Body	Rogers-Bennett	$y=(13.1*(1.63-(e^{-1.55x}))) - 8.28x$	0.99
L. persona		Weight	Rogers-Bennett	$y=(13.5*(1.71-(e^{-0.98x}))) - 1.70x$	0.99
L. digitalis		(g)	Rogers-Bennett	$y=(10.7*(0.987-(e^{-16.2x}))) -9.0x$	0.96
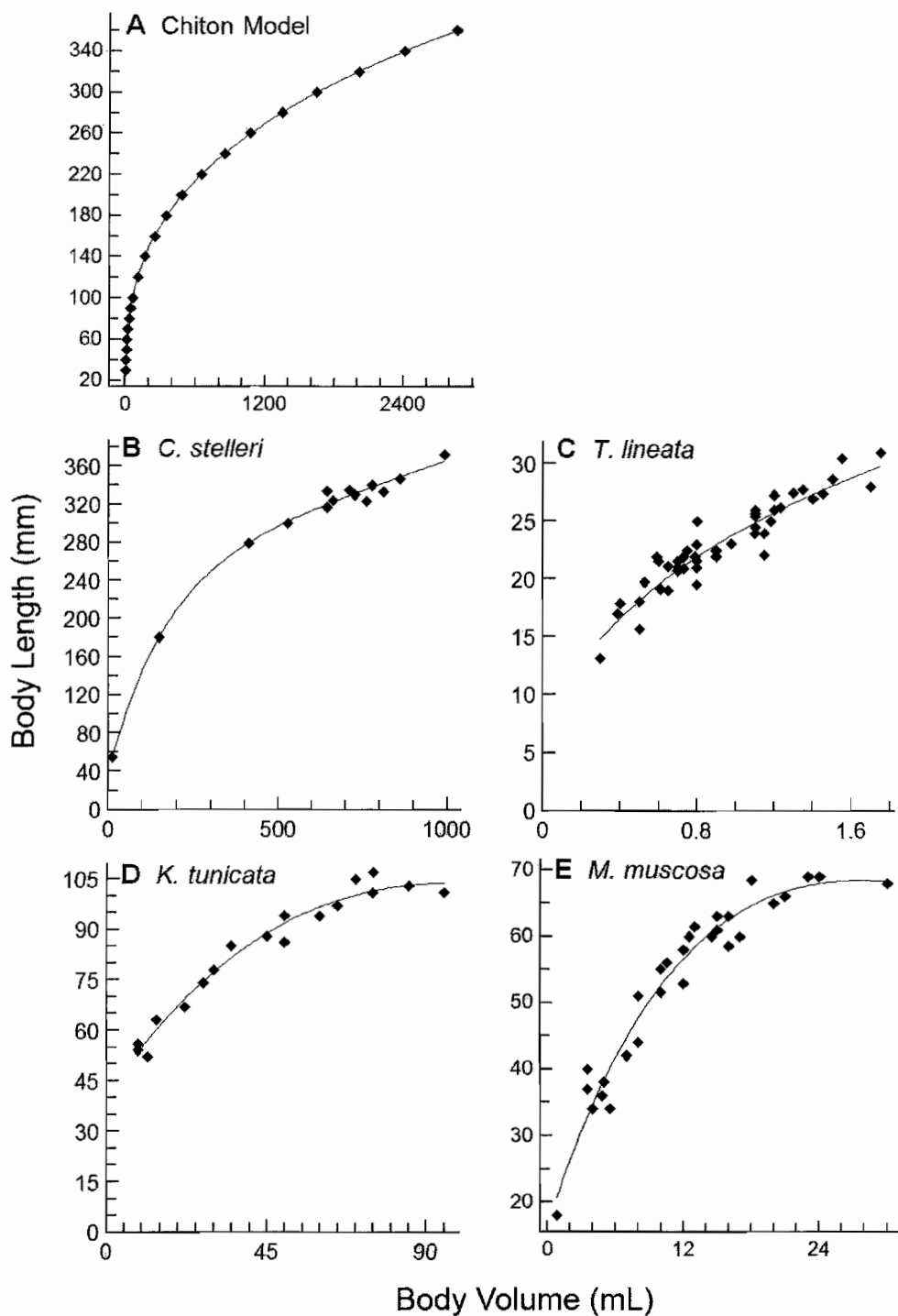
Figure 5.4. Body length (mm) plotted against body volume (mL) for four species of chitons, compared to dimensions of a multidimensional model of a chiton (Fig. 5.1A) that kept exactly the same body proportions as it increased in size (A). Chitons include (B) *Cryptochiton stelleri*; (C) *Tonicella lineata*; (D) *Katharina tunicata;* (E) *Mopalia muscosa.*
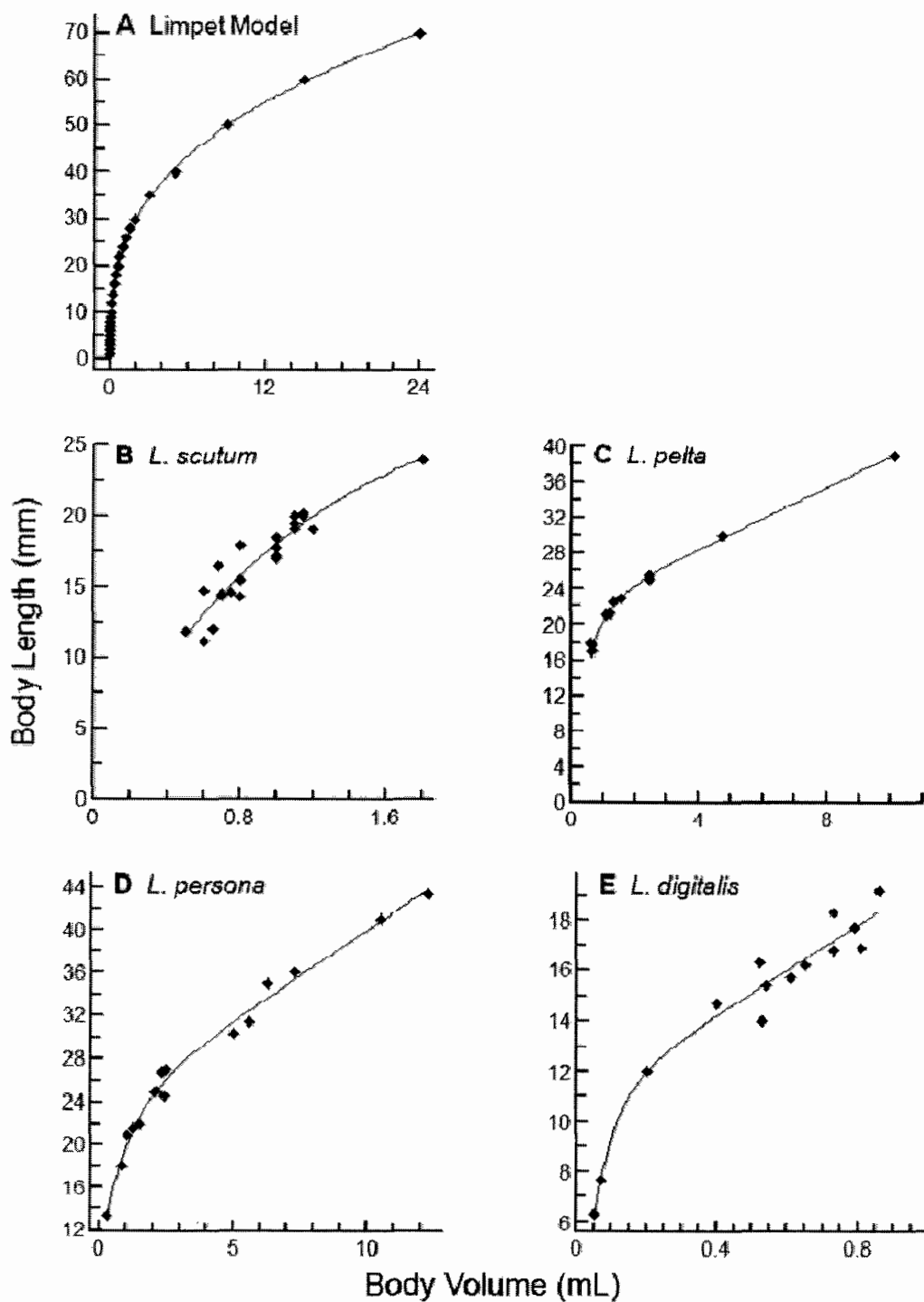
Figure 5.5. Body length (mm) plotted against body volume (mL) for four species of limpets, compared to a multidimensional model of a limpet (Fig. 5.1B) that kept the same body proportions as it increased in size (A). Limpets include (B) *Lottia scutum*; (C) *Lottia pelta*; (D) *Lottia persona*; (E) *Lottia digitalis.*

II. Size and reproductive output

Egg counts were related differently to linear and absolute measures of size. In all species examined, fecundity increased exponentially relative to body length (Figs. 5.6 A,C,E,G,I). However, these fecundity estimates varied linearly with body volume in all these species (Figs. 5.6 B,D,F,H,J). After comparison of hundreds of curve fits in XLFit®, the best fit curves for fecundity-length were all two parameter exponential growth functions and the best fits for fecundity-volume were all linear functions. All equations and correlation coefficients are presented in Table 5.4.

As a result of the linear relationship between egg count and body volume, size at first reproduction in females could be estimated using the x-axis intercept. Because growth rates are known for *K. tunicata* and *C. stelleri*, age estimates for first reproduction could be made as well (Lord, Chapter 4): first reproduction in *K. tunicata* occurs at two years and in *C. stelleri* at 14 years old.

Table 5.4. Relationships between egg counts of different measures of body size. Most relationships with body length are described by power functions, while most relationships with body volume are best fit with a line. The x and y variables are given for each function, as is the function type, formula, and correlation coefficient.

Species	x	y	Function Type	Formula	R^2
Tonicella lineata	Body Length		Exponential	$y = 16.7 * e^{0.25x}$	0.90
	Body Volume		Linear	$y = 13022x - 5.6*10^3$	0.84
Mopalia muscosa	Body Length		Exponential	$y = (5.60*10^2) * e^{0.072x}$	0.91
	Body Volume		Linear	$y = 3413.4x - 9.8*10^3$	0.98
Katharina tunicata	Body Length	Egg Count	Exponential	$y = (1.27*10^4) * e^{0.035x}$	0.94
	Body Volume		Linear	$y = 8000.0x - 4.2*10^4$	0.95
Cryptochiton stelleri	Body Length		Exponential	$y = (4.40*10^3) * e^{0.023x}$	0.95
	Body Volume		Linear	$y = 9914.2x - 4*10^6$	0.75
Lottia scutum	Body Length		Exponential	$y = (4.10*10^2) * e^{0.22x}$	0.93
	Body Volume		Linear	$y = 74295x - 48010$	0.87
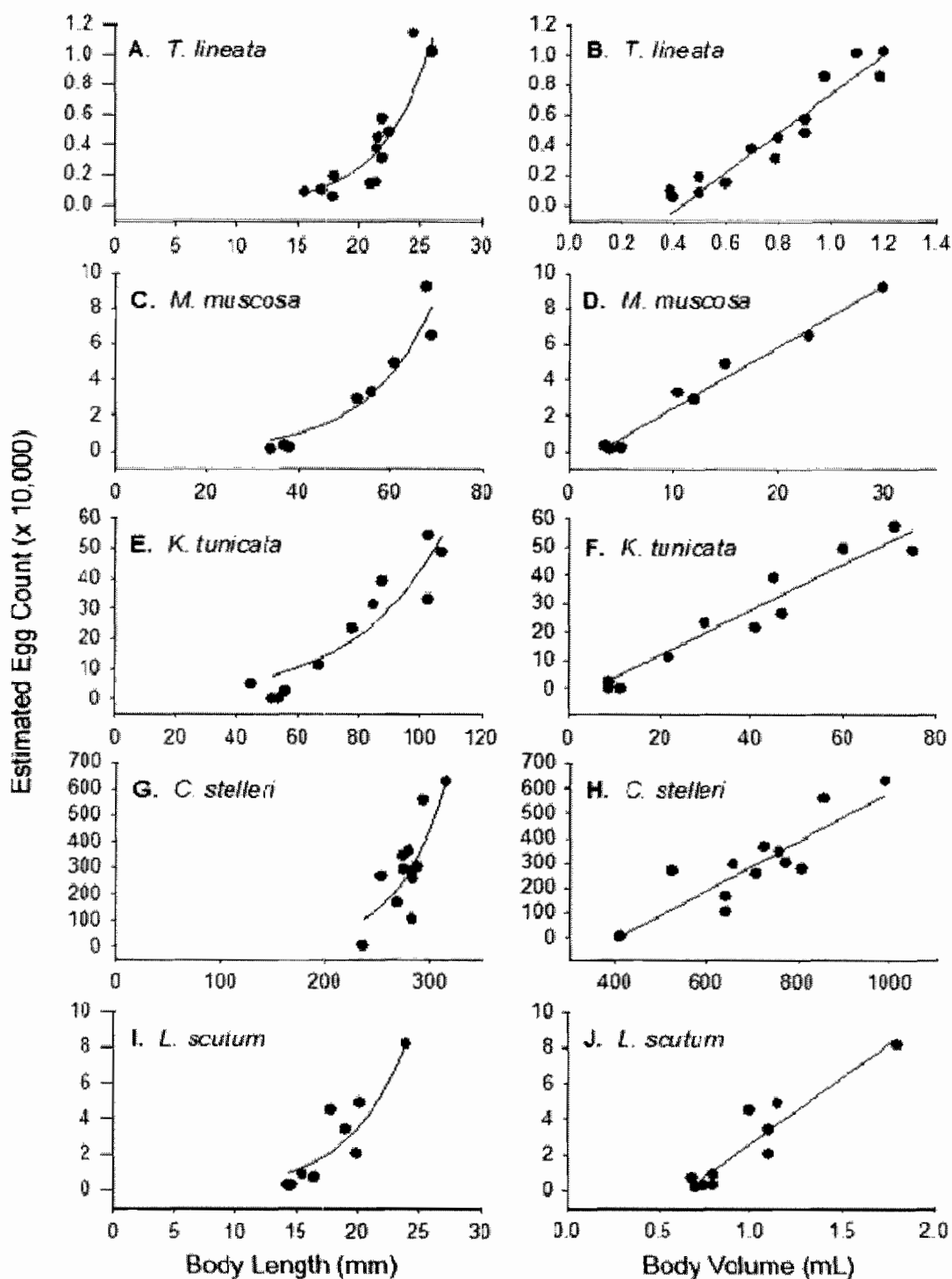
Figure 5.6. Estimated egg counts plotted against linear (length) and multidimensional (volume) measures of body size. All lengths are expressed in millimeters and all volumes are expressed in milliliters. All egg counts in the first column are plotted against length, and all in the second column are plotted against volume. (A,B) *Tonicella lineata,* (C,D) *Mopalia muscosa,* (E,F) *Katharina tunicata,* (G,H) *Cryptochiton stelleri,* (I,J) *Lottia scutum.*

III. Feeding experiments

The weight of seaweed consumed per day by both *Cryptochiton stelleri* and *Chlorostoma funebralis* was related exponentially to the length of the organism (Fig. 5.7) (Table 5.5). Seaweed consumption plotted against length for *C. stelleri* was best fit by a general exponential growth model ($r^2 = 0.96$). The best-fit function for *C. funebralis* shell width-feeding was a rational model ($r^2 = 0.92$). The amount of seaweed consumed plotted against body weight was best-fit by a linear function ($r^2 = 0.96$) for *C. stelleri* and by an indeterminate growth function published by Rogers-Bennett et al. (1992) ($r^2 = 0.89$) for *C. funebralis* (Table 5.5).

Table 5.5. Relationships between body length or total width and the amount of algae consumed per day for *Cryptochiton stelleri* (n = 30) and *Chlorostoma funebralis* (n = 26). The best fit functions are given for each relationship, as well as the formula and correlation coefficient. All data were best fit by curves in XLFit® 5.

Species	x	y	Function Type	Formula	R^2
Cryptochiton stelleri	Body Length		Linear	$y = 0.0061x + 0.23$	0.96
	Total Weight	Algae consumed per day (g)	General exponential growth model	$y = 0.14 * e^{0.14x}$	0.96
Chlorostoma funebralis	Shell Width		Rogers-Bennett et al.	$y = (0.89 * (0.31\text{-}(e^{-x}))) + 0.034x$	0.89
	Total Weight		Rational Model	$y = (\text{-}14 + (19x)) / ((1.0 + 76x) + (\text{-}2.0x^2))$	0.92
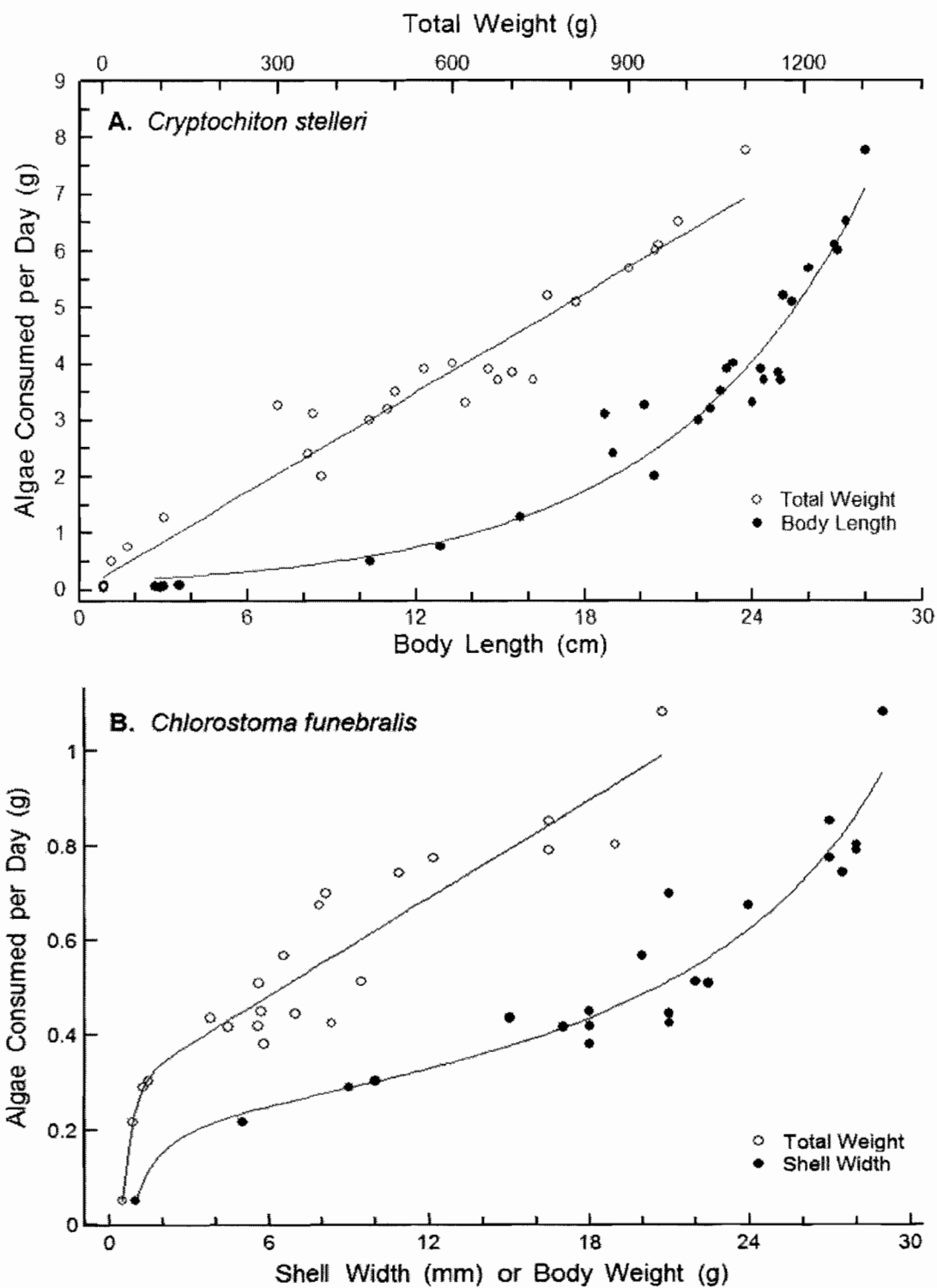
Figure 5.7. Algae consumed per day plotted against both body length and total weight (shell+soft tissue). Data for *Cryptochiton stelleri* (A) and *Chlorostoma funebralis* (B) are best fit by the curves on these graphs, with equations shown in Table 4.

Discussion

Models of energy allocation and life history strategies are based on the assumption that an important adaptive goal is to optimize lifetime reproductive output (R_o) (Rinke et al., 2008). While maintenance, growth, and reproduction are major factors in the energy budget of an organism, the balance between growth and reproduction is the most commonly modeled aspect of energy allocation models (Heino and Kaitala, 1996, 1999; Kozlowski, 1996a,b; Jokela, 1997; Chase, 1999b; Heino and Kaitala, 1999; Kozlowski and Gawelczyk, 2002). Organisms with indeterminate growth are more difficult to model because they do not undergo a complete shift from growth to reproduction as do organisms with determinate growth. While models of indeterminate growth vary, they are primarily based on linear measures of growth and show a decrease in growth rate as an increasing amount of energy is put towards reproduction, until the model organism is hardly growing at all (Heino and Kaitala, 1996, 1999; Kozlowski, 1996a,b; Jokela, 1997; Chase, 1999b; Kozlowski and Gawelczyk, 2002).

However, this pattern of slowing growth with age is not apparent when weight or volume is used instead of length or diameter to measure the size of the organism. All organisms included in this study display indeterminate growth, as do many invertebrates (Sebens, 1987; Kozlowski, 1996b; Rinke et al., 2008), and all displayed a continuous increase in size with age (Fig. 5.2). However, length-age curves (Fig. 5.2, Table 5.2) appear as typical asymptotic growth curves and are the predominant type of growth curves in the literature (Frank, 1965b,c; Kenny, 1969; Suchanek, 1981; Brown and Quinn, 1988; Ebert and Russell, 1992; Ebert and Lees, 1996; Steffani and Branch, 2003;

Grupe, 2006). The growth curves in Figure 2 plotting length against age show a clear decrease in growth rate with age, similar to that expressed by energy allocation models of indeterminate growth. Just like body length, linear shell growth slows dramatically with age for the chitons *K. tunicata* and *C. stelleri* (Fig. 5.3). This pattern has led to the idea of an ontogenetic shift in the allocation of energy from growth to reproduction (Heino and Kaitala, 1996; Kozlowski, 1996a,b; Jokela, 1997; Chase, 1999b; Heino and Kaitala, 1999; Kozlowski and Gawelczyk, 2002; Kozlowski et al., 2004).

However, this ontogenetic decrease in growth with age is not evident when volume or weight are used as an index of size and are plotted against age (Fig. 5.2). Volumetric or absolute growth did slow with age to some extent in *Chlorostoma funebralis* (Fig. 5.2C) and *Mytilus galloprovincialis* (Fig. 5.2E), but not abruptly and not to an asymptote. In sea urchins (Figs. 5.2A, 5.2B) volume and weight go up linearly with age after about 15 years, when the length-age curve would be flattening out. This linear growth rate later in life is especially relevant for red urchins, which can live over 100 years (Ebert and Southon, 2003). The California mussel *Mytilus californianus* (Fig. 5.2D), chitons *Katharina tunicata* (Fig. 5.2F) and *Cryptochiton stelleri* (Fig. 5.2G), and limpets *Lottia pelta* (Fig. 5.2H), *L. persona* (Fig. 5.2I), and *L. digitalis* (Fig. 5.2J) actually had a volumetric growth rate that increased with age: they add more shell (Fig. 5.3) and tissue (Fig. 5.2) each year when they are older than earlier in life. Similar patterns are evident for shell deposition rate, as the shell weight of chitons *K. tunicata* and *C. stelleri* showed an increase in growth rate with age.

Growth curves utilizing absolute measures such as volume and weight cannot be fit with the asymptotic growth functions that are often used to fit length-based growth curves (Ricker, 1975; Chen et al., 1992; Ebert and Russell, 1992; Hood and Schlieder, 1992; Ebert and Lees, 1996; Essington et al., 2001; Rogers-Bennett et al., 2003; Steffani and Branch, 2003; Lester et al., 2004). The most common and best (Kozlowski et al., 2004) growth function used to model indeterminate growth in fish, mussels, urchins, and other mollusks is the von Bertalanffy growth function, which has a built-in asymptote (von Bertalanffy, 1938). The maximum length of the organism is used as the asymptote for this growth function, so it cannot be used to plot continuous growth. As such, this function cannot be used to plot the growth of indeterminately growing organisms when absolute measures of size and growth are used.

The idea that some indeterminately growing organisms are not growing slower as they get older is unexpected because the paradigm for indeterminate growth is that at older ages, the vast majority of energy is shifted to reproduction (Heino and Kaitala, 1996; Kozlowski, 1996a,b; Jokela, 1997; Chase, 1999b; Heino and Kaitala, 1999; Kozlowski and Gawelczyk, 2002; Kozlowski et al., 2004). An extension of this is that organisms with indeterminate growth have minimal growth later in life because they are approaching an 'optimal size' (Sebens, 2002). However, if size is measured as weight or volume, then the organisms in this study do not approach any optimal size because their absolute size is continuously increasing instead of slowing to an asymptote. In addition, changing body shape is not the reason for increasing volume and weight with age, as evidenced by the length-volume relationships shown by chiton and limpet 3-D models

(Fig. 5.1) that did not change proportions as they expanded (Figs. 5, 6). The growth curves from the models were extremely similar to the curves for the live organisms in this study and in the literature (Boolootian, 1964; Frank, 1965b; Kenny, 1969; Glynn, 1970), indicating that changes in shape are not the reason why volume and weight continue to increase at old ages while linear growth slows down.

Steady or increasing growth rate with age makes sense from an energetic standpoint, because energy uptake is greater for larger organisms (Peters, 1983; Sebens, 1987; Chase, 1999a; Woodward, 2005), but this continuous growth is not apparent in length-based curves, which are asymptotic even for indeterminately growing organisms. In both *C. stelleri* and *C. funebralis,* food intake scaled linearly with weight (above 2g body weight for *C. funebralis*), and went up exponentially with body length (Fig. 5.7). Because both of these organisms grow approximately the same amount each year (Fig. 5.2) and their food intake is increasing, they are able to put more energy towards reproduction. *Cryptochiton stelleri* does display linearly increasing fecundity with volume (Fig. 5.6), and *Chlorostoma funebralis* gonad mass increases linearly with age as well (Cooper, 2010).

The evolutionary implications of indeterminate growth are largely unaffected by a change in the way size is measured, because the best strategy is still to maximize the lifetime reproductive output (R_o) of the individual (Kozlowski, 1996a; Kozlowski and Gawelczyk, 2002; Rinke et al., 2008). However, the weight and volume based growth curves presented in this study indicate that reproductive output does not increase at the expense of growth but rather as a result of a corresponding increase in energy intake.

Organisms with indeterminate growth are able to increase annual reproductive output because of growth rather than despite of it, since larger individuals can produce and contain more gametes (Hines, 1982). By continuing to grow steadily throughout their lives, the organisms in this study are able to keep increasing both food intake and reproductive output. This theoretically allows a higher percent of the energy budget to go to reproduction each year, but only because the budget itself increases each year and all excess can go to reproduction, not because growth rate decreases with time.

In models of energy allocation and life history strategies, length-based growth curves are used in combination with some measure of reproductive output to try to estimate and predict the amount of energy allocated to growth and reproduction throughout the life of the organism. Most studies of reproductive output measure reproduction in terms of fecundity (Lively, 1986; Liang et al., 2008; Jigyasu and Singh, 2010), gonad mass (Gilbert et al., 2006; Doall et al., 2008; Cooper, 2010), gonad index (Joaquim et al., 2008; Barbosa et al., 2009), or gonadosomatic index (Jessop, 1987; Tafur and Rabi, 1997; Cattaneo-Vietti et al., 1997; Perez et al., 2007). All of these measures of reproduction account for the size of the whole gonad, not just one dimension of its size. By using these measures of reproduction along with linear measures of body size, models of life history strategies and energy allocation can produce results that are artifacts of the allometric relationship between linear and absolute measures of size. This can result in a disproportionate amount of energy appearing to go towards reproduction, as growth appears to approach the 'asymptotic size' (Kozlowski et al., 2004) or 'optimal size' (Sebens, 2002).

When growth studies are just concerned with the size or growth of an organism, there is no problem with using linear measures of size. They are often less variable and have been used effectively for several growth rate studies (Frank, 1965b,c; Kenny, 1969; Suchanek, 1981; Brown and Quinn, 1988; Ebert and Russell, 1992; Ebert and Lees, 1996; Steffani and Branch, 2003; Grupe, 2006). However, when growth functions are incorporated into energetic or life history models, the means of measuring size becomes vital because the goal of the model is to account for all of the growth and reproduction for the organism involved. Using growth curves based on length or diameter only takes into account one dimension of the size and growth of the studied organism. By using these one-dimensional measures of size in conjunction with three-dimensional or absolute measures of reproduction, models can inherently underestimate both growth and the amount of energy allocated to growth. Only by taking into account absolute measures of size can energetic and life history models accurately assess the life history strategy and energy allocation of the study organism.

CHAPTER VI

CONCLUDING SUMMARY

The goal of this thesis was to fill in gaps of what was known about the life history of the gumboot chiton *Cryptochiton stelleri*. This species is charismatic (in my opinion) and relatively abundant in the intertidal zone for thousands of miles along the west coast of North America but not much was known about its growth or larval development. Because this species is the largest intertidal invertebrate herbivore throughout its range, it could have a large ecological impact like other large chitons do. As such, it was important to document the distribution of this species and determine how long they can live and how much they can eat. The life history of an organism in any habitat is vital to the ecology, reproduction, and evolution of that species, so I was drawn to investigate the life history and energy allocation of several intertidal species in southern Oregon.

Chapter II documented the distribution of *C. stelleri* at several sites along the southern Oregon coast, revealing that this species has a clumped distribution and prefers to inhabit small coves within rocky intertidal sites. The distribution of *C. stelleri* could be driven by recruitment patterns, though large-scale oceanographic conditions are not a likely cause of successful cohorts because the sites studied did not share peaks in cohort size. Chapter III described the larval development, metamorphosis, and juvenile behavior of *C. stelleri* and contradicted a previous study on the larval development of this species.

The metamorphosis cue for this species was found to be encrusting coralline algae, which is ubiquitous on the southern Oregon coast and therefore is not likely driving the distribution of *C. stelleri*. Chapter IV focused on the adult growth rates of *C. stelleri* and the leather chiton *Katharina tunicata*, using growth rings in the valves of these species to estimate age. These were found to be the oldest two known species of chiton in the world. Chapter V examined unusual growth patterns in these chitons and several other kinds of intertidal invertebrates with indeterminate growth and showed how growth and energetic models differ depending on the measure of size that is used.

Each chapter answered several questions about *C. stelleri* or other intertidal organisms but also raised several more questions that tied into the other chapters. The life history of *C. stelleri* that is described in Chapters III and IV has a strong influence on the distribution of this species described in Chapter II. Sporadic recruitment that is strongly influence by local conditions is the most likely cause of the patchy distribution of *C. stelleri*. The life history of this fascinating species brought up several intriguing questions and served as a useful model organism for examining models of indeterminate growth.

APPENDIX A

SIZE AND REPRODUCTIVE OUTPUT DATA FOR *CRYPTOCHITON STELLERI,*

TONICELLA LINEATA, KATHARINA TUNICATA, MOPALIA MUSCOSA, AND

LOTTIA SCUTUM

Presented below are additional tables showing the raw data comparing different measures

of body size with the reproductive output of four species of chiton and a limpet found on

the southern Oregon coast.

Table 1. Body and fecundity measurements of *Tonicella lineata* collected from Gregory Point, 5 km south of Charleston, Oregon in February 2010.

Specimen Number	Sex	Body Length (mm)	Body Weight (g)	Body Volume (mL)	Valve 4 Width (mm)	Valve 4 Weight (g)	Number of Gametes
1	F	17.9	0.4	0.4	8	0.03	540
2	F	22	0.7	0.79	11.5	0.06	3100
3	F	27.3	1.3	1.2	10.5	0.08	1680
4	F	17	0.3	0.39	7.1	0.02	980
5	F	26	1	1.1	11.3	0.05	10080
6	F	15.6	0.2	0.5	7	0.01	840
7	F	26	1.1	1.2	11.2	0.1	10240
8	F	26	1.2	1.2	12	0.08	1340
9	F	26.2	1.1	1.23	10.8	0.09	2540
10	F	21.5	0.5	0.6	8.5	0.04	1480
11	F	24.5	1	1.1	10.4	0.07	11380
12	F	22.1	0.9	1.15	11	0.07	200
13	F	25	1	1.18	10.6	0.08	1030
14	F	25.7	1	1.1	10.5	0.06	2240
15	F	27	1.2	1.4	11.2	0.08	940
16	F	21.5	0.5	0.7	8.5	0.03	3740
17	F	22.5	0.7	0.9	10.5	0.05	4800
18	F	21.6	0.6	0.8	10.3	0.05	4480
19	F	25.5	0.9	1.1	11.3	0.07	520
20	F	18	0.4	0.5	7.9	0.02	1880
21	F	27.8	1.1	1.35	11.4	0.08	660
22	F	22	0.7	0.9	10.3	0.04	5720
23	F	21	0.7	0.8	9.5	0.06	1420
24	M	22.5	0.9	0.75	10.9	0.05	8.16E+08
25	M	21.1	0.6	0.65	9.5	0.04	8.4E+08
26	M	21.9	0.6	0.59	8.1	0.04	1.17E+09
27	M	25	1	0.8	10.3	0.07	1.97E+09
28	M	19.1	0.5	0.61	9	0.03	8.4E+08
29	M	22	0.8	0.73	11	0.07	9.04E+08
30	M	28	1.9	1.7	12.4	0.12	2.02E+09
31	M	27.4	1.4	1.45	11.9	0.1	1.86E+09
32	M	27.5	1.2	1.3	10.9	0.08	2.46E+09
33	M	19.7	0.5	0.53	8.8	0.03	2.4E+08
34	M	19	0.4	0.65	8	0.02	7.04E+08
35	M	24	0.9	1.1	9.9	0.07	3.36E+08

Specimen Number	Sex	Body Length (mm)	Body Weight (g)	Body Volume (mL)	Valve 4 Width (mm)	Valve 4 Weight (g)	Number of Gametes
Table 1 (continued—page 2)							
36	M	13.1	0.1	0.3	5.3	0.01	2.24E+08
37	M	23.1	0.8	0.98	10	0.05	1.6E+09
38	M	24	1	1.15	10.7	0.08	1.52E+09
39	M	28.7	1.5	1.5	14	0.12	4.8E+08
41	M	22	0.8	0.9	10	0.05	3.84E+08
42	M	20.9	0.5	0.73	9	0.04	1.58E+09
43	M	31	1.9	1.75	14.1	0.12	8.64E+08
44	M	19.5	0.5	0.8	9.8	0.04	1.14E+09
45	M	23	0.7	0.8	10	0.05	1.19E+09
46	M	20.7	0.5	0.7	9.2	0.03	1.28E+08
47	M	30.5	1.7	1.55	12.8		2.03E+09

Table 2. Body and fecundity measurements of *Mopalia muscosa* collected from Gregory Point, 5 km south of Charleston, Oregon in February 2010.

Specimen Number	Sex	Body Length (mm)	Valve Width (mm)	Body Weight (g)	Body Volume (mL)	Number of Gametes
1	F	61	25	21.1	15	49000
2	F	60	23.5	20.3	14.5	14800
3	F	68	28.5	35.7	30	91600
4	F	53	22	15.1	12	29200
5	F	69	26	28.3	23	64600
6	F	58	22	17.3	12	17520
7	F	63	23.5	22.5	16	11480
8	F	37	14	4	3.5	3040
9	F	68	29.5	38.3	30	58400
10	F	38	19	6.6	5	1880
11	F	69	27.5	33.6	24	15280
12	F	56	23.5	15.6	10.5	32920
13	F	34	16	4.7	4	1240
14	M	40	15	5.3	3.5	2.02E+09
15	M	51.5	24	15.1	10	6.02E+09
16	M	36	14.5	6.6	4.8	5.63E+09
17	M	61.5	23	19.1	13	4.19E+09
18	M	68.5	25.5	25.7	18	5.79E+09
19	M	34	16	6.7	5.5	5.44E+08
20	M	58.5	24	21.9	16	8.35E+09
21	M	60	25	23.4	17	5.63E+09
22	M	42	17	8.4	7	5.63E+09
23	M	65	28	28.6	20	6.27E+09
24	M	63	26	23.5	15	1.5E+09
25	M	55	19.5	14.6	10	2.46E+09
26	M	51	18	12.1	8	5.28E+09
27	M	66	24	24.1	21	2.46E+09
28	M	60	24	18.4	12.5	3.46E+09

Table 3. Body and fecundity measurements of *Katharina tunicata* collected from Gregory Point, 5 km south of Charleston, Oregon in February 2010.

Specimen Number	Sex	Age	Body Length (mm)	Valve 4 Width (mm)	Valve 4 Weight (g)	Body Weight (g)	Body Volume (mL)	Number of Gametes
1	F	5	85	20.5	0.97	46.4	35	312240
2	F	3	56	15	0.37	12.4	9	24400
3	F	6	74	20	1	32.7	27	49680
4	F	4	54	15.5	0.44	11.7	9	1120
5	F	10	107	29	3.38	91.5	75	486000
6	F	6	78	20.5	0.92	42.2	30	233040
7	F	5	67	17.5	0.63	25.6	22	110880
8	F	9	94	27	3.05	69.9	50	98640
9	F	8	86	28	2.52	66.8	50	139440
10	F	3	52	15.5	0.42	13.8	11.5	320
11	F	6	88	23	1.47	59.9	45	390000
12	M	8	94	25	1.87	66.4	60	2E+11
13	M	9	97	27.1	1.87	79.5	65	2E+11
14	M	12	101	29	2.53	84.5	75	2E+11
15	M	12	103	31	3.59	104.8	85	2E+11
16	M	12	101	30	2.98	103.3	95	4E+11
17	M	10	105	28	2.31	84.7	70	3E+11
18	M	5	63	16	0.52	16.3	14	4E+09
19	M	16	103	30.5	3.14	108	85	3E+11

Table 4. Body and fecundity measurements of *Cryptochiton stelleri* collected from Gregory Point, 5 km south of Charleston, Oregon in February 2010.

Specimen Number	Sex	Age	Body Length (cm)	Body Circ. (cm)	Body Weight (g)	Body Volume (mL)	Valve 8 Width (mm)	Valve 8 Weight (g)	Number of Gametes
1	F	28	7.1	55	13.6	14			0
2	F	23	12.6	180	169	150			0
3	F	32	23.5	347	1020	858	4.7	15.18	5577000
4	F	29	19.8	317	740	643.5	4.3	9.44	1659000
5	F	23	25	372	1140	990	5.1	17.4	6300000
6	F	27	22.5	333	940	808.5	4.6	13.4	2775000
7	F	29	20.5	330	830	726	4.4	9.55	3645000
8	F	18	23.2	323	870	759	4.3	9.92	3455000
9	F	28	24.5	335	830	709.5	5.1	15	2562000
10	F	23	18	300	600	528	3.8	6	2685000
11	F	23	27	340	920	775.5	4.7	12.83	3021000
12	F	22	25	334	780	643.5	4.5	13.52	1032000
13	F	28	21.3	279	520	412.5	4.4	9.04	42000
14	F	23	20.7	324	750	660	4.4	9.52	2937000

Table 5. Body and fecundity measurements of *Lottia scutum* collected from Gregory Point, 5 km south of Charleston, Oregon in February 2010.

Specimen Number	Sex	Body Length (mm)	Shell Weight (g)	Body Weight (g)	Body Volume (mL)	Number of gametes
1	F	14.3	0.13	0.3	0.8	2900
2	F	14.6	0.1	0.3	0.75	2680
4	F	14.5	0.12	0.3	0.7	1980
7	F	20.2	0.44	1.1	1.15	49080
12	F	20	0.4	1	1.1	20420
13	F	17.8	0.28	0.8	1	45100
14	F	15.5	0.15	0.4	0.8	8860
15	F	24	0.6	1.7	1.8	81800
22	F	19.1	0.3	0.8	1.1	34200
23	F	16.5	0.2	0.6	0.68	6920
3	M	12.1	0.07	0.16	0.65	2E+08
5	M	19.5	0.35	0.8	1.1	3E+09
6	M	14.5	0.13	0.3	0.7	1E+09
8	M	20	0.28	0.8	1.15	2E+09
9	M	17	0.29	0.6	1	1E+09
10	M	11.2	0.04	0.1	0.6	7E+08
11	M	17.2	0.24	0.6	1	2E+09
16	M	14.3		0.3	0.7	9E+08
17	M	18.5	0.31	0.75	1	3E+09
18	M	11.9	0.06	0.1	0.5	2E+08
19	M	19.1	0.33	0.8	1.2	2E+09
20	M	14.8	0.17	0.4	0.6	1E+09
21	M	18		0.6	0.8	2E+09

APPENDIX B

DIFFERENT MEASURES OF SIZE FOR SEVERAL INTERTIDAL

INVERTEBRATES

These data show the sizes of different intertidal organisms when size is measured in linear terms such as length or diameter and absolute terms such as weight or volume. The relationships between linear and absolute measures of size were combined with previously published linear growth rate data to create growth curves based on absolute size in Chapter V. For all organisms included, when they are small, a little increase in length is accompanied by a little increase in weight or volume. When the organism is large, a little increase in length is accompanied by a large increase in weight or volume.

Table 1. Shell length and shell weight of *Acmaea mitra* collected from Gregory Point, Oregon.

Shell Length (mm)	Shell Weight (g)
14	0.38
15	0.44
18	0.71
24	1.54
25	1.7
26	2.22
27	2.88
27	3.25
28	3.18
32	5.86
32	7.89
33	3.19
33.5	5.78
37	8.49
39.5	9.52

Table 2. Shell length and shell weight of *Callianax biplicata* shells collected at Yoakim Point, Oregon.

Shell Length (mm)	Shell Weight (g)
0.79	0.05
0.86	0.07
1.69	0.54
1.78	0.66
1.95	0.9
2	0.84
2	0.89
2	1.03
2.07	1.31
2.07	1.08
2.1	1.13
2.13	1.26
2.15	1.2
2.28	1.4
2.34	1.61
2.4	1.61
2.4	1.38
2.5	1.57
2.6	2.07
2.75	2.73

Table 3. Shell length and shell weight of *Nucella lamellosa* collected from Yoakim Point, Oregon.

Shell Length (mm)	Shell Weight (g)
16	0.92
16.3	0.8
17	0.59
22.3	1.55
23	1.63
24	2.09
28	2.2
32.2	4.6
34	5.43
34	5.26
37	5.22
37.4	5.2
39.2	6.23
40.5	5.59
41.9	7.26
45	9.62
46.5	10.98
47	8.88
47.5	10.53
49	11.03
50.9	13.13

Table 4. Shell width and body volume of *Chlorostoma funebralis* collected from Gregory Point, Oregon.

Shell Width (g)	Body Volume (mL)
12.5	0.4
13.1	0.5
14.7	0.7
15	0.8
15.4	0.9
15.7	0.9
17	1.25
19.3	2
20	2.3
20	2.1
20.7	2.4
22	3.2
22.5	3.5
23.5	4.4
25.5	6.5
27.6	5.2
28.7	7.2
29	9
29.3	8.6
29.5	9
30	9.3
30.2	8.5

Table 5. Test diameter and total volume of *Strongylocentrotus purpuratus* at Gregory Point, Oregon.

Test diameter (mm)	Volume (mL)
22.1	4
32.5	12
38	20
42	27
46	33
47	35
49.5	43
49.5	40
59.5	90
63	85
67.5	98
68	101
70	115
70.5	107
72	135
72.5	130
74	130
76	150
77	145

Table 6. Test diameter and total volume of *Strongylocentrotus franciscanus* at Gregory Point, Oregon.

Test diameter (mm)	Body Weight (g)
105	360
136	780
137	805
125	700
117	680
102	400
143	1030
124	700
131	800
137	1000
120	640
118	600
44	37

Table 7. Shell length and total volume of *Mytilus californianus* at Gregory Point, Oregon.	
Shell Length (mm)	Total Volume (mL)
16	0.5
18	1
28	2.5
29	2.5
32.5	3.5
37	5
39	6
41.5	7.5
42	8
46	10
50	11.5
52	14
62.5	19
66.5	26
70.5	33
87	58
84	57
91	65
98.5	70
105	100
130	155
123	137

Table 8. Shell length and total weight of *Mytilus galloprovincialis* on the floating docks in Charleston, Oregon.	
Shell Length (mm)	Total Weight (g)
60	18
54	18.4
60	26.8
60	20.9
47	13.4
48	11.1
53	13.6
43	10
42	8.2
40	7.5
43	8.5
33.5	4
30	3.5
28	2.7
24	2
22	1.2
23	1.4
22	1.4

Table 9. Shell length and total weight of *Lottia pelta* at South Cove, Cape Arago, Oregon.	**Table 10.** Shell length and total weight of *Lottia persona* at South Cove, Cape Arago, Oregon.

Shell Length (mm)	Total Weight (g)	Shell Length (mm)	Total Weight (g)
22.5	1.33	26.8	2.36
21.2	1.19	13.5	.29
17.6	0.64	20.9	1.06
25.5	2.46	30.4	5.0
25	2.45	24.9	2.05
30	4.78	24.6	2.43
18	0.61	18	.84
22.9	1.56	35	6.24
39	10.1	36	7.26
17	0.64	22	1.54
21	1.1	21.6	1.29
		25	2.13
		27	2.49
		41	10.53
		43.4	12.24
		31.4	5.58

Table 11. Shell length and total weight
of *Lottia digitalis* at South Cove, Cape
Arago, Oregon.

Shell Length (mm)	Total Weight (g)
19.2	0.86
7.7	0.07
6.3	0.05
14	0.53
16.3	0.52
16.9	0.81
15.7	0.61
16.8	0.73
14.7	0.40
12	0.2
15.4	0.54
16.2	0.65
17.7	0.79
18.3	0.73

APPENDIX C

JUVENILE *CRYPTOCHITON STELLERI* GROWTH DATA

The following tables detail the growth of juvenile *Cryptochiton stelleri* that were raised in flowing seawater tables at the Oregon Institute of Marine Biology. Multiple measures of size are shown, including length, width, and body weight. The smallest individuals were approximately 8 mm in length when monitoring began. Specimens were raised until they were approximately one year old in April 2010. Additional information about *C. stelleri* adult growth and life history is described in Chapter IV.

Table 1. Individual juvenile *Cryptochiton stelleri* growth data in terms of body length, body width and body weight. Individuals were kept in a mesh container in a flowing seawater table at the Oregon Institute of Marine Biology from their collection date until the end of March 2010. Juveniles were fed the red leafy alga *Cryptopleura*.

Specimen Number	Date	Length (mm)	Width (mm)	Weight (g)
1	8/1/09	8.8	3.76	0.02666
2	8/1/09	7.68	3.52	0.01716
3	8/1/09	11.2	4.48	0.05815
4	8/1/09	12.64	5.92	0.08599
5	8/1/09	48	34	6.43734
1	8/14/09	10.08	4.8	0.04136
2	8/14/09	9.28	4.64	0.03165
3	8/14/09	12.16	5.92	0.07587
4	8/14/09	16.16	7.04	0.19034
5	8/14/09	53	38	8.86938
1	8/20/09	10.24	4.96	0.04352
2	8/20/09	9.472	4.64	0.03382
3	8/20/09	12	4.8	0.07269
4	8/20/09	14.72	6.64	0.14074
5	8/20/09	55	32	9.99823
1	9/6/09	10.56	6.56	0.04807
3	9/6/09	12.48	5.6	0.08252
4	9/6/09	16.48	4.16	0.2028
5	9/6/09	56	40	10.5982
1	9/17/09	10.72	5.28	0.05047
3	9/17/09	12.96	5.2	0.09323
4	9/17/09	16.8	7.68	0.21582
5	9/17/09	55.5	38.1	10.2952
1	9/23/09	12	5.76	0.07269
3	9/23/09	12.48	5.44	0.08252
4	9/23/09	17.12	8.32	0.2294
5	9/23/09	58	38	11.872
1	10/7/09	11.2	5.12	0.05815
3	10/7/09	13.6	5.44	0.10896
4	10/7/09	17.76	8	0.25831
5	10/7/09	63	39	15.5123
1	10/26/09	11.4	6.3	0.06158
3	10/26/09	12.4	7	0.08082
4	10/26/09	18	9.2	0.26977

Table 1 (continued—page 2)				
Specimen Number	Date	Length (mm)	Width (mm)	Weight (g)
5	10/26/09	63	47	15.5123
1	11/2/09	12.9	5.8	0.09184
3	11/2/09	13.4	7.4	0.10386
4	11/2/09	18.5	10.2	0.29477
6	11/2/09	14.8	7.5	0.14323
1	11/11/09	13	7.2	0.09417
3	11/11/09	13.4	8.2	0.10386
4	11/11/09	19.1	11.1	0.32682
5	11/11/09	63	48	15.5123
6	11/11/09	15.3	8.4	0.15948
1	11/18/09	13.5	6.7	0.10639
3	11/18/09	13.2	8.4	0.09893
4	11/18/09	20	11.6	0.37931
5	11/18/09	59	45	12.5468
6	11/18/09	16.6	8.4	0.20762
1	12/2/09	14.4	7.5	0.13109
3	12/2/09	15.2	8.5	0.15614
4	12/2/09	22	13.3	0.51626
6	12/2/09	17.9	8.7	0.26495
7	12/5/09	12.8	7	0.08956
1	12/9/09	13.9	8.4	0.11693
3	12/9/09	17.6	9.8	0.25086
4	12/9/09	23.2	14	0.61301
6	12/9/09	18.6	10.2	0.29995
7	12/9/09	14.7	8	0.14013
1	12/16/09	14.6	8.4	0.13707
3	12/16/09	15.4	9.7	0.16288
4	12/16/09	22.7	13.4	0.5713
6	12/16/09	16.6	11.7	0.20762
7	12/16/09	13.2	9.1	0.09893
1	12/30/09	16.2	8.4	0.19187
3	12/30/09	16.5	8.2	0.2036
4	12/30/09	23.8	15.1	0.66578
6	12/30/09	18.2	12.6	0.27959
7	12/30/09	15	8.6	0.14959
1	1/6/10	17	9	0.22424
3	1/6/10	15.4	10.2	0.16288
4	1/6/10	23.8	16	0.66578

Table 1 (continued—page 3)

Specimen Number	Date	Length (mm)	Width (mm)	Weight (g)
6	1/6/10	21	12	0.44414
7	1/6/10	15.6	8.5	0.16982
1	1/13/10	17.4	9.7	0.24176
3	1/13/10	18.3	10.5	0.28459
4	1/13/10	25	17	0.78059
6	1/13/10	22	13	0.51626
7	1/13/10	16.9	9.3	0.22
1	1/20/10	17.5	9.5	0.24628
3	1/20/10	17.7	10.7	0.2555
4	1/20/10	24.5	17.6	0.73122
6	1/20/10	22	14.7	0.51626
7	1/20/10	16.5	10.5	0.2036
1	1/27/10	19	9.8	0.32132
3	1/27/10	17.6	12.4	0.25086
4	1/27/10	25.5	17.9	0.83223
6	1/27/10	22.9	13.2	0.58774
7	1/27/10	17.6	10	0.25086
1	2/3/10	18.1	12.1	0.27465
3	2/3/10	17.3	12.3	0.23729
4	2/3/10	27.3	18.2	1.03764
6	2/3/10	24	15	0.68405
7	2/3/10	18.2	11.2	0.27959
8	2/3/10	19.3	11.7	0.33802
1	2/10/10	21	11.5	0.44414
3	2/10/10	19.9	12.8	0.37321
4	2/10/10	27	21.4	1.00122
6	2/10/10	25	15.9	0.78059
7	2/10/10	19	12.3	0.32132
8	2/10/10	20.3	12.4	0.39802
1	2/17/10	18.9	13.4	0.31588
3	2/17/10	20	13.4	0.37931
4	2/17/10	29	20.3	1.26154
6	2/17/10	25	17.1	0.78059
7	2/17/10	19	13.5	0.32132
8	2/17/10	19.7	13.5	0.36121
1	2/24/10	19.8	13.1	0.36717
3	2/24/10	20.7	14.6	0.42395
4	2/24/10	29	20.8	1.26154

Table 1 (continued—page 4)

Specimen Number	Date	Length (mm)	Width (mm)	Weight (g)
6	2/24/10	26.8	17.6	0.97743
7	2/24/10	19.8	14	0.36717
8	2/24/10	22	13.3	0.51626
1	3/3/10	20	14.8	0.37931
3	3/3/10	20.5	15.2	0.41084
4	3/3/10	29.3	22.5	1.30424
6	3/3/10	29	18.2	1.26154
7	3/3/10	21.6	14.6	0.48651
8	3/3/10	22.5	15	0.55518
1	3/10/10	21.3	14.8	0.46499
3	3/10/10	23.3	12.7	0.62159
4	3/10/10	30.5	24	1.48504
6	3/10/10	28.5	19	1.19254
7	3/10/10	22.4	14.2	0.54724
8	3/10/10	23	15.3	0.59608
1	3/24/10	25	15.3	0.78059
3	3/24/10	23	14.7	0.59608
4	3/24/10	32	24	1.7345
6	3/24/10	33	20.2	1.91601
7	3/24/10	23.5	15	0.63902
8	3/24/10	25	15.5	0.78059

APPENDIX D

ADDITIONAL AGE-FREQUENCY DATA FOR *CRYPTOCHITON STELLERI*

POPULATIONS ON THE SOUTHERN OREGON COAST

These figures show age-frequency data similar to that shown in Chapter II, but from different seasons. Surveys were done in July and August 2009, November and December 2009, and May and June 2010. The histograms shown in Chapter II are just from May and June 2010. Included in this section are data from the other two seasons. Size-frequency histograms do not change much within a site between dates because of the slow growth of *Cryptochiton stelleri*, but there is some variation due to different individuals being found during each survey. For all seasons, there is little overlap in peak cohorts between sites that are far away from each other, suggesting that recruitment and survival varies on a local scale.
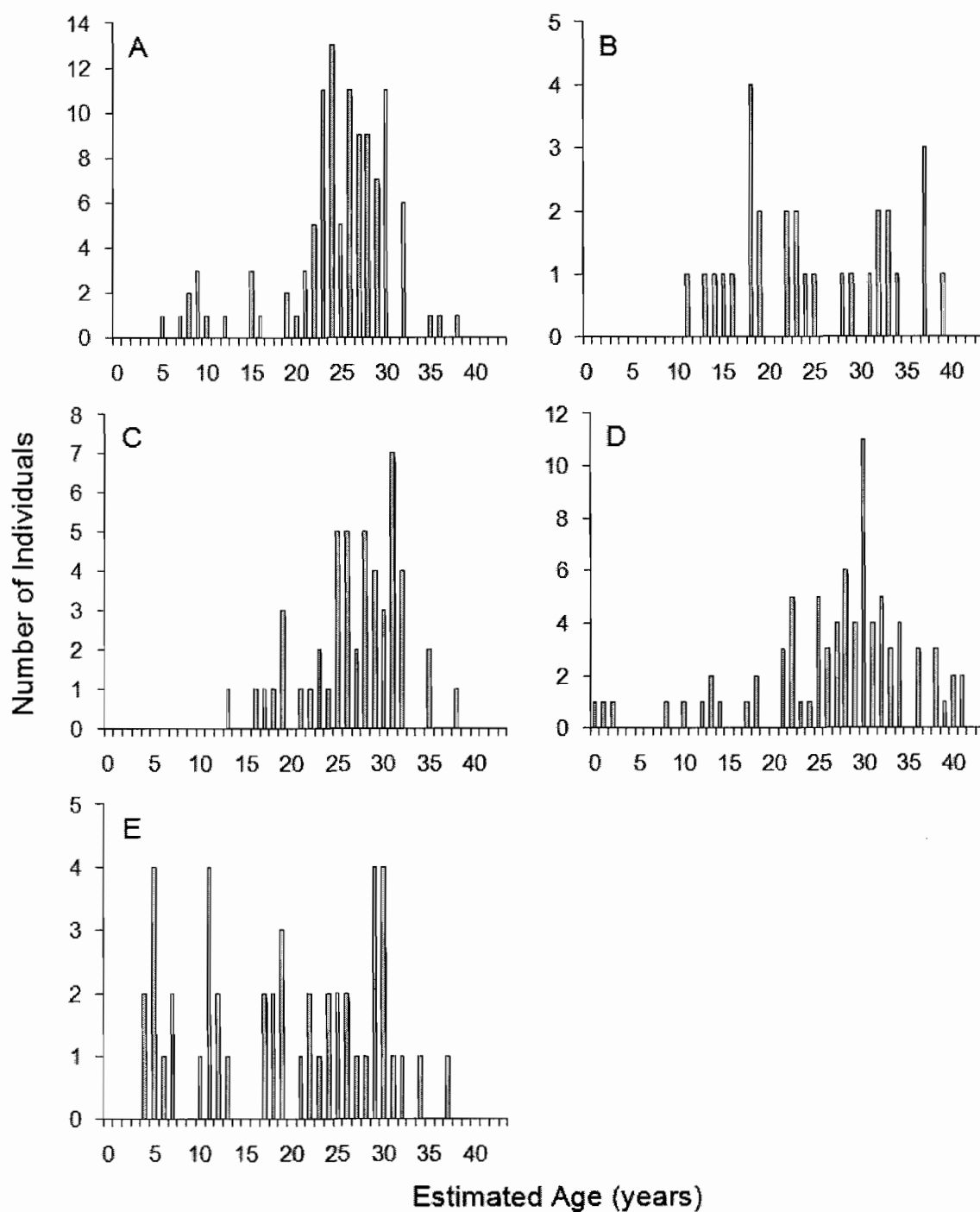
Figure 1. Age-frequency histograms for five sites along the southern Oregon coast during July and August 2009. Data shown were collected during intertidal surveys of these sites on tides below -0.3 m MLLW. (A) South Cove of Cape Arago; (B) Sunset Bay State park; (C) Middle Cove of Cape Arago; (D) Cape Blanco State Park; (E) Lighthouse Island.
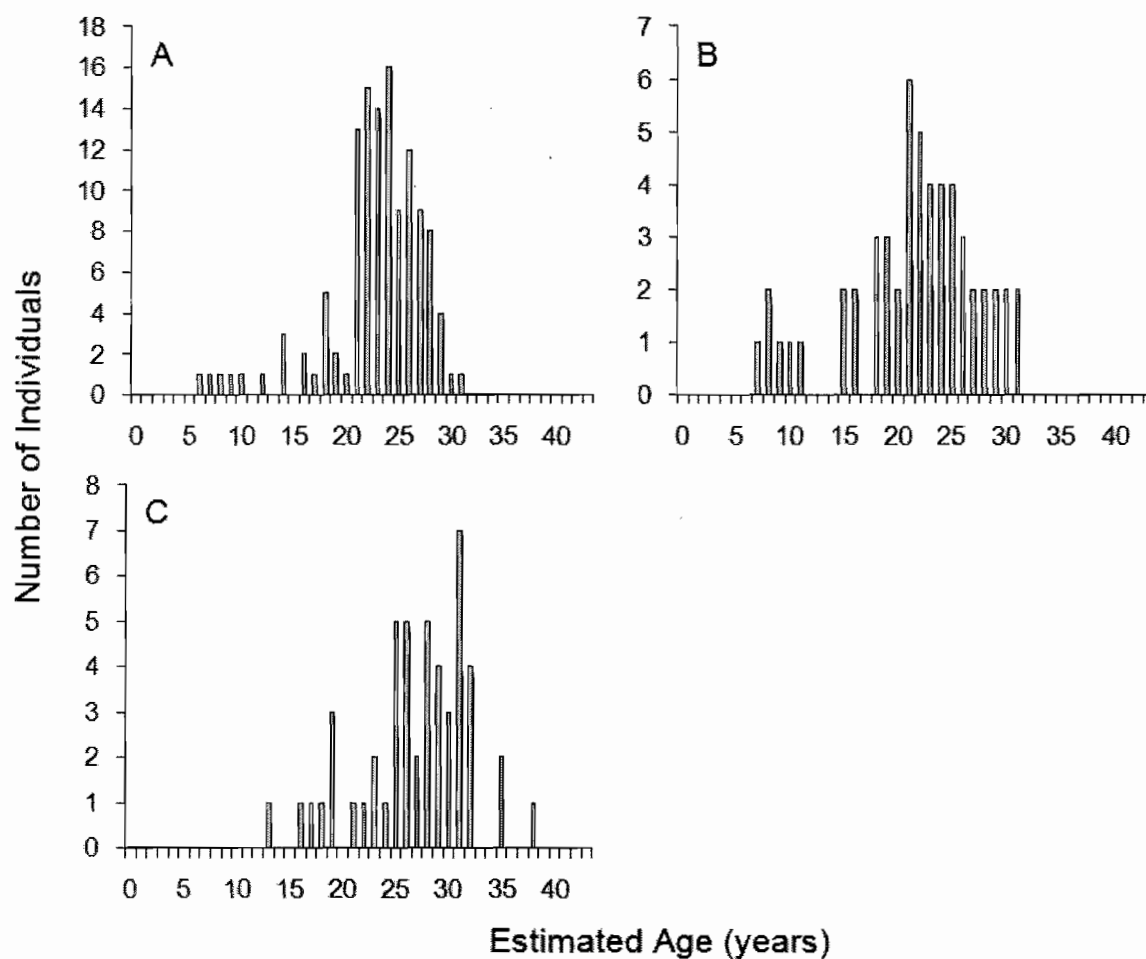
Figure 2. Age-frequency histograms for three sites along the southern Oregon coast during November and December 2009. Data shown were collected during intertidal surveys of these sites on tides below -0.3 m MLLW. (A) South Cove of Cape Arago; (B) Sunset Bay State park; (C) Middle Cove of Cape Arago.

REFERENCES

Abele, D., T. Brey, and E. Phillip. 2009. Bivalve models of aging and the determination of molluscan lifespans. *Experimental Gerontology* **44**: 307–315.

Arendt, J.D. and D.N. Reznick. 2005. Evolution of juvenile growth rates in female guppies (*Poecilia reticulata*): predator regime or resource level? *Proceedings of the Royal Society of Britain* **272**: 333-337.

Barbosa, S.S., M. Byrne, and B.P. Kelaher. 2009. Reproductive periodicity of the tropical intertidal chiton *Acanthopleura gemmata* at One Tree Island, Great Barrier Reef, near its southern latitudinal limit. *Journal of Experimental Marine Biology of the United Kingdom* **89(2):** 405-411.

Barnes, J.R., and J.J. Gonor 1973. The larval settling response of the lined chiton *Tonicella lineata. Marine Biology* **20(3):** 259-264.

Basson, M., A.A. Rosenberg, and J.R. Beddington. 1988. The accuracy and reliability of two new methods for estimating growth parameters from length-frequency data. *Journal du Conseil International pour l'Exploration de la Mer.* **44:** 277-285.

Baxter, J.M., and A.M. Jones. 1978. Growth and population structure of *Lepidochitona cinereus* (Mollusca: Polyplacophora) infected with *Minchinia chitonis* (Protozoa: Sporozoa) at Easthaven, Scotland. *Marine Biology* **46:** 305-313.

Bayne, B.L. 1969. The gregarious behavior of the larvae of *Ostrea edulis* L. at settlement. *Journal of the Marine Biological Association of the UK* **49:** 327-356.

Bayne, B.L. and C.M. Worrall 1980. Growth and production of mussels *Mytilus edulis* from two populations. *Marine Ecology Progress Series* **3:** 317-328.

Bennett, J.T., K.K. Turekian, W.J. Shaul, and W.J. Ropes. 1982. Using natural radionucleotides to measure shell growth rates and ages of the bivalves *Arctica islandica* (Linne) and *Panope generosa* Gould. *Journal of Shellfish Research* **2:** 88-89.

Black, B.A. 2009. Climate-driven synchrony across tree, bivalve, and rockfish growth-increment chronologies of the northeast Pacific. *Marine Ecology Progress Series* **378**: 37-46.

Black, B.A., C.A. Copenheaver, D.C. Frank, M.J. Stuckey, and R.E. Kormanyos. 2009. Multi-proxy reconstructions of northeastern Pacific sea surface temperature data from trees and Pacific geoduck. *Palaeogeography, Palaeoclimatology, Palaeoecology* **278**: 40–47.

Black, B.A., D.C. Gillespie, S.E. MacLellan, and C.M. Hand. 2008. Establishing highly accurate production-age data using the tree-ring technique of crossdating: a case study for Pacific geoduck (*Panopea abrupta*). *Canadian Journal of Fisheries and Aquatic Science* **65**: 2572–2578.

Boettcher, A.A. 2005. Heat shock induced metamorphosis of the queen conch, *Strombus gigas*: comparison with induction by algal associated cues. *Journal of Shellfish Research* **24(4):** 1123-1126.

Boolootian, R.A. 1964. On growth, feeding and reproduction in the chiton *Mopalia muscosa* of Santa Monica Bay. *Helgolander wissenschaftliche Meeresuntersuchungen* **11(3-4):** 186-199.

Bosman, A.L. and P.A.R. Hockey. 1988. Life-history patterns of populations of the limpet *Patella granularis*: the dominant roles of food supply and mortality rate. *Oecologia* **75**: 412-419.

Branch, G.M. 1975. Mechanisms reducing intraspecific competition in *Patella* spp.: migration, differentiation and territorial behavior. *Journal of Animal Ecology* **44(2):** 575-600.

Brousseau, D.J. 1979. Analysis of growth rate in *Mya arenaria* using the Von Bertalanffy equation. *Marine Biology* **51:** 221-227.

Brown, K.M. and J.F. Quinn. 1988. The effect of wave action on growth in three species of intertidal gastropods. *Oecologia* **75**: 420-425.

Bryan, P.J., and P.Y. Qian. 1998. Induction of larval attachment and metamorphosis in the abalone *Haliotis diversicolor* (Reeve). *Journal of Experimental Marine Biology and Ecology* **223(1):** 39-51.

Burke, R.D. 1984. Pheremonal control of metamorphosis in the Pacific sand dollar, *Dendraster excentricus*. *Science* **225:** 442-443.

Campana, S.E. 2001. Accuracy, precision and quality control in age determination, including a review of the use and abuse of age validation methods. *Journal of Fish Biology* **59:** 197-242.

Cattaneo-Vietti, R., M. Chiantore, and G. Albertelli. 1997. The population structure and ecology of the Antarctic scallop *Adamussium colbecki* (Smith, 1902) at Terra Nova Bay (Ross Sea, Antarctica). *Scientia Marina* **61 (suppl. 2):** 15-24.

Chapman, A.R.O., and C.R. Johnson. 1990. Disturbance and organization of macroalgal assemblages in the Northwest Atlantic. *Hydrobiologica* **192:** 77-121.

Chase, J.M. 1999a. Food web effects of prey size refugia: variable interactions and alternative stable equilibria. *American Naturalist* **154 (5):** 560-571.

Chase, J.M. 1999b. To grow or to reproduce? The role of life-history plasticity in food web dynamics. *American Naturalist* **154(5):** 571-586.

Chen Y., D.A. Jackson, and H.H. Harvey 1992. A comparison of von Bartalanffy and polynomial functions in modeling fish growth data. *Canadian Journal of Fisheries and Aquatic Sciences* **49:** 1228-1235.

Clauss, M.J., and L.W. Aarssen. 1994. Phenotypic plasticity of size—fecundity relationships in *Arabidopsis thaliana*. *Journal of Ecology* **82(3):** 447-455.

Comfort, A. 1957. The duration of life in molluscs. *Journal of Molluscan Studies* **32:** 219-241.

Connelly, P.W., and R.L. Turner. 2009. Epibionts of the eastern surf chiton, *Ceratozona squalida* (Polyplacophora: Mopaliidae), from the Atlantic coast of Florida. *Bulletin of Marine Science* **85(3):** 187-202.

Conover, D.O., and T.M.C. Present. 1990. Countergradient variation in growth rate: compensation for length of the growing season among Atlantic silversides from different latitudes. *Oecologia* **83(3):** 316-324.

Conover, D.O., J.J. Brown, and A. Ehtisham. 1997. Countergradient variation in growth of young striped bass (*Morone saxatilis*) from different latitudes. *Canadian Journal of Fisheries and Aquatic Science* **54(10):** 2401-2409.

Coon, S.L., D.B. Bonar, and R.M. Weiner. 1985. Induction of settlement and metamorphosis of the Pacific oyster, *Crassostrea gigas* (Thunberg), by L-DOPA and catecholamines. *Journal of Experimental Marine Biology and Ecology* **94:** 211-221.

Cooper, E.E. 2010. Population biology and reproductive ecology of *Chlorostomsa (Tegula) funebralis*, an intertidal gastropod. PhD dissertation, University of Oregon.

Cowden, R.R. 1961. A cytochemical investigation of oogenesis and development to the swimming larval stage in the chiton *Chiton tuberculatum* L. *Biological Bulletin* **120(3):** 313-325.

Crespi, B.J., and R. Teo. 2002. Phylogenetic analysis of the evolution of semelparity and life history in salmonid fishes. *Evolution* **56(5):** 1008-1020.

Crozier, W.J. 1918. Growth and duration of life of *Chiton tuberculatus*. *Proceedings of the National Academy of Science* **4:** 322-325.

Dayton, P.K. 1971. Competition, disturbance, and community organization: the provision and subsequent utilization of space in a rocky intertidal community. *Ecological Monographs* **41(4):** 351-389.

Dayton, P.K. 1973. Dispersion, dispersal and persistence of the annual intertidal alga *Postelsia palmaeformis* Ruprecht. *Ecology* **54(2):** 433-438.

Dehnel, P.A. 1955. Rates of growth of gastropods as a function of latitude. *Physiological Zoology* **28(2):** 115-144.

Dethier, M.N., and D.O. Duggins. 1984. An "indirect commensalism" between marine herbivores and the importance of competitive hierarchies. *The American Naturalist* **124(2):** 205-219.

Doall, M.H., D.K. Padilla, C.P. Lobue, C. Clapp, A.R. Webb, and J. Hornstein. 2008. Evaluating northern quahog (1/4 hard clam, *Mercenaria mercenaria* L.) restoration: are transplanted clams spawning and reconditioning? *Journal of Shellfish Research* **27(5):** 1069-1080.

Downing, J.A., Y. Roehon, M. Perusse, and H. Harvey. 1993. Spatial aggregation, body size, and reproductive success in the freshwater mussel *Elliptio complanata*. *Journal of the North American Benthological Society* **12(2):** 148-156.

Duggins, D.O. 1980. Kelp beds and sea otters: an experimental approach. *Ecology* **61(3):** 447-453.

Duggins, D.O. 1983. Starfish predation and the creation of mosaic patterns in a kelp-dominated community. *Ecology* **64(6):** 1610-1619.

Dyck, L.J., and R.E. DeWreede. 2006. Reproduction and survival in *Mazzaella splendens* (Gigartinales, Rhodophyta). *Phycologia* **45(3):** 302-310.

Ebert, T.A., and D.C. Lees. 1996. Growth and loss of tagged individuals of the predatory snail *Nucella lamellosa* in areas within the influence of the *Exxon Valdez* oil spill in Prince William Sound. *American Fisheries Society Symposium* **18:** 349-361.

Ebert, T.A., and M.P. Russell. 1992. Growth and mortality estimates for red sea urchin *Strongylocentrotus franciscanus* from San Nicolas Island, California. *Marine Ecology Progess Series* **81:** 31-41.

Ebert, T.A., and J.R. Southon. 2003. Red sea urchins (*Strongylocentrotus franciscanus*) can live over 100 years: confirmation with A-bomb [14]carbon. *Fisheries Bulletin* **101(4):** 915-922.

Eernisse, D.J. 2004. Foreword to Systematics, Phylogeny and Biology of Polyplacophora: Proceedings to the 4th International Workshop of Malacology held in Menfi, Sicily (14-18 June 2001) Istituzione Culturale Federico II. *Bollettino Malacologico* **40:** i-iv.

Essington, T.A., J.F. Kitchell, and C.J. Walters. 2001. The von Bertalanffy growth function, bioenergetics, and the consumption rates of fish. *Canadian Journal of Fisheries and Aquatic Sciences* **58:** 2129-2138.

Estes, J.A., and D.O. Duggins. 1995. Sea otters and kelp forests in Alaska-generality and variation in a community ecological paradigm. *Ecological Monographs* **65(1):** 75-100.

Feder, H.M., and A.J. Paul. 1974. Age, growth, and size-weight relationships of the soft-shell clam, *Mya arenaria* in Prince William Sound, Alaska. *Proceedings of the National Shellfish Association* **64:** 45-52.

Forseth, T., O. Ugedal, B. Jonsson. 1994. The energy budget, niche shift, reproduction and growth in a population of Arctic charr, *Salvelinus alpines*. *Journal of Animal Ecology* **63(1):** 116-126.

Fouda, M.M., and P.J. Miller. 1981. Age and growth of the common goby, *Pomatoschistus microps*, on the south coast of England. *Estuarine, Coastal and Shelf Science* **12:** 121-129.

Fournier, D.A., and P.A. Breen. 1983. Estimated abalone mortality rates with growth analyses. *Transactions of the American Fisheries Society* **112:** 403-411.

Frank, P.W. 1965a. The biodemography of an intertidal snail population. *Ecology*. **46(6):** 831-844.

Frank, P.W. 1965b. Growth of three species of *Acmaea. Veliger* **7(3):** 201-202.

Frank, P.W. 1965c. Shell growth in a natural population of the turban snail, *Tegula funebralis. Growth* **29:** 395-403.

Gang, H., B. Feng, L. Huosheng, Z. Junfeng. 2008. Age and growth characteristics of crimson sea bream *Paragyrops edita* Tanaka in Beibu Gulf. *Journal of the Oceanic University of China* **7:** 457-465.

Gappa, J.L., and A. Tablado. 1997. Growth and production of an intertidal population of the chiton *Plaxiphora aurata* (Spalowsky, 1795). *Veliger* **40(3):** 263-270.

Gibbons, M.M., and T.K. McCarthy 1986. The reproductive output of frogs *Rana temporaria* (L.) with particular reference to body size and age. *Journal of Zoology* **209(4):** 579-586.

Giese, A.C., J.S. Tucker, and R.A. Boolootian. 1959. Annual reproductive cycles of the chitons, *Katharina tunicata* and *Mopalia hindsii. Biological Bulletin* **117:** 81-88.

Giese, A.C., and J.S. Pearse. 1979. Reproduction of Marine Invertebrates: Molluscs: Pelecypods and Lower Classes. New York: Academic Press, 369 pp.

Gilbert, A., S. Andre'foue"t, L. Yan, and G. Remoissenet. 2006. The giant clam *Tridacna maxima* communities of three French Polynesia islands: comparison of their population sizes and structures at early stages of their exploitation. *ICES Journal of Marine Science* **63:** 1573-1589.

Glynn, P.W. 1970. On the ecology of the Caribbean chitons *Acanthopleura granulata* Gmelin and *Chiton tuberculatus* Linne: density, mortality, feeding, reproduction, and growth. *Smithsonian Contributions to Zoology* **66.** 23 pp.

Grayson, J.E., and M.G. Chapman. 2004. Patterns of distribution and abundance of chitons of the genus *Ischnochiton* in intertidal boulder fields. *Austral Ecology* **29(4):** 363-373.

Grupe, B.M. 2006. Purple sea urchins (*Strongylocentrotus purpuratus*) in and out of pits: the effects of microhabitat on population structure, morphology, growth, and mortality. Univ. of Oregon Master's Thesis. 278 pp.

Hansen, J.E., and W.T. Doyle. 1976. Ecology and natural history of *Iridea cordata* (Rhodophyta: Gigartinaceae): population structure. *Journal of Phycology* **12**: 273-278.

Heath, H. 1897. External features of young *Cryptochiton. Proceedings of the National Academy of Sciences* **49**: 299-302.

Heath, H. 1905a. The breeding habits of chitons of the Californian coast. *Zoologischer Anzeiger* **29**: 390-393.

Heath, H. 1905b. The excretory and circulatory systems of *Cryptochiton stelleri* Midd. *Biological Bulletin* **9(4)**: 213-225.

Heino, M., and Kaitala, V. 1996. Optimal resource allocation between growth and reproduction in clams: why does indeterminate growth exist? *Functional Ecology* **10(2)**: 245-251.

Heino, M. and Kaitala, V. 1999. Evolution of resource allocation between growth and reproduction in animals with indeterminate growth. *Journal of Evolutionary Biology* **12**: 423-429.

Himmelman, J.H. 1978. The reproductive cycle of *Katharina tunicata* Wood and its controlling factors. *Journal of Experimental Marine Biology and Ecology* **31(1)**: 27-41.

Himmelman, J.H. 1984. Urchin feeding and macroalgal distribution in Newfoundland, eastern Canada. *Canadian Naturalist* **111**: 337-348.

Hines, A.H. 1982. Allometric constraints and variable of reproductive effort in brachyuran crabs. *Marine Biology* **69(3)**: 309-320.

Hood, P.B., and R.A. Schlieder. 1992. Age, growth, and reproduction of gag, *Mycteroperca microlepis* (Pisces: Serranidae), in the eastern Gulf of Mexico. *Bulletin of Marine Science* **51(3)**: 337-352.

Howes, B.J., and S.C. Lougheed. 2007. Male body size varies with latitude in a temperate lizard. *Canadian Journal of Zoology* **85(5)**: 626-633.

Hunter, E. and E. Naylor. 1993. Intertidal migration by the shore crab *Carcinus maenas. Marine Ecology Progress Series* **101**: 131-138.

Huxley, J.S. 1932. Problems of relative growth. Dial Press, New York.

Jenkins, S.R., and R.G. Hartnoll. 2001. Food supply, grazing activity and growth rate in the limpet *Patella vulgata* L.: a comparison between exposed and sheltered shores. *Journal of Experimental Marine Biology and Ecology* **258:** 123-139.

Jessop, B.M. 1987. Migrating American eels in Nova Scotia. *Transactions of the American Fisheries Society* **116:** 161-170.

Jigyasu, H.V., and V.K. Singh. 2010. Effect of environmental factors on the fecundity, hatchability and survival of snail *Lymnaea* (Radix) *acuminate* (Lamarck): vector of fascioliasis. *Journal of Water and Health* **8(1):** 109-115.

Joaquim, S., D. Matias, B. Lopes, W.S. Arnold, and M.B. Gaspar 2008. The reproductive cycle of white clam *Spisula solida* (L.) (Mollusca: Bivalvia): implications for aquaculture and wild stock management. *Aquaculture* **281:** 43-48.

Johnson, M.S., and R. Black. 2008. Effects of contrasting tidal habitats on growth, survivorship and dispersal in an intertidal snail. *Journal of Experimental Marine Biology and Ecology* **363:** 96-103.

Jokela, J. 1997. Optimal energy allocation tactics and indeterminate growth: life-history evolution of long-lived bivalves. Pages 179-196 *in* eds. Streit B, Stadler T, and Lively CM. Evolutionary ecology of freshwater animals. Birkhauser-Verlag, Germany.

Jones, D.S. 1981. Annual growth increments in shells of *Spisula solidissima* record marine temperature variability. *Science* **211:** 165-167.

Jones, P., and M. Crisp. 1985. Microgrowth bands in chitons: evidence of tidal periodicity. *Journal of Molluscan Studies* **51:** 133-137.

Katsanevakis, S. 2006. Modeling fish growth: model selection, multi-model inference and model selection uncertainty. Fisheries Research **81:** 229-235.

Kenny, R. 1969. Growth characteristics of *Acmaea persona*. *Veliger* **11(4):** 336-339.

Kent. A., S.J. Hawkins, and C.P. Duncaster. 2003. Population consequences of mutual attraction between settling and adult barnacles. *Journal of Animal Ecology* **72:** 941-952.

Kilada, R.W., S.E. Campana, D. Roddick. 2009. Growth and sexual maturity of the northen propellerclam (*Cyrtodaria siliqua*) in Eastern Canada, with bomb radiocarbon age validation. *Marine Biology* **156:** 1029-1037.

Kniprath, E. 1980. Ontogenetic plate and plate field development in two chitons, *Middendorffia* and *Ischnochiton*. *Development Genes and Evolution* **189(2):** 97-106.

Kozlowski, J. 1996a. Energetic definition of fitness? Yes, but not that one. *American Naturalist* **147(6):** 1087-1091.

Kozlowski, J. 1996b. Optimal allocation of resources explains interspecific life-history patterns in animals with indeterminate growth. *Proceedings of the Royal Society of London: Biological Sciences* **263(1370):** 559-566.

Kozlowski, J., and Gawelczyk, A.T. 2002. Why are species' body size distributions usually skewed to the right? *Functional Ecology* **16:** 419-432.

Kozlowski, J., M. Czarnoleski, and M. Danko. 2004. Can optimal resource allocation models explain why ectotherms grow larger in cold? *Journal of Integrative and Comparative Biology* **4:** 480-493.

Kunin, W.E. 1997. Population size and density effects in pollination: pollinator foraging and plant reproductive success in experimental arrays of *Brassica kaber*. *Ecology* **85(2):** 225-234.

Lawrence, A.L., and J.M. Lawrence. 1965. Cyclic variations in the digestive gland and glandular oviduct of chitons (Mollusca). *Science* **147:** 508-510.

Leighton, D.L., L.G. Jones, and W.J. North 1966. Ecological relationships between giant kelp and sea urchins in southern California. *Proceedings of the International Seaweed Symposium* **5:** 141-153.

Lester, N.P., B.J. Shuter, and P.A. Abrams. 2004. Interpreting the von Bertalanffy model of somatic growth in fishes: the cost of reproduction. *Proceedings of the Royal Society of London: Biological Sciences* **271:** 1625-1631.

Levitan, D.R., M.A. Sewell, F.S. Chia. 1992. How distribution and abundance influence fertilization success in the sea urchin *Strongylocentrotus franciscanus*. *Ecology* **73(1):** 248-254.

Liang, I., and J. Lopez-Alvarado. 2008. Effect of dried algae diets on conditioning and fecundity of Manila clam, *Tapes philippinarum* (Adams and Reeve). *Aquaculture Research* **25(2):** 157-166.

Linse, K., D.K.A. Barnes, and P. Enderlein. 2006. Body size and growth of benthic invertebrates along an Antarctic latitudinal gradient. *Deep Sea Research* **53:** 921-931.

Lively, C.M. 1986. Competition, comparative life histories, and maintenance of shell dimorphism in a barnacle. *Ecology* **67(4):** 858-864.

Lubchenco, J. 1978. Plant species diversity in a marine intertidal community: importance of herbivore food preference and algal competitive abilities. *American Naturalist* **112:** 23-39.

MacDonald, B.A., and M.L.H. Thomas. 1980. Age determination of the soft-shell clam *Mya arenaria* using shell internal growth lines. *Marine Biology* **58:** 105-109.

MacGinitie, G.E., and N. MacGinitie. 1968. Notes on *Cryptochiton stelleri* (Middendorff, 1846). *Veliger* **11(1):** 59-61.

Merrill, A.S., J.A. Posgay, F.E. Nichy. 1961. Annual marks on shell and ligament of sea scallop (*Placopecten magellanicus*). *Fisheries Bulletin* **65(2):** 299-311.

Miyazaki, N. 1977. Growth and reproduction of *Stenella coeruleoalba* off the Pacific coast of Japan. *The Scientific Reports of the Whales Research Institute* **29:** 21-48.

Moreno, C.A., E. Jaramillo. 1983. The role of the grazers in the zonation of intertidal macroalgae of the Chilean coast near of Valdivia, Chile. *Oikos* **41:** 73–76.

Morse, D.E., N. Hooker, H. Duncan, and L. Jensen. 1979. γ-Aminobutyric acid, a neurotransmitter, induces planktonic abalone larvae to settle and begin metamorphosis. *Science* **204:** 407-410.

Munroe, D.M., and T. Noda. 2009. Spatial pattern of rocky intertidal barnacle recruitment: comparison over multiple tidal levels and years. *Journal of the Marine Biological Association of the UK* **89(2):** 345-353.

Navarte, M., V. Willers, M.S. Avaca, M.E. Echave. 2008. Population structure of the snail *Buccinanops globulosum* (Prosobranchia, Nassariidae) in San Matias Gulf, Patagonia Argentina: isolated enclaves? *Journal of Sea Research* **60(3):** 144-150.

O'Farrell, M.R., and L.W. Botsford. 2005. Estimation of change in lifetime egg production from length-frequency data. *Canadian Journal of Fisheries and Aquatic Science* **62:** 1626–1639.

Okuda, S. 1947. Notes on the post-larval development of the Giant Pacific chiton, *Cryptochiton stelleri* (Middendorff). *Journal of the Faculty of Science, Hokkaido Imperial University* **9(3):** 267-275.

Osenberg, C.W., and G.G. Mittelbach 1989. Effects of body size on the predator-prey interaction between pumpkinseed sunfish and gastropods. *Ecological Monographs* **59(4):** 405-432.

Paine, R.T. 1969. The *Pisaster-Tegula* interaction: prey patches, predator food preference, and intertidal community structure. *Ecology* **50(6):** 950-961.

Paine, R.T. 1976. Size-limited predation: an observational and experimental approach with the *Mytilus-Pisaster* interaction. *Ecology* **57(5):** 858-873.

Paine, R.T. 1988. Habitat suitability and local population persistence in the sea palm *Postelsia palmaeformis*. *Ecology* **69(6):** 1787-1794.

Palmer, J.B. and P.W. Frank. 1974. Estimates of growth in *C. stelleri* (Middendorff, 1846) in Oregon. *Veliger* **16(3):** 301-304.

Parry, G.D. 1978. Effects of growth and temperature acclimation on metabolic rate in the limpet, *Cellana tramoserica*. *Journal of Animal Ecology* **47(2):** 351-368.

Perez, M.C., M.L. Gonzalez, and D.A. Lopez. 2007. Breeding cycle and early development of the keyhole limpet *Fissurella nigra* Lesson, 1831. *Journal of Shellfish Research* **26(2):** 315-318.

Peters, R.H. 1983. The ecological implications of body size. Cambridge University Press, New York.

Petersen, J.A., and K. Johansen. 1973. Gas exchange in the giant sea cradle *Cryptochiton stelleri* (Middendorff). *Journal of Experimental Marine Biology and Ecology* **12:** 27-43.

Picken, G.B. 1980. The distribution, growth, and reproduction of the Antarctic limpet *Nacella (Patinigera) concinna* (strebel, 1908). *Journal of Experimental Marine Biology and Ecology* **42:** 71-85.

Rao, M.B. 1976. Studies on the growth of the limpet *Cellana radiata* (Born) (Gastropoda: Prosobranchia). *Journal of Molluscan Studies* **42:** 136-144.

Reiss, M.J. 1989. The allometry of growth and reproduction. Cambridge University Press, Cambridge.

Ricker, W.E. 1975. Computation and interpretation of biological statistics of fish populations, bulletin 19. Ottawa: Department of the Environment, Fisheries and Marine Service.

Rinke, K., S. Hulsmann, and W.M. Mooij. 2008. Energetic costs, underlying resource allocation patterns, and adaptive value of predator-induced life-history shifts. *Oikos* **117(2):** 273-285.

Rogers-Bennett, L., D.W. Rogers, W.A. Bennett, and T.A. Ebert. 2003. Modeling red sea urchin growth using six growth functions. *Fisheries Bulletin* **101:** 614-626.

Ropes, J.W. 1987. Preparation of acetate peels of valves from the ocean quahog, *Arctica islandica,* for age determinations. NOAA Technical Report NMFS 50. 12 pp.

Royo, C., D. Villegas, Y. Rharrabti, R. Blanco, V. Martos, and L.F. Garcia de Moral. 2006. Grain growth and yield formation of durum wheat grown at contrasting latitudes and water regimes in a Meditteranean environment. *Cereal Research Communications* 34.

Rumrill, S.S., and R.A. Cameron. 1983. Effects of gamma-aminobutyric acid on the settlement of larvae of the black chiton *Katharina tunicata. Marine Biology* **72 (3):** 243-247.

Schone, B.R. 2003. A 'clam-ring' master-chronology constructed from a short-lived bivalve mollusc from the northern Gulf of California, USA. *The Holocene* **13:** 39.

Sebens, K.P. 1987. The ecology of indeterminate growth in animals. *Annual Review of Ecology and Systematics* **18:** 371-407.

Sebens, K.P. 2002. Energetic constraints, size gradients, and size limits in benthic marine invertebrates. *Integrative and Comparative Biology* **42:** 853-861.

Shanks, A.L. 2001. An Identification Guide to the Larval Marine Invertebrates of the Pacific Northwest. Corvallis: Oregon State University Press.

Shanks, A.L., and A. McCulloch. 2003. Topographically generated fronts, very nearshore oceanography, and the distribution of chlorophyll, detritus, and selected diatom and dinoflagellate taxa. *Marine Biology* **143:** 969-980.

Shields, J.D. 1991. The reproductive ecology and fecundity of *Cancer* crabs. Pages 193-213 *in* eds. Wenner A and Kuris A. Crustacean Egg Production. A.A. Balkema, Rotterdam.

Snow, C.D. 1951. Notes on the life history of the giant chiton: *Cryptochiton stelleri* (Middendorff). Linfield College: 6 pp.

Soliman, F.E., M.A. Hussein, A. Almaraghy, and T. Habib. 1996. Population structure and growth curve of *Acanthopleura gemmata* (Mollusca: polyplacophora) in the northwestern Red Sea. *Qatar University Science Journal* **16(2):** 307-314.

Steffani, C.N., and G.M. Branch. 2003. Growth rate, condition, and shell shape of *Mytilus galloprovincialis*: responses to wave exposure. *Marine Ecology Progress Series* **246:** 197-209.

Steinberg, P.D. 1985. Feeding preferences of *Tegula funebralis* and chemical defenses of marine brown algae. *Ecological Monographs* **55(3):** 333-349.

Strathmann, M.F. 1985. Feeding and nonfeeding larval development and life-history evolution in marine invertebrates. *Annual Review of Ecology and Systematics* **16:** 339-361.

Suchanek, T.H. 1981. The role of disturbance in the evolution of life history strategies in the intertidal mussels *Mytilus edulis* and *Mytilus californianus*. *Oecologia* **50:** 143-152.

Tafur, R., and M. Rabi. 1997. Reproduction of the jumbo flying squid, *Dosidicus gigas* (Orbigny, 1835) (Cephalopoda: Ommastrephidae) off Peruvian coasts. *Sciencia Marina* **61 (suppl. 2):** 33-37.

Takada, Y. 1996. Vertical migration during the life history of the intertidal gastropod *Monodonta labio* on a boulder shore. *Marine Ecology Progress Series* **130:** 117-123.

Tanaka, M. 1982. A new growth curve which expresses infinite increase. *Publications of the Amakusa Marine Biology Laboratory* **6:** 167-177.

Tegner, M.J. and P.K. Dayton. 1981. Population structure, recruitment and mortality of two sea urchins (*Strongylocentrotus franciscanus* and *S. purpuratus*) in a kelp forest. *Marine Ecology Progress Series* **5:** 255-268.

Thompson, I., D.S. Jones, and D. Dreibelbis. 1980. Annual internal growth banding and life history of the ocean quahog *Arctica islandica* (Mollusca: Bivalvia). *Marine Biology* **57:** 25-34.

Thompson, R.J. 1979. Fecundity and reproductive effort in the blue mussel (*Mytilus edulis*), the sea urchin (*Strongylocentrotus drobachiensis*), and the snow crab (*Chionoecetes opilio*) from populations in Nova Scotia and Newfoundland. *Journal of the Fisheries Research Board of Canada* **36:** 955-964.

Thorpe, S.R. 1962. A preliminary report on spawning and related phenomena in California chitons. *Veliger* **4:** 202-210.

Tucker, J.S., and A.C. Giese. 1962. Reproductive cycle of *Cryptochiton stelleri* (Middendorff). *Journal of Experimental Zoology* **150(1):** 33-43.

Vendrasco, M.J., C.Z. Fernandez, D.J. Eernisse, and B. Runnegar. 2008. Aesthete canal morphology in the Mopaliidae (Polyplacophora). *American Malacological Bulletin* **25(1):** 51-69.

von Bertalanffy, L. 1938. A quantitative theory of organic growth (inquires on growth laws II). *Human Biology* **10:** 181-213.

Voronozhskaya, E.E., S.A. Tyurin, and L.P. Nezlin. 2002. Neuronal development in larval chiton *Ischnochiton hakodadensis* (Mollusca: Polyplacophora). *Journal of Comparative Neurology* **444:** 25-38.

Watanabe, J.M., and L.R. Cox. 1975. Spawning behavior and larval development in *Mopalia lignosa* and *Mopalia muscosa* (Mollusca: Polyplacophora) in central California. *Veliger* **18 (suppl):** 18-27.

Winship, A.J., A.W. Trites, and D.G. Calkins. 2001. Growth in body size of the Steller sea lion (*Eumetopias jubatus*). *Journal of Mammalogy* **82(2):** 500-519.

Woodward, G., B. Ebenman, M. Emmerson, J.M. Montoya, J.M. Oleson, A. Valido, and P.H. Warren. 2005. Body size in ecological networks. *Trends in Ecology and Evolution* **20(7):** 402-409.

Yates, K.R. 1989. Notes on the feeding ecology of the gumboot chiton, *Cryptochiton stelleri* (Middendorff). PhD thesis, Dept. of Zoology, Oregon State University. 206 pp.

Young, C.M., P.K. Tyler, J.L. Cameron, and S.G. Rumrill. 1992. Seasonal breeding aggregations in low-density populations of the bathyal echinoid *Stylocidaris lineata*. *Marine Biology* **113:** 603-612.